DYNAMIC RESPONSE FUNCTION AND THE THEORY OF SPIN WAVES IN METALLIC OVERLAYERS

by

Minh Son Phan, BSc

A Thesis Submitted for the Degree of

Doctor of Philosophy

Department of Mathematics

The City University, London

November, 1989

To my Parents

CONTENTS

CHAPTER 3

FIRST PRINCIPLE CALCULATION OF SPIN WAVES IN AN OVERLAYER

page

ACKNOWLEDGEMENTS

I am deeply indebted to my supervisor Prof. J Mathon for his guidance, encouragement, helpful criticism and energetic interest in the development of this thesis.

Financial support from the Science and Engineering Research Council is gratefully acknowledged. Computations, in the present thesis, were performed at the CRAY X-MP at University of London Supercomputer centre (ULCC) is also gratefully acknowledged.

ABSTRACT

A general recursion method (method of adlayers) for calculating the exact Green function in an arbitrary overlayer is developed. The method as presented applies to an s-band tight-binding Hamiltonian with hopping between nearest-neighbours only. The generalisation of the method to a multi-orbital band structure is described. The overlayer we consider is deposited above the (100) surface of a simple cubic semi-infinite nonmagnetic metallic substrate occupying the half-space $z<0$. The aim of the present thesis is twofold: firstly, the ground state of a ferromagnetic overlayer is investigated. In particular, the local densities of states (LDOS) of an overlayer are calculated using the method of adlayers. The method of adlayers is very simple, computationally stable and extremely accurate. The numerical results for the LDOS and the Hartree-Fock (HF) occupation numbers of a single-adlayer and a seven-adlayer overlayer are presented. The surface and bulk DOSs for an overlayer of seven atomic planes are compared. The presence of an adlayer may induce surface states if a strong enough perturbation occurs at the surface. Such surface states are automatically included in our method of adlayers. Secondly, spin waves in a transition metal overlayer are investigated within the framework of the itinerant theory of magnetism. The overlayer is modelled by a single-orbital tight-binding band with a strong intra-atomic repulsion U (one band Hubbard model). All the matrix elements of the HF dynamic unenhanced susceptibility in the overlayer are computed from the HF one-electron Green functions. Spin waves are then poles of the full dynamic enhanced susceptibility which is determined in the random phase approximation (RPA). It is demonstrated that a very high accuracy in solving the HF ground state is needed to determine correctly spin wave modes. When this requirement is fulfilled, the Goldstone theorem at zero wavevector and zero frequency is very well satisfied. Numerical results for the spin wave spectra of a single-adlayer are presented for a range of values of U. Spin wave energies for a single-adlayer, for an unsupported layer and the exchange stiffness constant D of an unsupported layer are compared. Finally, all the computed spin wave branches of an overlayer of seven atomic planes are presented and discussed. The disappearance of spin waves in the Stoner continuum is illustrated and the possibility that a surface spin wave mode might occur is briefly discussed.

Chapter 1.

1.1 Introduction

The surface magnetism of transition metals has been studied extensively in recent years and is now a subject of great interest both theoretically and experimentally. One of the factors behind this development is the dramatic improvement in experimental methods, the preparation of good thin films and surfaces and in particular the development of local spin-density functional method together with high-speed computers.

There is a great impact of many techniques familar in solid state technology for example, molecular or atom beam epitaxy which are being transferred to surface and interface magnetism. Another important factor arises from the fact that the surface methods are now being employed widely to study the fundamental processes in magnetic materials. For example, information about the ferromagnetic band structure, the effect of correlations and finite-temperature magnetism is currently obtained from photoemission data.

One of the fundamental problems of surface magnetism is the effect of surface on the ground-state magnetisation. The ground state surface problem of magnetic transtion metals is now quite well understood.The main factor here is the Stoner-Wohlfarth theory (see Wohlfarth, 1980) and in

particular,the local-spin-density-functional theory, (see Hohenberg and Kohn, 1964, Kohn and Sham, 1965 and Rajagopal, 1980), which applies to ferromagnetic as well as antiferromagnetic metals. However, unlike the ground state problem, the effect of surface on excited states is not fully understood and is still one of the major challenges in surface physics and in solid state physics.

The main factors which motivated the present work on spin waves in magnetic overlayers can be summarised as follows:

(i) theoretically, the local-spin-density-functional formalism has been very successful in the calculations of the ground-state properties of some metallic layer structure and superlattices, for example, see Freeman and Fu (1987),

(ii) experimentally, the magnetic layer structures hold the promise of new device applications. For example, layer structures with a magnetic anisotropy perpendicular to the surface are prime candidates for high-density (perpendicular) recording (Iwasaki 1984,Carcia et al. 1985). This is why such structures are now studied extensively in industrial laboratories such as IBM (Siegmann et al.1989, Mauri et al. 1988).

(iii) Using the method of atomic beam deposition, it has recently becomes possible to farbricate magnetic layer structures with atomic precision (Gradmann 1985, Bader and Moog 1987, Arrot et al. 1987).

(iv) Local exchange interactions and anisotropy (crucial for perpendicular recording) have become accessible to experiment.This has been achieved through interpretation of finite-temperature measurements of the local magnetisation carried out at IBM San Jose and ETH Zurich (see Siegmann et al.1989 and Mauri et al.1988) on the basis of our theory of spin waves in layer structures (Mathon and Ahmad 1988, Mathon 1988a, Mathon 1989b, Ahmad et al. 1989). An essential ingredient here is the high spatial resolution of "magnetometry" with spin-polarised electrons (Siegmann et al. 1989) which makes meaningful comparison with theory possible.

1.2 The ground state of an itinerant ferromagnet

The main ingredients of the classical Stoner-Wohlfarth model of ferromagnetism are (Wohlfarth 1980)

(i) the carriers of magnetism in ferromagnetic transition metals, such as,iron, cobalt, nickel, are the electrons in 3d band The respective approximate saturation magnetisation values are 2.2, 1.7 and $0.6\mu_B$/atom .

(ii) the distribution of itinerant electrons among the energy levels is determined by the band structure and $N(E_F)$, the density of states at the Fermi energy E_F is the key quantity.

(iii) The interaction between the itinerant electrons may be described in the molecular field approximation.The molecular field is proportional to the magnetisation and the associated energy per atom is

$$E_\zeta = -\frac{1}{4} n^2 \zeta^2 U \qquad (1.1)$$

Here,

n is the number of electrons per atom,

U is an interaction parameter,

ζ is the relative magnetisation.

When the density of states at the Fermi level $N(E_F)$ is high and U is strong, the Stoner condition $U.N(E_F) > 1$ is satisfied and the energy bands for up and down-spin carriers become split, resulting in a spontaneous magnetisation ζ.

In this original formulation of the Stoner model the calculation of the band structure is made neglecting the effect of electron interactions. The electron interactions are then treated in the lowest Hatree-Fock (HF) approximation and U is assumed to be independent of the electron wavevector.

A microscopic basis of the Stoner model was provived by Hubbard (1963,1964), and the Hubbard Hamiltonian combined with a tight-binding scheme for calculating the band structure remains the only theoretical framework for discusing excited states in itinerant ferromagnet.

Application of the HF theory to Hubbard model leads to the Stoner model of ferromagnetism in which the two bands are split by a constant factor (an energy) $\Delta = U^{Hub}.(n_{\uparrow}-n_{\downarrow})$. In the paramagnetic regime, the interaction between electrons is not strong enough to split the band and the number of spin-up electrons and spin-down electrons are equal, (Δ = 0). Now we can discuss the orgin and magnitude of the parameter U.

When discussing the origin of ferromagnetism within the HF approximation we must consider the exchange integral U dependening on the Bloch wavefunction $\Psi_{nk}(n=1,2,...,5)$ in the d-band. In general it is of the form (with correlation negelected)

$$U_{m\underline{k},n\underline{k}'}=\iint d\underline{r}_1 d\underline{r}_2 \psi^*_{m\underline{k}}(\underline{r}_1)\psi^*_{n\underline{k}'}(\underline{r}_2)V(\underline{r}_1-\underline{r}_2)\psi_{m\underline{k}}(\underline{r}_2)\psi_{n\underline{k}'}(\underline{r}_1) \qquad (1.2)$$

where $V(\underline{r}_1-\underline{r}_2) = e^2/r_{12}$ is the screened Coulomb

interaction within a unit cell and the relationship between Bloch and Wannier function $\omega_m(\underline{r}-\underline{R}_i)$ for the m-th band is given by

$$\psi_{m\underline{k}}(\underline{r}) = \frac{1}{\sqrt{N}} \sum_{\underline{R}_i} e^{i\underline{K}\underline{R}_i} \omega_m(\underline{r}-\underline{R}_i) \qquad (1.3)$$

where N is, the number of atomic cells in the crystal; $\underline{r}$ is the electron position vector; $\underline{R}_i$ is the atomic site.

Within the tight-binding approximation, and upon substitution eq.(1.3) into (1.2) we find that there are two most important factors independent of k and k′ which contribute to U :

(1) The intra-atomic Coulomb interaction for two electrons on the same site with opposite spins in the same orbital, which is defined by

$$I_{mm} = \iint |\omega_m(\underline{r}_1)|^2 \frac{e^2}{r_{12}} |\omega_m(\underline{r}_2)|^2 \, d\underline{r}_1 d\underline{r}_2 \qquad \text{(if m=n)} \qquad (1.4)$$

(2) The intra-atomic exchange interaction or the Hund's rule exchange integral, between two electrons on the same site in different orbitals but with parallel spin :

$$J_{mn} = \iint \omega_m^*(\underline{r}_1) \, \omega_n^*(\underline{r}_2) \, \frac{e^2}{r_{12}} \omega_m(\underline{r}_2)\omega_n(\underline{r}_1) \, d\underline{r}_1 d\underline{r}_2 (m \neq n) \qquad (1.5)$$

These integrals have values $I_{mm} \approx 22$eV, $J_{mn} \approx 0.8$eV for a metal such as nickel (Edwards 1977). Screening by s electrons reduces I_{mm} to $I \approx 5$-8eV, although Herring (1966) and Mott (1964) gave the value of I as about 2eV. The Hund's rule J_{mn} is important when the number of electrons

(holes) per atom is large, as in Fe and Co but less significant for a ferromagnet such as Ni with 0.6 holes per atom since it is unlikely to find two holes on the same atom due to correlation effects not included in the HF approximation.

The bare interaction parameters are reduced not only by screening but also by correlations in the d-band. Both Hubbard (1963) and Kanamori (1963) had studied the effect of correlation on U. They showed that for a low density of holes,such as Ni, the ground state properties of itinerant electron ferromagnet (see Hubbard Hamiltonian Eq(1.9) may be treated in the HF approximation provided the bare interaction U is replaced by a weaker effective interaction U^{eff} .

The effective interaction parameter U^{eff} which should be used in the Stoner model is of the order 0.5 to 1eV and is remarkably constant across the transition metal series (Wohlfarth 1980).

It is clear that Kanamori formalism only applies to nickel with 0.6 holes per atom ($U^{eff} \approx 0.5$eV). For iron and cobalt the above formalism is not justified since the density of holes is too high (2.2,1.7 μ_B/atom respectively)

The above estimates of U^{eff} are clearly only qualitative and that is the main reason why the classical Stoner model (1938) fails to predict the saturation moment, exchange splitting of the (up and down) bands and other fundamental properties of ferromagnetic metals.

Since the original Stoner model was first proposed, the local-spin-density-functional (LSDF) method has been developed to describe exchange and correction effects within a one-body formulation. The LSDF method is based on the exact results of Hohenberg and Kohn (1964) and has been very successful in explaining many ground states properties of magnetic transition metals.

For the purpose of calculating the ground-state properties, it is clear that the LSDF method has now replaced the Stoner model and allows us to include correlation effects quite naturally. Another serious problem with Stoner model is that it ignores spin waves. This is because it uses the molecular field approximation which precludes spin wave excitations from the begining. In fact, in the Stoner model, single particle spin-flip excitations is the only mechanism to reduce the magnetisation ζ. This mechanism leads to $\zeta \propto T^2$, while spin wave excitations first derived for a metal by Herring and Kittel (1951) predict a $T^{3/2}$ dependence of the magnetisation at low temperature.

From the above disscusion, we can conclude that:a satisfactory theory must include both Stoner and spin wave excitations.Such a theory certainly can not be developed within the LSDF theory since it valid only for the ground state. To calculate spin waves we have to use a model Hamiltonian and we are going to consider this prolem in the next section.

1.2.1 The Hubbard model

As already discussed, the complete Hamiltonian for n interacting electrons is very complicated and too difficult to handle. Therefore, a simple model hamiltonian has to be developed.

The carriers of magnetism in transition metals are 'holes' in the d band which contains five sub-bands. To discuss the magnetism of a transition metal, a model of d electrons is needed. S band electrons are free electron like and their contribution to magnetism is small (Herring 1966). Therefore in general, when discussing the phenomenon of magnetism of transition metals, one needs to consider a degenerated band.Any treatment of the d-band in transition metals must include electron-electron correlation effect since the d electrons are concentrated near the nucleus of each atom, making it possible to speak with some meaning of an electron being 'on 'a particular atom. This is because the width of the d band is narrower than that of s band. For example, in the iron group, the width of the d band is about 4eV while the width of the s band is about 20eV (Shimizu 1981).It was Hubbard (1963,1964) who had originally put forward a simple model for treating correlation in narrow bands (see also Penn 1979 and Liebsch 1979).

It is in fact found experimentally that the d electrons in transition metals exhibit behaviour characteristic of both the 'itinerant electron model'

and the 'localized spin model'. By the localized spin model, we mean that the magnetic electrons are localized around the atom in the crystal. This is the Heisenberg model or localized model applicable to insulator. In the itinerant electron model (or band model), we start from the one-electron eigenstates or Bloch states in the metal and take into account screening, electron correlations and exchange interactions among electrons. In this model the magnetic electrons are supposed to be band electrons and run over the whole crystal. This model was employed by Bloch (1929), Mott(1935), Stoner (1936) (1936) and Slater (1936) to explain the ferromagnetism of the iron group metals.

In the present thesis, we shall adopt the itinerant electron model to discuss the magnetism of transition metals. We shall therefore, build a model including electron-electron interactions through the Hartree-Fock approximation.Our model is based upon the tight-binding approximation which is known to be a good staring point for transition metals.The general Hamiltonian describing the d electrons is, in fact, the degenerate Hubbard Hamiltonian given by (Hubbard 1964) :

$$H=\sum_{\substack{ij\\ \mu\nu\sigma}} T_{ij}^{\mu\nu} c_{i\mu\sigma}^{+} c_{j\nu\sigma} + \frac{1}{2} \sum_{\substack{ijkl\\ \mu\nu\eta\xi\\ \sigma\sigma'}} \langle i\mu\sigma j\nu\sigma' | \frac{1}{r} | k\eta\sigma l\xi\sigma \rangle (c_{i\mu\sigma}^{+} c_{j\nu\sigma'}^{+} c_{l\xi\sigma'} c_{k\eta\sigma}) \tag{1.6}$$

Where

$$T_{ij}^{\mu\nu} = \int \Phi_{\mu\sigma}^{*}(\underline{r}-\underline{R}_i) \left[-\frac{\hbar}{2m}\nabla^2 + V \right] \Phi_{\nu\sigma}(\underline{r}-\underline{R}_j) d\underline{r}^3 \tag{1.7a}$$

with

$$\langle i\mu\sigma, j\nu\sigma|\frac{1}{r}|k\eta\sigma, l\xi\sigma = e^2\int \Phi^*_{\mu\sigma}(\underline{r}-\underline{R}_i)\Phi^*_{\nu\sigma'}(\underline{r}'-\underline{R}_j)\ \frac{1}{r-r'}$$

$$\Phi_{k\sigma}(\underline{r}-\underline{R}_k)\Phi_{l\sigma}(\underline{r}'-\underline{R}_l)d\underline{r}^3 d\underline{r}'^3 \qquad (1.7b)$$

Here, V represents the nuclear potential acting on the eletron; $\Phi_{\mu\sigma}(\underline{r}-\underline{R}_i)$ is the atomic wavefunction of an electron on a site $\underline{R}_i$ in an orbital μ; $C^+_{i\mu\sigma}$ ($C_{i\mu\sigma}$) are the creation (annihilation) operators for an electron at a site $\underline{R}_i$ with spin σ in an orbital μ.

The first term in Eq.(1.6) is just the ordinary band Hamiltonian while equation (1.7b) giving the second term in Eq.(1.6) represents the Coulomb interaction between electrons . It is convenient to follow Hubbard (1963) and make the following assumptions :

(i) Neglect degeneracy, i.e., drop all the band indices, the model is now reduced to a simple one-band model,

(ii) Neglect all interaction terms other than those whose matrix elements involve electrons on the same site, i.e., $\langle ii|1/r|ii\rangle$, which is the diagonal terms .

we thus obtain

$$H = \sum_{ij\sigma} T_{ij}C^+_{i\sigma}C_{j\sigma} + \frac{1}{2}\sum_{i\sigma\sigma'}\langle ii|1/r|ii\rangle C^+_{i\sigma}C_{i\sigma}C^+_{i\sigma'}C_{i\sigma'} \qquad (1.8)$$

Eq(1.8) is the simplest one-band model in which electrons interact only when they are in the Wannier function $\Phi_\sigma(\underline{r}-\underline{R}_i)$ To simplify it further we write:

$$H = \sum_{ij\sigma} T_{ij} c^{+}_{i\sigma} c_{j\sigma} + \frac{U}{2} \sum_{i\sigma} n_{i\sigma}\, n_{i-\sigma} \qquad (1.9)$$

where $U = \langle ii|1/r|ii\rangle$, T_{ij} is the hopping integral, $n_{i\sigma}=c^{+}_{i\sigma}c_{i\sigma}$ is the occupation number where the Wannier operator $c^{+}_{i\sigma}$ is related to the Bloch operator $c^{+}_{k\sigma}$ by the following equation

$$c^{+}_{i\sigma} = \frac{1}{\sqrt{N}} \sum_{k} c^{+}_{k\sigma} e^{-ikR_i} \qquad (1.10)$$

1.2.2 Hubbard model in the HF ground state

As already discussed, all the main features of the Stoner model can be obtained by treating the Hubbard model in the HF approximation. We first replace the bare interaction U in Eq.(1.9) by an effective U^{eff} to take into account the effect of correlations and we can rewrite Eq.(1.9) as follow:

$$H = \sum_{ij\sigma} T_{ij} c^{+}_{i\sigma} c_{j\sigma} + U^{eff} \sum_{i} n_{i\uparrow} n_{i\downarrow} \qquad (1.11)$$

Now, the second term in Eq.(1.11) can be written as

$$\sum_{i} n_{i\uparrow} n_{i\downarrow} \xrightarrow{\text{HF, RPA}} \sum_{i} \frac{1}{2} \left\{ \langle n_{i\uparrow} \rangle n_{i\downarrow} + n_{i\uparrow} \langle n_{i\downarrow} \rangle \right\}$$

$$= n_{\uparrow} n_{\downarrow} \qquad (1.12)$$

where $n_{\uparrow} = \langle n_{i\uparrow} \rangle$ and $n_{\sigma} = \sum_{\sigma} n_{k\sigma}$ have been used.

Therefore, the total energy in the HF approximation is given by

$$E_{HF} = \sum_{k\sigma} E_k \, n_{k\sigma} + U^{eff} \, n_{\uparrow} n_{\downarrow} \qquad (1.13)$$

We can write

$$U^{eff} n_{\uparrow} n_{\downarrow} = \frac{1}{4} U^{eff} \left[(n_{\uparrow} + n_{\downarrow})^2 - (n_{\uparrow} - n_{\downarrow})^2 \right] \qquad (1.14)$$

Then (Thompson 1963)

$$U^{eff} n_{\uparrow} n_{\downarrow} = - \frac{U^{eff}}{4} (n_{\uparrow} - n_{\downarrow})^2 + \text{constant}$$

$$= - \frac{U}{4} \zeta^2 n^2 + \text{constant} \qquad (1.15)$$

where

$\zeta = \dfrac{n_\uparrow - n_\downarrow}{n}$ is the relative magnetisation and

$n = n_\uparrow + n_\downarrow$ is the total number of particles in the system

Eq(1.15) is in fact the expression for the additional energy of the system in the Stoner model (1938,1946).

It follows that (Thompson,Wohlfarth and Bryan 1964)

$$n_\sigma = \begin{cases} \frac{n}{2}(1+\zeta) & \text{if } \sigma = \uparrow \\ \frac{n}{2}(1-\zeta) & \text{if } \sigma = \downarrow \end{cases} \qquad (1.16)$$

or

$$n_\sigma = \int_0^\infty N(E) f^\sigma(E)\, dE \qquad (1.17)$$

where

$$f^\sigma(E) = \frac{1}{1 + e^{(E-\mu^\sigma)/K_B T}} \qquad (1.18)$$

is the 'Fermi-Dirac function' for σ-spin particles, μ^σ are the corresponding chemical potentials, K_B is the Boltzmann constant, T is the temperature and N(E) is the density of states.

The total energy in the 'Stoner model' is given by

$$E^{\text{Stoner}} = \sum_{k\sigma} E_{k\sigma} n_{k\sigma} - \frac{1}{4} U^{\text{eff}} \zeta^2 n^2 \qquad (1.19)$$

At T=0 , Eq(1.19) is equivalent to

$$E^{Stoner} = \int_0^{E_{F\uparrow}} EN(E)dE + \int_0^{E_{F\downarrow}} EN(E)dE - \frac{U^{eff}}{4}\zeta^2 n^2 \qquad (1.20)$$

where Ef is the Fermi energy for the σ-spin bands and

$$n_{\uparrow\downarrow} = \int_0^{E_{F\uparrow\downarrow}} N(E)dE \qquad (1.21)$$

The criterion for ferromagnetism is obtained by comparing the energy E^{Stoner} for small ζ at T=0 with the paramagnetic energy E_o. It is found (Thompson,Wohlfarth and Bryan 1964) that

$$E_\zeta = E_o + \frac{n^2\zeta^2}{4N(E_F)}\left[1 - U^{eff}N(E_F)\right] \qquad (1.22)$$

From eq(1.22) it is clear that the system becomes ferromagntic if the energy of the system is less on magnetizing if

$$U^{eff}\, N(E_F) > 1 \qquad (1.23)$$

which is known as the Stoner criterion. In fact more carefull analysis shows that Stoner criterion together with the positive exchange stiffness D form a necessary and sufficient conditions forthe stability of ferromagtism. If D is negative, the ferromagnetic ground state is unstable even if (1.23) holds. For further discusion of the ground state stability (see Katsuki and Wolhfarth (1966)).

If the condition (1.23) is satisfied either all spins are line up as in the case of Ni and we have a strong ferromagnet shown in figure (1) :

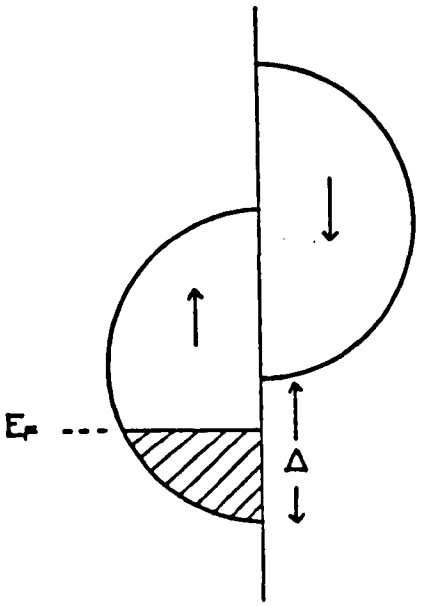

Fig.1 Strong ferromagnetic $\Delta=nU^{eff}>E_{F\uparrow}$, $\zeta=1$ at $T=0^0K$

For a strong ferromagnet the HF ground state is an exact eigenstate since particles of the same spin do not interact in this model (Pauli principle).If a point of balance is reached with both sub-bands occupied then we have a weak ferromagnets as in the case of iron (see figure 2.). The bands are shifted by Δ defined as the exchange spliting where

$$\Delta = n\zeta U^{eff} \qquad (1.24)$$

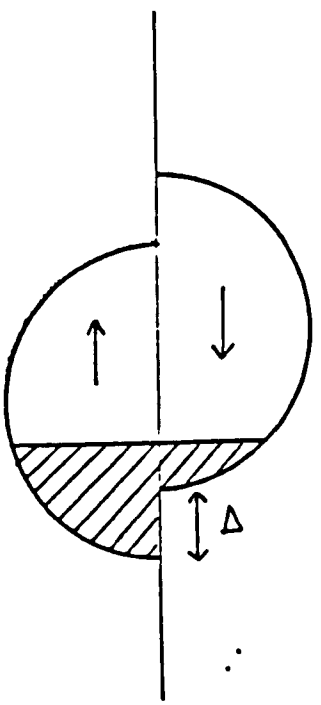

Fig.2 Weak ferromagnetic $\Delta=nU^{eff}\zeta$, $\zeta<1$.

1.3 Green's Function and Resolvents

Green's functions or propagators play a very important role in the theory of many particle systems and in solid state theory. For example, the one-particle Green's function G yields directly the energies of particles, the number of up and down spin electron electrons, particle density and can be used to calculate the ground state energy. The two-particle propagator, on the other hand, gives us collective excitation energies as poles of the dynamic susceptibility. Since the whole thesis is based on the Green's function formulation, we shall now summarise the main results we shall need, following the paper by Zubarev (1960).

1.3.1 The Retarded and Advanced Green's Function

The retarded $G_R(t,t')$ and advanced $G_A(t,t')$ Green functions are defined as follow :

$$G_R(t,t') = \langle\langle A(t);B(t')\rangle\rangle_R$$

$$= -i\theta(t-t')\langle[A(t),B(t')]\rangle \qquad (1.25)$$

$$G_A(t,t') = \langle\langle A(t);B(t')\rangle\rangle_A$$

$$= i\theta(t-t')\langle[A(t),B(t')]\rangle \qquad (1.26)$$

where $\theta(t)$ is the step function being equal to unity if $t>0$ and zero otherwise, and $\langle\langle A(t);B(t')\rangle\rangle_{R,A}$ are the abbreviated notations for the corresponding Green functions, and $\langle \cdots \rangle$ denotes averaging over a grand canonical ensemble defined by

$$\langle \cdots \rangle = Q^{-1}\, Tr(e^{-\mathbb{H}/\theta}) \qquad (1.27)$$

$$Q = Tr(e^{-\mathbb{H}/\theta}) = e^{\Omega/\theta} \qquad (1.28)$$

Here $\theta = K_B T$ where K_B is the Boltzmann constant and T is the absolute temperature, Q is the grand partition function, and Ω is the thermodynamic potential.

The operator $\mathbb{H} = H-\mu N$ is the generalized Hamiltonian where H is the time-independent Hanmitonian operator and N is the operator for the total number of particles and μ is the chemical potential. A(t) and B(t') in eqs.(1.25 and 1.26) are the operators in the Heisenberg representation which can be expressed in terms of a product of the quantized field operators, i.e.,

$$A(t) = e^{iHt} A(0) e^{-iHt} \qquad (1.29)$$

Also [A,B] is the commutator or anticommutator,

$$[A,B] = AB - \eta BA \qquad (1.30)$$

where

$$\eta = \begin{cases} +1 \text{ if A,B are Boson operator} \\ -1 \text{ if A,B are Fermion operator} \end{cases} \qquad (1.31)$$

It is most convenient to choose the sign of η depending on the condition of the problem.Upon substitution (1.30) into eqs.(1.25 and 1.26) to get

$$G_R(t,t') = -i\theta(t-t')\{\langle A(t)B(t')-\eta\langle B(t')A(t)\rangle\} \qquad (1.32)$$

$$G_A(t,t') = i\theta(t-t')\{\langle A(t)B(t')-\eta\langle B(t')A(t)\rangle\} \qquad (1.33)$$

Note that from Eqs. (1.25) and (1.32) we see that

$$G_{R,A}(t,t') = \begin{cases} 0 \text{ if } (t-t') < 0 \\ \neq 0 \text{ if } (t-t') > 0 \\ \text{undefined if } (t-t') = 0 \text{ because of the discontinuity of } \theta(t) \text{ at } t=0 \end{cases} \qquad (1.34)$$

Since $G_{R,A}(t,t')$ are the functions of $(t-t')$ only it is in fact very useful to introduce Fourier integral representation

$$G_{R,A}(t,t') = \int_{-\infty}^{\infty} dE\, G_{R,A}(E)\, e^{-iE(t-t')} \qquad (1.35)$$

or

$$G_{R,A}(E) = \int_{-\infty}^{\infty} dt\, G_{R,A}(t,t')\, e^{iE(t-t')} \qquad (1.36)$$

1.3.2 Equation of motion of the Green's Function

The operators A(t) and B(t′) satisfy equations of motion of the form

$$i\frac{dA}{dt} = [A,H] \qquad (1.37)$$

By differentiating the Green function (1.25) and (1.26) w.r.t.t to obtain

$$i\frac{dG_{R,A}}{dt} = i\frac{d}{dt}\ll A(t);B(t')\gg$$

$$= \frac{d}{dt}\theta(t-t')\langle[A(t),B(t')]\rangle + \theta(t-t')\langle[\frac{d}{dt}A(t),B(t')]\rangle$$

$$= \frac{d}{dt}\theta(t-t')\langle[A(t),B(t')]\rangle + \ll i\frac{d}{dt}A(t);B(t')\gg \qquad (1.38)$$

Here, we have used

$$\frac{d}{dt}\theta(-t) = -\frac{d}{dt}\theta(t),\ \theta(t) = \int_{-\infty}^{t}\delta(t)dt \text{ and } \frac{d}{dt}\theta(t) = \delta(t) \qquad (1.39)$$

Finally, we obtain

$$i\frac{d}{dt}G_{R,A} = \delta(t-t')\langle[A(t),B(t')]\rangle + \ll[A(t),H];B(t')\gg \qquad (1.40)$$

The second term in the RHS of eq(1.40) is also a Green function of a higher order involving the commutator or anticommutator of products of two or more operators with B(t′). The equation of motion of this Green function may be written in the same fashion as in Eq(1.40) and we can obtain a chain of coupled equations of motion for the Green functions. They must be supplemented by boundary conditions and this can be done by means of spectral theorems which will be discussed in the next section.

1.3.3 Spectral representation for time correlation function

The time correlation functions $\langle A(t)B(t')\rangle$ and $\langle B(t')A(t)\rangle$ are the averages over the statistical ensemble of the product of operators A and B in the Heisenberg representation. We shall now derive the spectral representation for $\langle A(t)B(t')\rangle$ and $\langle B(t')A(t)\rangle$

Let $|n\rangle$, E_n be the eigenfunctions and eigenvalues of the Hamiltonian ($\mathcal{H} = H-\mu N$), i.e,

$$\mathcal{H}|n\rangle = E_n|n\rangle \qquad (1.41)$$

The time correlation function $\langle B(t')A(t)\rangle$ can be write in the form

$$\begin{aligned}\langle B(t')A(t)\rangle &= Q^{-1}\,\mathrm{Tr}(e^{-\mathcal{H}/\theta}\,B(t')A(t)) \\ &= Q^{-1}\sum_n \langle n|e^{-\mathcal{H}/\theta}\,B(t')A(t)|n\rangle \\ &= Q^{-1}\sum_n \langle n|B(t')A(t)|n\rangle e^{-E_n/\theta} \qquad (1.42)\end{aligned}$$

where $\theta = K_B T$.

We insert a complete set of states which is unity, i.e., $1=\sum|m\rangle\langle m|$ in eq(1.42), which gives

$$\langle B(t')A(t)\rangle = Q^{-1}\sum_{m,n} \langle n|B(t')|m\rangle\langle m|A(t)|n\rangle e^{-E_n/\theta} \qquad (1.43)$$

Upon substitutions

$$\begin{aligned}A(t) &= e^{i\mathcal{H}t}A(0)e^{-i\mathcal{H}t'} \\ B(t') &= e^{i\mathcal{H}t}B(0)e^{-i\mathcal{H}t'}\end{aligned} \qquad (1.44)$$

into eq(1.43) to obtain

$$<B(t')A(t)>=Q^{-1}\sum_{m,n}<n|e^{i\mathbb{H}t'}B(0)e^{-i\mathbb{H}t}\ m><m|e^{i\mathbb{H}t}A(0)e^{-i\mathbb{H}t}|n>e^{-E_n/\theta}$$

$$=Q^{-1}\sum_{m,n}B_{nm}A_{mn}e^{-E_n/\theta}e^{-i(E_n-E_m)(t-t')} \qquad (1.45)$$

The last equation holds since

$$e^{-i\mathbb{H}t}|n> = e^{-iE_nt}|n>$$
$$<n|e^{i\mathbb{H}t} = <n|e^{iE_nt} \qquad (1.46)$$

and we have used the notation

$$B_{nm} = <n|B(0)|m>$$
$$A_{mn} = <m|A(0)|m> \qquad (1.47)$$

Similarly,

$$<A(t)B(t')> = Q^{-1}\sum_{m,n}A_{nm}B_{mn}e^{-E_n/\theta}e^{-i(E_n-E_m)(t'-t)} \qquad (1.48)$$

Now interchanging the summation indices in Eq.(1.45) and (1.46) we get

$$<B(t')A(t)> = Q^{-1}\sum_{m,n}B_{mn}A_{nm}e^{-E_m/\theta}e^{-i(E_m-E_n)(t-t')} \qquad (1.49)$$

and

$$<A(t)B(t')> = Q^{-1}\sum_{m,n}A_{mn}B_{nm}e^{-E_m/\theta}e^{-i(E_m-E_n)(t-t')} \qquad (1.50)$$

or we can write (1.49) and (1.50) as follow

$$<B(t')A(t)> = \int_{-\infty}^{\infty}J(\omega)e^{-i\omega(t-t')}d\omega \qquad (1.51)$$

$$<A(t)B(t')> = \int_{-\infty}^{\infty}J(\omega)e^{w/\theta}\ e^{-i\omega(t-t')}d\omega \qquad (1.52)$$

Where we have introduced $J(\omega)$, the spectral density function, is the Fourier transform of $\langle A(t)B(t')\rangle$ and $\langle B(t')A(t)\rangle$ defined by the equation

$$J(\omega) = Q^{-1} \sum_{m,n} A_{mn}B_{nm}e^{-E_m/\theta}\delta(\omega-E_n+E_n) \qquad (1.53)$$

Equations (1.51) and (1.52) are the required spectral representations for the time-correlation functions.

1.3.4 Spectral representations for $G_{R,A}$

We shall now consider the spectral representation of $G_{R,A}(t,t')$ .These are obtained by means of the time correlation functions (1.51 and 1.52).

Now we can restate Eq.(1.32) as

$$G_R(t,t') = -i\theta(t-t')\{<A(t)B(t')> + <B(t')A(t)>\} \quad (1.54)$$

Fourier transforming Eq.(1.54) we have

$$G_R(E) = \int_{-\infty}^{\infty} dt G_R(t) e^{iEt}$$

$$= -i\int_{-\infty}^{\infty} dt\ \theta(t)\{<A(t)B(0)>+<B(0)A(t)>\}e^{iEt} \quad (1.55)$$

Now inserting the time correlation functions (1.51 and 1.52) into Eq.(1.55) to obtain

$$G_R(E) = -i \int_{-\infty}^{\infty} d\omega\ J(\omega)(e^{\omega/\theta} + 1) \int_{-\infty}^{\infty} dt\ \theta(t) e^{i(E-\omega)t} \quad (1.56)$$

Here we write the discontinous function $\theta(t)$ in the form

$$\theta(t) = \int_{-\infty}^{t} e^{\varepsilon t}\ \delta(t)dt \qquad (\varepsilon \to 0, \varepsilon>0) \quad (1.57)$$

where

$$\delta(t) = \frac{1}{2\pi}\int_{-\infty}^{\infty} e^{-ixt} dx \quad (1.58)$$

Thus,

$$\theta(t) = \frac{1}{2\pi}\int_{-\infty}^{\infty}\int_{-\infty}^{t} e^{(\varepsilon-ix)t}\ dtdx$$

$$= \lim_{\varepsilon \to 0} \frac{1}{2\pi}\int_{-\infty}^{\infty} \frac{\exp(\varepsilon-ix)t}{\varepsilon-ix}\ dx = \lim_{\varepsilon \to 0} \frac{i}{2\pi}\int_{-\infty}^{\infty} \frac{e^{-ixt}}{x+i\varepsilon}\ dx \quad (1.59)$$

We shall consider x as a complex variable and assume that the integral (1.59) is taken over the contour depicted in Fig.(3)

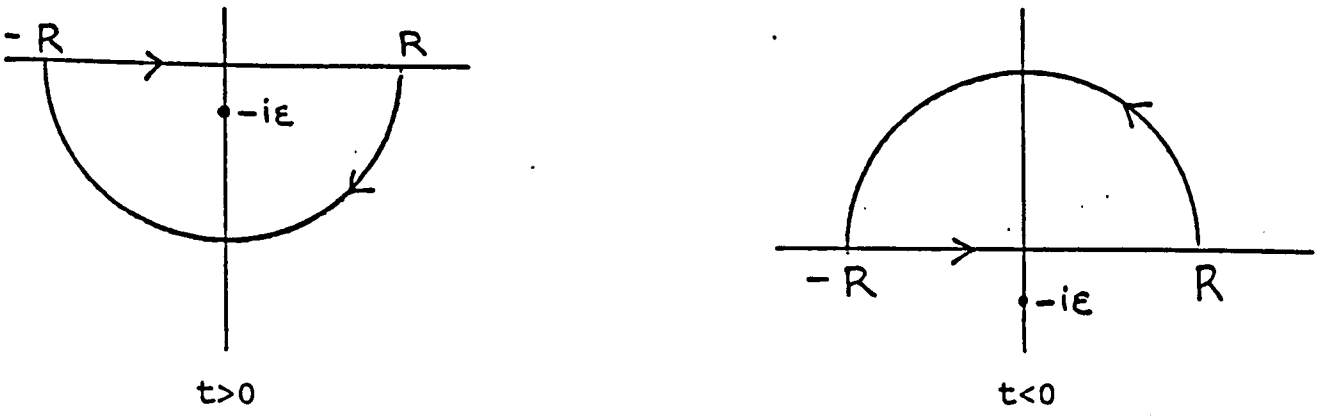

Fig.3 Contour of integration in a complex plane.

We note that the integrand in Eq.(1.59) has a simple pole in the lower half-plane at $x = -i\varepsilon$ and

$$e^{-ixt} = e^{-iRe(x)t} \cdot e^{Im(x)t}$$

If $t>0$, we must take the semi circle in the lower half-plane since $|e^{-ixt}| = e^{Im(x)t}$ which is bounded only for $Im(x) > 0$. Only the residue at the simple pole $x = -i\varepsilon$ which lies inside the lower half contour contributes to the integral.

If $t<0$, then $Im(x)>0$ and the contour must be closed in the upper half-plane. The integral then vanishes since the pole is not situated in the uper half-plane.

Using Eq.(1.59) we can write

$$\int_{-\infty}^{\infty} dt\theta(t) e^{i(E-\omega)t} = \int_{-\infty}^{\infty} dt e^{i(E-\omega)t} \frac{i}{2\pi} \int_{-\infty}^{\infty} \frac{e^{-ixt}}{x + i\varepsilon} dx$$

$$= \frac{i}{2\pi} \int_{-\infty}^{\infty} \frac{dx}{x + i\varepsilon} \delta(E-\omega-x)$$

$$= \frac{i}{2\pi} \frac{1}{E - \omega + i\varepsilon} \qquad (1.60)$$

Thus Eq(1.56) now reduces to

$$G_R(E) = \frac{1}{2\pi} \int_{-\infty}^{\infty} J(\omega) \, (e^{\omega/\theta} + 1) \, \frac{d\omega}{E - \omega + i\varepsilon} \qquad (1.61)$$

Similarly, the advanced Green function can be written as follows

$$G_A(E) = \frac{1}{2\pi} \int_{-\infty}^{\infty} J(\omega) \, (e^{\omega/\theta} + 1) \, \frac{d\omega}{E - \omega - i\varepsilon} \qquad (1.62)$$

If E is assumed to be complex then $G_{R,A}(E)$ can be continued analytically in the complex E-plane, thus

$$\frac{1}{2\pi} \int_{-\infty}^{\infty} J(\omega) \, (e^{\omega/\theta} + 1) \, \frac{d\omega}{E - \omega} = \begin{cases} G_R(E) & \text{if Im } E > 0 \\ G_A(E) & \text{if Im } E > 0 \end{cases} \qquad (1.63)$$

Ommiting the indices 'R' and 'A', we can write

$$G(E) = \begin{cases} G_R(E) & \text{if Im } E > 0 \\ G_A(E) & \text{if Im } E < 0 \end{cases} \qquad (1.64)$$

where $G_{R,A}(E)$ can be considered to be two branches in the upper and lower half-planes of the complex E-plane, of the same analytic function G(E) determined by the singularity on the real axix. Interchanging E and ω in Eqs.(1.61) and (1.62) and subtracting, we obtain ∞

$$G(\omega+i\varepsilon) - G(\omega-i\varepsilon) = \frac{1}{2\pi} \int_{-\infty}^{\infty} J(E) \, (e^{E/\theta} + 1) \left(\frac{1}{\omega - E + i\varepsilon} - \frac{1}{\omega - E - i\varepsilon} \right) \qquad (1.65)$$

Using δ-function representation we may write

$$\delta(x) = \frac{1}{2\pi}\left(\frac{1}{x - i\varepsilon} - \frac{1}{x + i\varepsilon}\right) \tag{1.66}$$

to obtain

$$G(\omega+i\varepsilon)-G(\omega-i\varepsilon) = -i\int_{-\infty}^{\infty} J(E)\,(e^{E/\theta}+1)\,\delta(\omega-E)\,dE$$

$$= -iJ(\omega)\,(e^{\omega/\theta}+1) \tag{1.67}$$

Using also

$$G(\omega+i\varepsilon)-G(\omega-i\varepsilon)=2i\,\mathrm{Im}G(\omega+i\varepsilon) \tag{1.68}$$

and Eq.(1.67) we obtain the spectral density function

$$J(\omega) = -\frac{2\ \mathrm{Im}G(\omega+i\varepsilon)}{(e^{\omega/\theta}+1)} \tag{1.69}$$

It is clear that for a given G(E) we can obtain J(ω) and the correlation functions given by Eqs.(1.51 and 1.52) in the form

$$\langle B(t')A(t)\rangle = \lim_{\varepsilon\to 0}\int_{-\infty}^{\infty} -\frac{2\ \mathrm{Im}\ G(\omega+i\varepsilon)}{(e^{\omega/\theta}+1)}\ e^{-i\omega(t-t')}\,d\omega \tag{1.70}$$

Setting t=0 and using $f(\omega)=1/(e^{\omega/\theta}+1)$, we can reduce Eq.(1.70) to

$$\langle B(t')A(t)\rangle = \lim_{\varepsilon\to 0}\int_{-\infty}^{\infty} -2\ \mathrm{Im}\ G(\omega+i\varepsilon)\,f(\omega)\,e^{i\omega t}\,d\omega \tag{1.71}$$

1.4 Derivation of RPA equation for the Dynamic susceptibility

The aim of this section is to generalize the results of Wolfram, (1969) and derive an integral equation for the full dynamic susceptibility $\chi^{-+}(\omega,q_{\parallel})$ which is exact in the random phase approximation (RPA) and is valid for both the bulk ferromagnet and the ferromagnet with a surface. This equation for χ^{-+} will then be employed in chapter 3 to determine the transverse spin susceptibility χ^{RPA} for an overlayer.

We begin by deriving a matrix equation for the dynamic susceptibility which is connected to a certain two-particle Green's function. In order to calculate the two-particle Green's function, a generalized RPA is adopted to decouple the equation of motion and we assume that the electrons move in an energy band that may be described in the tight-bingding approximation.

The model we consider is a simple one-band itinerant ferromagnet which may contain impurities or surface,described by the standard Hubbard Hamitonian

$$H = \sum_{ij\sigma} E_{ij} c^{+}_{i\sigma} c_{j\sigma} + \sum_{i} U_i n_{i\uparrow} n_{i\downarrow} + \sum_{i} V_i n_{i\sigma} \qquad (1.72)$$

Where $c^{+}_{i\sigma}(c_{j\sigma})$ are the creation (annihilation) operators in the Wannier states on site $\underline{R}_i$ with spin σ and $n_{i\sigma} = c^{+}_{i\sigma} c_{i\sigma}$ is the number operator for the Wannier states.The quantities E_{ij}, U_i and V_i are the hopping integrals,

intra-atomic Coulomb interaction which is different at the surface (or impurity) and potential scattering from impurities (surface), respectively (Note that U_i is the effective interaction).

The transverse dynamic susceptibility matrix $\chi_{ij}(t)$ in the Wannier representation is defined by :

$$\chi_{ij}(t) = \langle\langle S_i^+(t) ; S_j^-(0)\rangle\rangle_R \tag{1.73}$$

where $\langle\langle \quad ; \quad \rangle\rangle_R$ denotes the retarded Green's function given by Eq(1.25) and

$$\begin{aligned} S_i^+ &= C_{i\uparrow}^+ C_{i\downarrow} \\ S_j^- &= C_{j\downarrow}^+ C_{j\uparrow} \end{aligned} \tag{1.74}$$

Or in the Bloch representation we can write the operators in Eq.(1.74) as follow (see Izuyama et al. 1963)

$$S_{-q}^+ = \sum_k C_{k\uparrow}^+ C_{k+q\downarrow} \tag{1.75a}$$

$$S_q^- = \sum_k C_{k+q_\downarrow}^+ C_{k_\uparrow} \tag{1.75b}$$

Where the operator S_q^- excites an electron in the state q with $\downarrow$-spin into a state (k+q) with $\uparrow$-spin.

In terms of two-particle Green's function, Eq.(1.73) may be writen as

$$\chi_{ij}(t) = -i\theta(t)\langle[C_{i\uparrow}^+(t)C_{i\downarrow}(t), C_{j\downarrow}^+(0)C_{j\uparrow}(0)]\rangle \tag{1.76}$$

and $\chi_{ij}(t)$ satisfies the equation of motion given by

Eq.(1.40) Izuyama et al (1963) showed that the equation of motion for $\chi_{ij}(t)$ can be solved in the RPA in closed form and for a homogenous ferromagnet.

Wolfram (1969) studied $\chi_{ij}(t)$ for a ferromagnet with an isolates impurity. He showed that it is necessary to consider a more general two-particle Green's function:

$$\begin{aligned} S_{ijkl}(t) &= \langle\langle S^{+}_{ij}(t) \; ; \; S^{-}_{kl}(0)\rangle\rangle_{R} \\ &= -i\theta(t)\langle[S^{+}_{ij}(t), S^{-}_{kl}(0)]\rangle \\ &= -i\theta(t)\langle[C^{+}_{i\uparrow}(t)C_{j\downarrow}(t), C^{+}_{k\downarrow}(0)C_{l\uparrow}(0)]_{-}\rangle \end{aligned} \qquad (1.77)$$

The susceptibility is then defined by

$$\chi_{ij}(t) = - S_{iijj}(t) \qquad (1.78)$$

Now to evaluate $S_{ijkl}(t)$ we set up its equation of motion and solve it in RPA for the simple one-band itinerant ferromagnet Hamiltonian(1.72), i.e.,

$$\begin{aligned} i\frac{d}{dt}S_{ijkl}(t) &= \delta(t)\langle[C^{+}_{i\uparrow}(t)C_{j\downarrow}(t) \; , \; C^{+}_{k\downarrow}(0)C_{l\uparrow}(0)]_{-}\rangle \\ &+ \langle\langle[C^{+}_{i\uparrow}(t)C_{j\downarrow}(t) \; , \; H]_{-} \; ; \; C^{+}_{k\downarrow}(0)C_{l\uparrow}(0)\rangle\rangle \end{aligned} \qquad (1.79)$$

To evaluate the RHS of Eq(1.79) we need the following anticommutation relations :

$$\begin{aligned} [C_{i\sigma} \; , \; C_{j\sigma'},]_{+} &= C_{i\sigma}C_{j\sigma'} + C_{j\sigma'}C_{i\sigma} = 0 \\ [C^{+}_{i\sigma} \; , \; C^{+}_{j\sigma'},]_{+} &= 0 \\ [C_{i\sigma} \; , \; C^{+}_{j\sigma'},]_{+} &= C_{i\sigma}C^{+}_{j\sigma'} + C^{+}_{j\sigma'}C_{i\sigma} = \delta_{ij}\delta_{\sigma\sigma'} \end{aligned} \qquad (1.80)$$

It is clear that when the commutator of $[C^{+}_{i\uparrow}(t)C_{j\downarrow}(t),H]_{-}$

is evaluated, the kinetic energy term and the potential scattering V_i term from the impurities (or surface) give a contribution to the commutator involving one creation and one annihilation operators which make the derivation straight forward.However, the major difficulties in dealing with the commutator $[C^+_{i\uparrow}(t)C_{j\downarrow}(t)\ ,H]_-$ arise from the presence of the intra-atomic Coulomb interaction U_i terms which contain the products of four operators, namely, two creation and two annihilation operators. This results in a term in the equation of motion (1.79) involving an average of six operators, making it extremely difficult task to try to find an exact solution for this Hamiltonian .

In order to terminate the hierarchy of the Green's function equations and to obtain a closed equation for our two-particle function $S_{ijkl}(t)$, it is necessary to make an approximation method which produce adequate solutions for a particular purpose. The RPA which we now develop provides such an approximation. The RPA is based on the following decoupling of the four-operator term at the time t:

$$\langle c_i^+ c_j c_k^+ c_l \rangle \xrightarrow{\text{RPA}} \langle c_i^+ c_j \rangle c_k^+ c_l + \langle c_k^+ c_l \rangle c_i^+ c_j - \langle c_i^+ c_l \rangle c_k^+ c_j - \langle c_k^+ c_j \rangle c_i^+ c_l \qquad (1.81)$$

We note that all Green function techniques treat the kinetic energy part and the potential part of the Hubbard Hamiltonian (1.72) exactly while approximating the interaction part. It is clear that our two-particle function $S_{ijkl}(t)$ depend strongly on the model which we consider, i.e., the on form of Hamiltonian H.

Here we shall deal with two cases:

(1) pure crystal (or unperturbed ferromagnet) having a single-band Hubbard Hamiltonian (Hubbard 1963)

$$H = \sum_{ij\sigma} E_{ij} c^{+}_{i\sigma} c_{j\sigma} + \sum_{i} U n_{i\uparrow} n_{i\downarrow} \tag{1.82}$$

Where U an interaction parameter which is constant across the system.

(2) Crystal with a surface at R_z=a (see Asadi, 1980) having a simple one-band Hamiltonian defined by Eq.(1.72) where the parameter U_i may be different in the surface plane R_z=a, i.e,

$$U_i = \begin{cases} U & \text{if } R_\perp \neq a \\ U + \Delta U & \text{if } R_\perp = a \end{cases} \tag{1.83}$$

Decoupling the four operator terms in the commutator in the RPA and taking into account the fact that the average product of up and down-spin operators are zero, we obtain the following equation of motion:

$$i\frac{d}{dt}\hat{S}_{ijkl}(t) = \delta(t)\hat{D}_{ijkl} + \sum_{m,n}(K_{ijmn} + W_{ijmn} + J_{ijmn} + j_{ijmn})S_{mnij} \tag{1.84}$$

We shall now Fourier transform this equation using

$$S(\omega) = \int_{-\infty}^{\infty} dt S(t) e^{i\omega t} \tag{1.85}$$

Where

$$S(t) = \frac{1}{2\pi}\int_{-\infty}^{\infty} d\omega S(\omega) e^{-i\omega t} \tag{1.86}$$

Therefore we obtain a matrix equation

$$\omega\hat{S}(\omega) = (\hat{K} + \hat{W} + \hat{J} + \hat{j})\hat{S}(\omega) + \hat{D} \qquad (1.87)$$

Where $\hat{K},\hat{W},\hat{J},\hat{j}$ are the generalized matrices depending on four indices and the matrix multiplication for such generalized matrices is defined by:

If $A = B.C$

then
$$\hat{A}_{ijkl} = \sum_{m,n} \hat{B}_{ijmn}\,\hat{C}_{mnkl} \qquad (1.88a)$$

and the unit matrix has components $\hat{I}_{ijkl} = \delta_{ik}\delta_{jl}$ (1.88b)

For arbitrary potentials V_i and U_i, the generalized matrices K, J and D are found to be:

$$\hat{K}_{ijkl} = E_{lj}\delta_{ik} - E_{ik}\delta_{lj} \qquad (1.89a)$$

$$\hat{J}_{ijkl} = U\,\delta_{kl}\{\,\delta_{ik}\langle c_{i\downarrow}^{+}c_{j\downarrow}\rangle - \delta_{jl}\langle c_{i\uparrow}^{+}c_{j\downarrow}\rangle\,\} \qquad (1.89b)$$

$$\hat{D}_{ijkl} = \delta_{jk}\langle c_{i\uparrow}^{+}c_{l\uparrow}\rangle - \delta_{il}\langle c_{k\downarrow}^{+}c_{j\downarrow}\rangle \qquad (1.89c)$$

On the other hand, the expressions for the generalized matrices $\hat{W}$ and $\hat{j}$ depend upon the system we are dealing with.

(1) For a pure infinite crystal, we find that:

$$\hat{j}_{ijkl} = 0 \qquad (1.90a)$$

and

$$\hat{W}_{ijkl} = \delta_{ik}\delta_{jl}\delta_{ij}\,[U(\langle n_{i\uparrow}\rangle - \langle n_{j\downarrow}\rangle)] \qquad (1.90b)$$

(2) For a system with a surface at $R_z = a$, we can generalize the results of Wolfram (1969) to our surface problem to obtain:

$$\hat{J}_{ijkl} = \Delta U\ \delta_{kl}[\delta_{ik}\delta_{li_\perp}\langle c^+_{i\downarrow} c_{j\downarrow}\rangle - \delta_{jl}\delta_{lj_\perp}\langle c^+_{i\uparrow} c_{j\downarrow}\rangle] \quad (1.91a)$$

$$\hat{W}_{ijkl} = \hat{V}_{ijkl\downarrow} - \hat{V}_{ijkl\uparrow} \quad (1.91b)$$

where

$$\hat{V}_{ijkl\uparrow} = \delta_{ik}\delta_{lj}\ [U\langle n_{j_\downarrow}\rangle + [\Delta U\langle n_{j_\downarrow}\rangle \delta_{lj_\perp} + V\delta_{aj_\perp}] \quad (1.92a)$$

$$\hat{V}ijkl\downarrow = \delta_{ik}\delta_{lj}\ [U\langle n_{i_\uparrow}\rangle + [\Delta U\langle n_{i_\uparrow}\rangle \delta_{li_\perp} + V_{ai_\perp}] \quad (1.92b)$$

and
$$\delta_{li_\perp} = \begin{cases} 1 \text{ if } R^l_\perp = R^l_\perp \\ 0 \text{ if } R^l_\perp \neq R^l_\perp \end{cases} \quad (1.92c)$$

For both the cases considered, we have a formal solution of Eq.(1.87) in the form

$$\hat{S}(\omega) = (\omega I - \hat{K} - \hat{W} - \hat{J} - \hat{j}).\hat{D}^{-1} \quad (1.93)$$

where I is the unit matrix.

To solve Eq.(1.93) explicitly, we let

$$\hat{S}^{(1)}(\omega) = [\omega I - (\hat{K}+\hat{W})].\hat{D}^{-1} \quad (1.94)$$

Using the standard Dyson's equation

$$[\omega I - (A+B)]^{-1} = (\omega I - A)^{-1} + (\omega I - A)^{-1}.B.[\omega I - (A+B)]^{-1},$$

we have

$$[\omega\hat{I} - \{(\hat{K}+\hat{W}) + (\hat{J}+\hat{j})\}]^{-1}.\hat{D} = [\omega\hat{I} - (\hat{K}+\hat{W})]^{-1}.\hat{D} + [\omega\hat{I} - (\hat{K}+\hat{W})]^{-1}.$$

$$\hat{D}\ \hat{D}^{-1}(\hat{J}+\hat{j})[\omega\hat{I} - (\hat{K}+\hat{W}+\hat{J}+\hat{j})]^{-1}\ \hat{D} \quad (1.95)$$

so that

$$\hat{S}(\omega) = \hat{S}^{(1)}(\omega) + \hat{S}^{(1)}(\omega)[\hat{D}(\hat{J}+\hat{j})]\hat{S}(\omega) \quad (1.96)$$

Now setting $\hat{P} = \hat{D}^{-1}(\hat{J}+\hat{j})$ to satisfy $\hat{D}\hat{P} = \hat{J}+\hat{j}$, we find:

(1) For an infinite isotropic ferromagnet j=0 and P is given by

$$P_{ijkl} = -U\,\delta_{il}\,\delta_{ik}\,\delta_{jk} \tag{1.97a}$$

and

$$[S(\omega)]_{ijkl}=[S^{(1)}(\omega)]_{ijkl}-U\sum_{m,n}[S^{(1)}(\omega)]_{ijmn}[S(\omega)]_{mnkl} \tag{1.97b}$$

(2) For the surface problem, we can generalize Wolfram's result to obtain

$$P_{ijkl} = -U\,\delta_{il}\delta_{ik}\delta_{jk} - \Delta U\delta_{il}\delta_{jk}\delta_{ij}\delta_{ij_\perp} \tag{1.98a}$$

and

$$[S(\omega)]_{ijkl}=[S^{(1)}(\omega)]_{ijkl}-U\sum_{m,n}[S^{(1)}(\omega)]_{ijmn}[S(\omega)]_{mnkl} - \Delta U\,[S^{(1)}(\omega)]_{i_\perp j_\perp 11}\,[S(\omega)]_{11K_\perp l_\perp} \tag{1.98b}$$

Now returning to the susceptibility $\chi_{ij}(\omega)=-S_{iijj}(\omega)$ we can write Eqs(1.97b) and (1.98b) in the universal form

$$\chi_{ij}(\omega) = \chi^{HF}_{ij}(\omega) + \sum_m \chi^{HF}_{im}(\omega)\,U_m\,\chi_{mj}(\omega) \tag{1.99}$$

which is exact in the RPA and valid both for the bulk and semi-infinite ferromagnets (Wolfram 1969, Gumbs and Griffin 1980 and Mathon 1981)

Since we shall deal with a surface problem the translational symmetry in the direction parallel to the surface is preserved and the wave vector $q_\parallel$ is a good quantum number.It is, therefore, convenient to use the mixed Bloch-Wannier representation (see Mills et al. 1972)

$\chi_{ij} \equiv \chi_{ij}(q_\parallel,\omega)$ where i,j label the planes parallel to the surface. Eq(1.99) may be then written as follows:

$$\chi_{ij}(q_\parallel,\omega) = \chi^{HF}_{ij}(q_\parallel,\omega) + \sum_m \chi^{HF}_{im}(q_\parallel,\omega)\ U_m\ \chi_{mj}(q_\parallel,\omega) \qquad (1.100)$$

The kernel $\chi^{HF}_{ij}(q_\parallel,\omega)$ is the transverse unenhanced susceptibility of non-interacting electrons moving in a spin dependent HF potential:

$$V_{i\sigma} = V_i + U_i\langle n_{i,-\sigma}\rangle \qquad (1.101)$$

where

$$V_i = \begin{cases} V & \text{at the surface} \\ 0 & \text{in the bulk} \end{cases} \qquad (1.102)$$

and $U_i\langle n_{i,-\sigma}\rangle$ is the HF exchange potential. For a semi-infinite ferromagnet, this HF exchange potential is highly inhomogenous since both U_i and $\langle n_{i,-\sigma}\rangle$ vary near the surface. As a result, the kernel χ^{HF} is an essentially off-diagonal matrix both in the Wannier and Bloch representations (Mathon, 1981). Thus, direct solution of Eq.(1.100) with the exact kernel χ^{HF} is equivalent to the inversion of an infinite matrix and is therefore not feasible.

However, as we shall show later in chapter 3 that a solution of Eq.(1.100) which is exact in RPA can be obtained for a magnetic overlayer.

Eq.(1.100), which is the fundamental formula for calculating spin wave energies in transition metals, was derived earlier by Mills et al (1972) in the paramagnetic case in an approximation which replaced the kernel $\chi^{HF}(\omega,q_\parallel)$

by the response function of non-interacting electrons in an infinite paramagnet.

For a semi-infinite ferromagnet, Griffin and Gumb (GG) (1976,1980) replaced the kernel χ^{HF} in the so-called classical infinite barrier model (CIBM) in which they found a surface spin wave mode split-off above the bulk spin wave band as $q_{\parallel} \rightarrow 0$. More discussion on the work of GG will be given later on chapter 3.

Before we apply Eq.(1.100) to an overlayer, let us review briefly the situation for an infinite ferromagnet. Since $U_m = U$ = constant and all the matrices in Eq(1.100) are diagonal, we can write Eq.(1.100) in the form:

$$\chi^{-+}(q,\omega) = \chi^{HF}(q,\omega) + \chi^{HF}(q,\omega)\ U\ \chi^{-+}(q,\omega) \qquad (1.103a)$$

or

$$\chi^{-+}(q,\omega) = \frac{\chi^{HF}(q,\omega)}{1 - U\,\chi^{HF}(q,\omega)} \qquad (1.103b)$$

Eq.(1.103b) is the standard formula for the dynamic susceptibility which was obtained by Izuyama, Kim and Kubo (1963). It folows from the structure of Eq(1.103b) that $\chi^{-+}(q,\omega)$ has two types of poles

(i) poles arise out of the singularities of $\Gamma = \chi^{HF}(q,\omega)$ which is given in Bloch representation by (see Mattis, 1964)

$$\Gamma = \sum_{K} \frac{f_{K\uparrow} - f_{K+q\downarrow}}{\varepsilon_{K+q} - \varepsilon_{K} + \Delta - \hbar\omega + i\delta} \qquad (1.104)$$

These are called single-particle or Stoner excitations; (ii) other type of poles arise from the zero of the denominator $1-U\chi^{HF}(q,\omega)$ at some real ω for a given q. If a

real ω is found then this pole would correspond to an undamped spin wave mode, if ω is complex then the mode will be damped. In fact, the kernel χ^{HF} is usually considered to be complex function but the spin wave excitation energy is given as the energy at which the real part of the denominator vanishes, i.e.,

$$1 - \text{Re}\ \chi^{HF}(q,\omega) = 0 \qquad (1.105a)$$

To clarify this expression, we can use Eq.(1.103b) to write

$$\text{Im}\ \chi^{-+}(\omega, q_{\parallel}) = -\frac{1}{U} \frac{(U\Gamma'')}{(1-U\Gamma')^2 + (U\Gamma'')^2} \qquad (1.105b)$$

where the functions $\Gamma'$and Γ'' are respectively the real and imaginary parts of Γ given by Eq.(1.105b) which have the form:

$$\Gamma' = \sum_{K} \frac{f_{K\uparrow} - f_{K+q\downarrow}}{\varepsilon_{K+q} - \varepsilon_{K} + \Delta - \hbar\omega} \qquad (1.106a)$$

and

$$\Gamma'' = -\pi \sum_{K} \frac{(f_{K\uparrow} - f_{K+q\downarrow})\ \delta}{(\varepsilon_{K+q} - \varepsilon_{K} + \Delta - \hbar\omega)^2 + \delta^2}$$

$$= -\pi \sum_{K} (f_{K\uparrow} - f_{K+q\downarrow})\ \delta(\varepsilon_{K+q} - \varepsilon_{K} + \Delta - \hbar\omega) \qquad (1.106b)$$

Here δ is the Dirac delta function which enforces $\Gamma'' \neq 0$ only when spin wave spectrum is inside Stoner continum. It follows that spin wave modes are delta function poles outside the continum hence $\Gamma'' = 0$ in the region where spin waves exist.

Outside the Stoner band, $\varepsilon_{K+q\downarrow} - \varepsilon_{K\downarrow} + \Delta - h\omega \neq 0$, thus we get

$$\Gamma'' \propto \delta \tag{1.106c}$$

It follows from Eq.(1.105b) that

$$\text{Im}\ \chi^{-+}(\omega, q_{\parallel}) = \frac{\pi}{U}\,\delta(1 - U\Gamma') \tag{1.107}$$

In the next section we shall show how the kernel χ^{HF} can be expressed in terms of the HF one-electron Green functions for the surface problem.

1.5 Properties of the Hartree-Fock transverse susceptibility

In this section we shall obtain an expression for the HF transverse susceptibility $\chi^{HF}_{ij}(q_{\parallel},\omega)$ that appears in Eq.(1.103b), and is needed for solving the dynamic susceptibility $\chi^{-+}(q_{\parallel},\omega)$. The kernel $\chi^{HF}(q_{\parallel},\omega)$ can be quite generally expressed (Wolfram, 1969) in terms of HF one-electron Green's function $G^{\sigma}_{ij}(t)$ in the Wannier representation

$$\chi^{HF}_{ij}(t)=<c^{+}_{i\uparrow}(t)c_{j\downarrow}(0)>G^{\downarrow}_{ij}(t)+<c^{+}_{j\downarrow}(0)c_{i\downarrow}(t)>G^{*\uparrow}_{ij}(t) \qquad (1.108)$$

Following Mills et al.(1972) and Gumbs and Griffin (1980) we can write the kernel in the Wannier representation as:

$$\chi^{HF}_{ij}(\omega)=\int_{-\infty}^{\infty}\int_{-\infty}^{\infty}d\Omega_1 d\Omega_2 \frac{[f(\Omega_1)-f(\Omega_2)]}{\omega+i\delta-(\Omega_1-\Omega_2)} A^{\uparrow}_{ij}(\Omega_1)\, A^{\downarrow}_{ij}(\Omega_2) \qquad (1.109)$$

where $f(\Omega)$ is the Fermi-Dirac function and $A^{\sigma}_{ij}(\Omega)$ is the single particle spectral density in the Wannier representation defined by

$$A^{\sigma}_{ij}(\Omega) = -\frac{1}{\pi}\,\mathrm{Im}G^{\sigma}_{ij}(\Omega+i\delta) \qquad (1.110)$$

Substituting Eq(1.110) into Eq(1.109) we obtain

$$\chi^{HF}_{ij}(\omega) = \frac{1}{\pi^2}\int_{-\infty}^{\infty}\int_{-\infty}^{\infty}d\Omega_1 d\Omega_2 \frac{[f(\Omega_1)-f(\Omega_2)]}{(\omega-\Omega_1+\Omega_2)+i\delta}\,\mathrm{Im}G^{\downarrow}_{ij}(\Omega_1)\,\mathrm{Im}G^{\uparrow}_{ij}(\Omega_2) \qquad (1.111)$$

Using the identity

$$\frac{1}{x\pm i\delta} = P\frac{1}{x} \mp i\pi\delta(x) \qquad (1.112)$$

We can write Eq(1.111) as follow :

$$\chi_{ij}^{HF}(\omega) = P \frac{1}{\pi^2} \int_{-\infty}^{\infty}\int_{-\infty}^{\infty} d\Omega_1 d\Omega_2 \, [f(\Omega_1)-f(\Omega_2)] \, \frac{\mathrm{Im}G_{ij}^{\downarrow}(\Omega_1)\,\mathrm{Im}G_{ij}^{\uparrow}(\Omega_2)}{\omega - \Omega_1 + \Omega_2}$$

$$- \frac{i}{\pi} \int_{-\infty}^{\infty}\int_{-\infty}^{\infty} d\Omega_1 d\Omega_2 \, [f(\Omega_1)-f(\Omega_2)] \, \delta(\omega-\Omega_1+\Omega_2)\,\mathrm{Im}G_{ij}^{\downarrow}(\Omega_1)\,\mathrm{Im}G_{ij}^{\uparrow}(\Omega_2)$$

$$= \mathrm{Re}\,\chi_{ij}^{HF}(\omega) + i\,\mathrm{Im}\,\chi_{ij}^{HF}(\omega) \qquad (1.113)$$

We shall now derive expressions for Re $\chi_{ij}^{HF}(\omega)$ and Im $\chi_{ij}^{HF}(\omega)$ in terms of the HF one-electron Green's functions.

1.5.1 Equation for Re$\chi_{ij}^{HF}(\omega, q_{\parallel})$

We can separate the first part of Eq(1.113) into two parts:

$$\mathrm{Re}\,\chi_{ij}^{HF}(\omega) = \mathrm{Re}\,\chi_{(1)}^{HF} + \mathrm{Re}\,\chi_{(2)}^{HF} \qquad (1.114)$$

where

$$\mathrm{Re}\,\chi_{(1)}^{HF} = \frac{1}{\pi} \int_{-\infty}^{\infty} d\Omega_1 f(\Omega_1)\,\mathrm{Im}G_{ij}^{\downarrow}(\Omega_1) \left\{ - P \frac{1}{\pi} \int_{-\infty}^{\infty} d\Omega_2 \frac{\mathrm{Im}G_{ij}^{\uparrow}(\Omega_2)}{(\Omega_1-\omega) - \Omega_2} \right\}$$

$$= - \frac{1}{\pi} \int_{-\infty}^{\infty} d\Omega_1 f(\Omega_1) \; \mathrm{Im}G_{ij}^{\downarrow}(\Omega_1)\,\mathrm{Re}G_{ij}^{\uparrow}(\Omega_1-\omega) \qquad (1.115)$$

and similarly,

$$\mathrm{Re}\,\chi_{(2)}^{HF} = - \frac{1}{\pi} \int_{-\infty}^{\infty} d\Omega_2 f(\Omega_2) \; \mathrm{Im}G_{ij}^{\uparrow}(\Omega_2) \; \mathrm{Re}G_{ij}^{\downarrow}(\omega + \Omega_2) \qquad (1.116)$$

Note that we have used the Kramer-Kronig relations in

obtaining Eqs.(1.115) and (1.116), i.e.,

$$\text{Re } G^{\sigma}_{ij}(\Omega) = P\frac{1}{\pi}\int_{-\infty}^{\infty} d\Omega' \frac{\text{Im } G^{\sigma}_{ij}(\Omega')}{\Omega - \Omega'} \qquad (1.117)$$

Adding (1.115) and (1.116) we get

$$\text{Re } \chi^{HF}_{ij}(\omega) = -\frac{1}{\pi}\int_{-\infty}^{\infty} d\Omega_2\ f(\Omega_2)\ \text{Im}G^{\uparrow}_{ij}(\Omega_2)\ \text{Re}G^{\downarrow}_{ij}(\Omega_2 + \omega)$$

$$-\frac{1}{\pi}\int_{-\infty}^{\infty} d\Omega_1 f(\Omega_1)\ \text{Im}G^{\downarrow}_{ij}(\Omega_1)\ \text{Re}G^{\uparrow}_{ij}(\Omega_1 - \omega) \qquad (1.118)$$

Since we are interested only in the ground state ($T=0^{\circ}K$) the Fermi function has the value 0 or 1 depending upon whether Ω is above or below the Fermi energy E_F. We can now write in the mixed Bloch-Wannier representation (see section 2.1).

$$\text{Re } \chi^{HF}_{ij}(q_{\parallel},\omega) = -\frac{1}{\pi N_{\parallel}}\sum_{K_{\parallel}}\int_{-\infty}^{E_F} d\Omega\ \text{Im}G^{\uparrow}_{ij}(\Omega,q_{\parallel})\text{Re}G^{\downarrow}_{ij}(K_{\parallel}+ q_{\parallel}+G,\Omega + \omega)$$

$$+\ \text{Im}G^{\downarrow}_{ij}(\Omega,q_{\parallel})\text{Re}G^{\uparrow}_{ij}(K_{\parallel}+ q_{\parallel}+G,\Omega - \omega) \qquad (1.119)$$

where $q_{\parallel}$ is the wave vector from the first Brillouin Zone and the sum $(K_{\parallel}+ q_{\parallel}+ G)$ is used to bring the vector $(K_{\parallel}+ q_{\parallel})$ lies within the first Brillouin Zone (Umklapp process); and G is the reciprocal lattice vector.

It should be noted that for a very strong ferromagnet the contribution from the second term in Eq.(1.119) vanishes since $\text{Im}G^{\downarrow}_{ij}=0$ above the Fermi level E_F.

1.5.2 Equation for Im $\chi_{ij}^{HF}(\omega, q_{\parallel})$

Splitting the second part of Eq(1.113) into two terms, we obtain

$$\text{Im } \chi_{ij}^{HF}(\omega) = \text{Im } \chi_{(1)}^{HF} + \text{Im } \chi_{(2)}^{HF} \qquad (1.120)$$

where

$$\text{Im } \chi_{(1)}^{HF} = -\frac{1}{\pi} \int_{-\infty}^{\infty}\int_{-\infty}^{\infty} d\Omega_1 d\Omega_2 f(\Omega_1)\delta(\omega-\Omega_1+\Omega_2)\ \text{ImG}_{ij}^{\downarrow}(\Omega_1)\,\text{ImG}_{ij}^{\uparrow}(\Omega_2)$$

$$= -\frac{1}{\pi}\int_{-\infty}^{\infty} d\Omega_1 f(\Omega_1)\,\text{ImG}_{ij}^{\downarrow}(\Omega_1)\int_{-\infty}^{\infty}\delta(w-\Omega_1+\Omega_2)\,\text{ImG}_{ij}^{\uparrow}(\Omega_2)\,d\Omega_2$$

$$= -\frac{1}{\pi}\int_{-\infty}^{\infty} d\Omega_1 f(\Omega_1)\,\text{ImG}_{ij}^{\downarrow}(\Omega_1)\,\text{ImG}_{ij}^{\uparrow}(\Omega_1 - \omega) \qquad (1.121)$$

where

$$\int_{-\infty}^{\infty}\delta(x-a)f(x) = f(a) \quad \text{has been used}$$

and

$$\text{Im } \chi_{(2)}^{HF} = \frac{1}{\pi}\int_{-\infty}^{\infty} d\Omega_1 d\Omega_2 f(\Omega_2)\delta(\omega - \Omega_1 + \Omega_2)\,\text{ImG}_{ij}^{\downarrow}(\Omega_1)\,\text{ImG}_{ij}^{\uparrow}(\Omega_2)$$

$$= \frac{1}{\pi}\int_{-\infty}^{\infty} d\Omega_2 f(\Omega_2)\,\text{ImG}_{ij}^{\uparrow}(\Omega_2)\int_{-\infty}^{\infty}\delta(\Omega_1 - (\omega + \Omega_2))\ \text{ImG}_{ij}^{\downarrow}(\Omega_1)\,d\Omega$$

$$= \frac{1}{\pi}\int_{-\infty}^{\infty} d\Omega_2 f(\Omega_2)\,\text{ImG}_{ij}^{\uparrow}(\Omega_2)\,\text{ImG}_{ij}^{\downarrow}(\Omega_2 + \omega) \qquad (1.122)$$

Combining Eqs(1.121) and (1.122) we obtain

$$\text{Im } \chi_{ij}^{HF}(\omega) = \frac{1}{\pi}\int_{-\infty}^{\infty} d\Omega_2\ f(\Omega_2)\,\text{ImG}_{ij}^{\uparrow}(\Omega_2)\ \text{ImG}_{ij}^{\downarrow}(\Omega_2 + \omega)$$

$$- \frac{1}{\pi} \int_{-\infty}^{\infty} d\Omega_1 f(\Omega_1) \mathrm{Im}G_{ij}^{\downarrow}(\Omega_1) \mathrm{Im}G_{ij}^{\uparrow}(\Omega_1 - \omega) \qquad (1.123)$$

Assuming again zero temperature and using the mixed Bloch-Wannier representation we arrive at

$$\mathrm{Im}\,\chi_{ij}^{HF}(q_\parallel,\omega) = \frac{1}{\pi N_\parallel} \sum_{K_\parallel} \int_{-\infty}^{E_F} d\Omega\ \mathrm{Im}G_{ij}^{\uparrow}(\Omega,q_\parallel)\ \mathrm{Im}G_{ij}^{\downarrow}(K_\parallel + q_\parallel, \Omega + \omega)$$

$$-\mathrm{Im}G_{ij}^{\downarrow}(\Omega,q_\parallel)\mathrm{Im}G_{ij}^{\uparrow}(K_\parallel + q_\parallel, \Omega - \omega) \qquad (1.124)$$

The imaginary part of $\chi_{ij}^{HF}(q_\parallel,\omega)$ determines the spin wave relaxation time for decay into the Stoner excitations, and

$$\lim_{q_\parallel \to 0} \mathrm{Im}\,\chi_{ij}^{HF}(q_\parallel,\omega) \longrightarrow 0$$

(for small $q_\parallel$) so that in the RPA long-wave length (low-frequency ω) spin waves are undamped.

CHAPTER 2

METHODS FOR CALCULATING THE GROUND-STATE ELECTRON GREEN'S FUNCTION OF A SEMI-INFINITE CRYSTAL

2.Introduction

There has been considerable amount of effort, both theoretical and experimental, to gain understanding of the electronic properties of surfaces from the fundamental point of view. It is shown in the literature that, the tight-binding (TB) or linear-combination-of-atomic-orbital (LCAO) formalism is the simplest and most useful method for studying the electronic structure of transition metals.

Compared to LCAO, local-spin-density-functional (LSDF) method is a more reliable method for calculating from the first principal the ground-state properties of transition metals (see e.g. Kohn and Sham 1965, Rajagopal 1980). However, LSDF can not be used to study excited states such as spin waves and it is also unsuitable for complicated multilayers;the computationally effort involve in LSDF is too big to handle even on fastest computers. We shall therefore employ the LCAO formalism in the present thesis.

Several techniques are used in the LCAO-TB formalism to study the surface problem.Among these techniques, the most powerful is the formalism which is known as the Green's function (or resolvent) technique. For an infinite crystal, this technique starts with the Green's function and the

surface is regarded as a perturbation. With the aid of the Green's function method quantities such as the local density of states (LDOS) can be readily determined. Several methods have been developed to calculate the LDOS within the tight-binding formalism. In particular, we can mention the recursion method (RM) of Haydock et al (1972);the method of moment (MM) of Cyrot-Lackmann (1973,1975); resolvent method of Kalkstein and Soven (1971); the transfer matrix methods of Falicov and Yndurain (1975); Lee and Joannopoulos (1981a,b) and Lopez Sancho et al (1985). Finally, Mathon and coworkers (1988a,1988b,1989) have recently developed a new version of the recursion method and we shall called it the method of adlayers.

Both (RM) and (MM) make use of large clusters surrouding an atomic site under study and the size of the cluster is determined from the requirement that the LDOS should reach a stable value.

In constrast to both these methods, Kalkstein and Soven (KS) had taken advantage of the plannar translational symmetry to construct their Green function using the mixed Bloch-Wannier representation. They solve directly for the surface Green's function. This allows them to calculate directly the LDOS for each layer in the crystal. The advantage of their method is that their formalism is very simple and convenient and that their result are exact. The disadvantages are that they take into account surface perturbations at only a few atomic layers and it would be very difficult to calculate the LDOS for realistic degenerate bands.

Lopez Sancho et al (1985) have developed a new version of the transfer matrix method based on the decimation technique, which is formulated with the help of a principal layer concept. In their method a stack of atomic layers can be mapped on a chain of atoms separated by equal distances.

Their important new idea is that they eliminate the two nearest-neighbours of each atom and replace the original chain by an effective chain of atoms with double the distance between the atoms. In this process both the on-site energies and the hopping integrals are renormalized. This step can be repeated until the effective interactions between atoms are as weak as one wishes.The advantage of their method is that LDOS of the bulk and surface are easily obtained and the method is readily applicable to realistic degenerate bands.

From the discussion above, it is obvious that the method of Sancho et al works only for a system consisting of atomic planes which all have the same properties. For an inhommogenous system the method is not directly applicable.

Another disadvantage of all the traditional recursion methods (see e.g. Haydock 1982; Lopez Sancho et al 1985 and references therein) is that they are iterative and give only an approximate Green's function. In surface applications, the RM and MM methods require long computing times since they do not take advantage of the translational symmetry in the surface plane.

In the applications described in section 2.3 an exact rather than approximate Green's function is required. We have, therefore, developed a new version of the recursion method which gives the exact surface Green's function for an arbitrary overlayer. We shall also describe the computational methods required to generate the Green's functions in every other layer of the overlayer.

In this chapter, we explain our new recursion method for calculating the one-electron Green function in magnetic surfaces and multilayers. The LDOS of the surface layer of an overlayer and also all the LDOS of very atomic layer in the overlayer will be calculated for an s-band tight-binding crystal with nearest-neighbour hopping. In constrast to Lopez Sancho et al's transfer matrix method the perturbations present in each atomic layer of an overlayer can be arbitrary.

Our method can be immediately generalized to multiple band structure; this is achieved using the concept of principal layers (see Lee and Joannopuolos 1981). This states that any layer structure with an arbitrary orientation of its atomic planes and with an arbitrary range of interactions both between and within the planes and with only number of atomic orbitals is always equivalent to a simple stack of (100) principal layers coupled by an effective nearest-neighbour interaction. This means that we can restrict ourselves, without loss of generality, to a simple cubic tight-binding band with nearest-neighbour hopping integrals.

The plan of chapter 2 is as follows : First the KS formalism for a simple cubic (100) surface with a localized perturbation will be briefly given in section 2.1. The formalism is revisited for the purpose of introducing necessary notation and,above all, because our overlayer system sits on top of a nonmagnetic substrate. This substrate can either be generated by KS formalism or by transfer matrix method. The concept of transfer matrix method will then be discussed in section 2.2. Finally, in section 2.3 our new recursion method will be discribed in detail.

2.1 Kalkstein and Soven Method Revisited

The purpose of this section is to introduce the notation and the fundamental concepts necessary to develope our thery in section 2.3. Thus the Kalkstein and Soven (KS) formalism will be briefly described.

We shall start with a perfect (infinite) crystal and denote by H^0 its Hamiltonian. We generate artificially two semi-infinite (cleaved) crystals by passing an imaginary cleavage plane in some crystallographic direction of the perfect crystal (see Fig.4.)

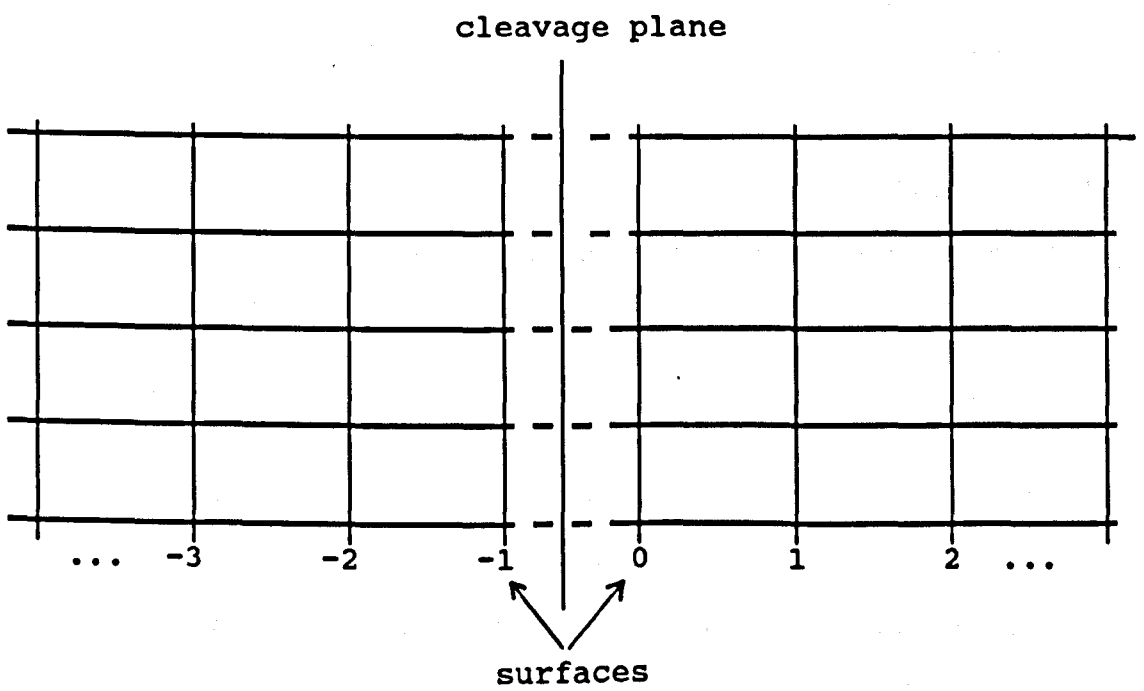

Fig.4. Two surfaces are created by cutting a perfect crystal.

If H is the one-electron Hamiltonian of these two semi-infinite crystals then

$$H = H^0 + V \qquad (2.1)$$

where V is the perturbation to an infinite crystal due to creation of both surfaces, i.e.,

$$V = H - H^{\circ} \qquad (2.2)$$

Let

$$(E+i\delta-H)G = 1 \qquad (2.3)$$

be the equation which defines the Green's function of a semi infinite crystal with a surface described by the Hamiltonian H and let the corresponding equation for a perfect crystal be

$$(E+i\delta-H^{\circ})G^{\circ} = 1 \qquad (2.4)$$

Here E is the energy and δ is a positive infinitesimal.

The Green's operators G and G° are related by the Dyson equation

$$G = G^{\circ} + G^{\circ}VG \qquad (2.5)$$

In the tight-binding approximation, the Green's function matrix elements are described in the atomic site representation. The general coordinate of an atomic site on the nth plane is defined by

$$\underline{R} = n\underline{d} + \underline{R}_{\parallel} \qquad (2.6)$$

where $\underline{R}_{\parallel}$ is a general translational vector parallel to the surface; $\underline{d}$ is a vector normal to the surface; the integer n labels the planes paralell to the surface. For consistency, we call the semi-infinite crystal with n = 0,1,2,3,... the right-surface whereas n = -1,-2,-3,... corresponding the left surface (see Fig.4).

Let $|\underline{R}\rangle$ denote a localized function centred on a lattice site $\underline{R}$. We then have

$$\langle\underline{R}|H|\underline{R}'\rangle = 0 \qquad (2.7)$$

whenever R $\in$ right surface and R′ $\in$ left surface or $\underline{R}$ $\in$ left surface and R′ $\in$ right surface. It follows that

$$\langle \underline{R}|V|\underline{R}'\rangle = - \langle \underline{R}|H^{\circ}|\underline{R}'\rangle \tag{2.8}$$

We further assume that when both R and R′ are on the same side of the cleavage plane,

$$\langle R|V|R'\rangle = \langle R|U|R'\rangle \tag{2.9}$$

is known and U denotes the difference between the potentials in the cleaved and uncleaved crystals. Since there is translational symmetry in the direction paralell to the surface, the wave vector paralell to the surface $K_{\parallel}$, is a good quantum number.It is, therefore ,convenient to introduce the mixed Bloch-Wannier representation by the following two-dimensional Bloch-sum

$$|K_{\parallel},n\rangle = (N_{\parallel})^{-1/2} \sum_{\underline{R}_{\parallel}} |n\underline{d} + \underline{R}_{\parallel}\rangle e^{i\underline{K}_{\parallel}\underline{R}_{\parallel}} \tag{2.10}$$

where $N_{\parallel}$ is the number of atoms in the surface plane. These functions are Wannier-like in the direction normal to the surface and Bloch-type parallel to it. Obviously $|K_{\parallel},n\rangle$ is localized around the nth plane parallel to the surface.In this representation G, G° and V will be diagonal in the wave vector index $\underline{K}_{\parallel}$, and we have

$$\begin{aligned}
\langle m,\underline{K}_{\parallel}|G^{\circ}|n,\underline{K}'_{\parallel}\rangle &= \delta(\underline{K}_{\parallel}-\underline{K}'_{\parallel})\ G^{\circ}(m-n,\underline{K}_{\parallel}) \\
\langle m,\underline{K}_{\parallel}|G|n,\underline{K}'_{\parallel}\rangle &= \delta(\underline{K}_{\parallel}-\underline{K}'_{\parallel})\ G(m,n,\underline{K}_{\parallel}) \\
\langle m,\underline{K}_{\parallel}|V|n,\underline{K}'_{\parallel}\rangle &= \delta(\underline{K}_{\parallel}-\underline{K}'_{\parallel})\ V(m,n,\underline{K}_{\parallel})
\end{aligned} \tag{2.11}$$

Omitting the explicit $\underline{K}_{\parallel}$ dependence, the matrix equation of Eq.(2.5) becomes

$$G(m,n) = G^{\circ}(m,n) + \sum_{p,q} G^{\circ}(m,p)V(p,q)G(q,n) \qquad (2.12)$$

We assume that

$$\langle R|H^{\circ}|R'\rangle = \begin{cases} E_o & \text{if } \underline{R} = \underline{R}' \\ T & \text{if } \underline{R} = \underline{R}' \pm 1 \\ 0 & \text{otherwise} \end{cases} \qquad (2.13)$$

(The standard tight-binding approximation for infinite crystal)

Here E_o is the middle of the bulk band and T is the nearest-neighbour hopping integral for the perfect crystal. Both E_o and T are kept as adjustable parameters.

We further assume

$$\langle R|U|R'\rangle = \begin{cases} U_o & \text{if } R = R' = \text{site on surface plane} \\ 0 & \text{otherwise} \end{cases} \qquad (2.14)$$

The implication of Eqs.(2.13) and (2.14) is that the only nonzero elements in V(m,n) are V(0,0), V(-1,0), V(0,-1) and V(-1,-1). Thus with the help of G(-1,m) = 0 for all $m \geq 0$, we write Eq(2.12) as follows

$$G(m,n) = G^{\circ}(m-n) + G(0,n)[G^{\circ}(m,0)V(0,0) + G^{\circ}(m,-1)V(-1,0)] \quad \text{for all } m \geq 0 \qquad (2.15a)$$

It is clear that the diagonal matrix elements of the cleaved Green function is now given by

$$G(m,m) = G^{\circ}(0) + [G^{\circ}(m)V(0,0)+G^{\circ}(m+1)V(-1,0)]G^{\circ}(-m)[1-G^{\circ}(0) \times V(0,0) - G^{\circ}(1)V(-1,0)]^{-1} \quad \text{for all } m \geq 0 \qquad (2.15b)$$

To obtain an explicit formula for G(m,m) we have first to find $G^{\circ}(m)$.The functions of Eq(2.10) are related to the Bloch functions defined by

$$|\underline{K}\rangle = |\underline{K}_\perp, \underline{K}_\parallel\rangle = (N_\perp)^{-1/2} \sum_n |n\underline{d}, \underline{K}_\parallel\rangle e^{ink_\perp d} \qquad (2.16)$$

where $N_\perp$ is the number of planes paralell to the surface. Here $\underline{K} = \underline{K}_\parallel + \underline{K}_\perp$ and $\underline{K}_\perp$ is a normal vector to the surface plane and satisfies the restriction $|K_\perp| \leq \pi/d$. Now in the Bloch representation G° is diagonal and defined by

$$\langle \underline{K}|G^\circ|\underline{K}'\rangle = \delta(\underline{K}-\underline{K}')/(E - E_\circ(\underline{K}) + i\delta) \qquad (2.17)$$

Where $E_\circ(\underline{K})$ is the energy eigenvalue of an electron in a perfect crystal. It follows that

$$G^\circ(n) = (N_\perp)^{-1} \sum_{\underline{K}_\perp} \frac{epx(inK_\perp d)}{E + i\delta - E_\circ(\underline{K})} \qquad (2.18)$$

with

$E_\circ(\underline{K}) = \langle \underline{K}|H^\circ|\underline{K}\rangle$ and using Eqs(2.13, and 2.16) to get

$$= H^\circ(n,n,\underline{K}_\parallel) + H^\circ(n,n\pm1,\underline{K}_\parallel)$$

$$= w(\underline{K}_\parallel) + 2T\cos(K_\perp d) \qquad (2.19)$$

Here we assume that $H^\circ(n,n) = 0$ thus for the case where only nearst-neighbour interactions are concerned, we find

$$w(\underline{K}_\parallel) = 2T[\cos(K_x d) + \cos(K_y d)] \qquad (2.20)$$

where K_x and K_y are components of $\underline{K}_\parallel$. Upon substitution Eqs.(2.19) into (2.18) and by changing to a continous reoresentation $\underline{K}_\perp$ in which case we replace the summation by an integral,

$$\frac{1}{N_\perp} \sum_{\underline{K}_\perp} \longrightarrow \frac{d}{2\pi} \int_{1BZ} dK_\perp \qquad (2.21)$$

to obtain

$$G^{\circ}(n) = \frac{d}{2\pi}\int_{-\pi/d}^{\pi/d} dK_{\perp}\,\frac{epx(inK_{\perp}d)}{\omega - 2T\cos(K_{\perp}d) + i\delta} \qquad (2.22)$$

where $\omega = E - w(\underline{K}_{\parallel})$ (2.23a)

and $-2 \le w(\underline{K}_{\parallel}) \le 2$ (2.23b)

Eq.(2.22) can be easily solved by means of contour integration in the complex plane over a unit circle. There are two possibilities to be considered

(i) $\underline{\omega^2-4T^2 \le 0}$

We obtain

$$G^{\circ}(n) = i\mu^{-1}\left(\frac{\omega + i\mu}{2T}\right)^{|n|} \qquad (2.24)$$

and $\mu = \sqrt{4T^2 - \omega^2}$ (2.25)

(ii) $\underline{\omega^2-4T^2 \ge 0}$

We replace μ in Eq.(2.24) by $i\,\mathrm{sign}(w)\alpha$ to obtain

$$G^{\circ}(n) = \frac{1}{\mathrm{sign}(\omega)\alpha}\left[\frac{\omega - \mathrm{sign}(\omega)\alpha}{2T}\right]^{|n|} \qquad (2.26)$$

where $\alpha = \sqrt{\omega^2 - 4T^2}$ (2.27)

and

$$\mathrm{sign}(\omega) = \begin{cases} 1 & \text{if } \omega > 0 \\ -1 & \text{if } \omega < 0 \end{cases} \qquad (2.28)$$

We are now in a position to calculate the semi-infinite Green's function G(m,m). We first substitute the explicit Eqs.(2.24) and (2.26) into Eq.(2.15a) and make use of the fact that V(-1,0) = -T (Note: This is the potential to cancell the interactions across the cleavage plane between n = 0 and n = -1).

We then to obtain the following two cases :

(i) $\underline{\text{For } \omega^2 - 4T^2 \le 0 \quad \text{i.e.} \quad -2T \le \omega \le 2T}$

We have

$$G(m,n) = G^{\circ}(m-n) + \frac{i}{\mu}\left(\frac{\omega + i\mu}{2T}\right)^{|m|+|n|}\left[\frac{\mu - i(\omega-2U_o)}{\mu + i(\omega-2U_o)}\right] \tag{2.29}$$

where $m \geq 0$

$\mu = \sqrt{4T^2 - \omega^2}$

G° is given by Eq.(2.24)

It is clear that the diagonal matrix elements of the cleaved Green function are given by

$$G(m,m) = i\mu^{-1}\left\{1 + \left(\frac{\omega+i\mu}{2T}\right)^{2|m|}\left[\frac{\mu - i(\omega-2U_o)}{\mu + i(\omega-2U_o)}\right]\right\} \tag{2.30}$$

(ii) <u>For $\omega^2-4T^2 > 0$,i.e., $\omega>2T$ and $\omega<-2T$</u>

We have

$$G(m,n) = G^{\circ}(m-n) + \frac{1}{\eta}\left(\frac{\omega - \eta}{2T}\right)^{|m|+|n|}\left[\frac{\eta - (\omega-2U_o)}{\eta + (\omega-2U_o)}\right] \tag{2.31}$$

where $\eta = \alpha\ \mathrm{sign}(\omega)$

G° is defined by Eq.(2.26)

Again the diagonal matrix elements of the cleaved Green's function are given by

$$G(m,m) = \eta^{-1}\left\{1 + \left(\frac{\omega - \eta}{2T}\right)^{2|m|}\left[\frac{\eta - (\omega - 2U_o)}{\eta + (\omega - 2U_o)}\right]\right\} \tag{2.32}$$

In the mixed representation, the local density of states (LDOS) is defined by

$$\rho_m(E) = -\frac{1}{\pi N_{\parallel}} \sum_{\underline{K}_{\parallel}} \mathrm{Im}G(m,m,\underline{K}_{\parallel}) \tag{2.33}$$

Using Eq.(2.33), we have performed numerical calculation of the LDOS for the surface (n=0) and the first two interior

planes of an s-band of a semi-infinite (100) simple cubic tight-binding crystal. Here the summation over $\underline{K}_{\parallel}$ is converted to an integral and numerically performed by Simpson's rule. The details of the computation of the two-dimensional Brillouin zone sums will be described in subsection 2.3.4. The numerical result are presented in figure 5.

Finally, we wish to mention that we shall employ both Eqs.(2.30) and Eq(2.32) as the surface Green's functions of a (100) substrate in the development of our new recursion method for an overlayer system (see section 2.3).

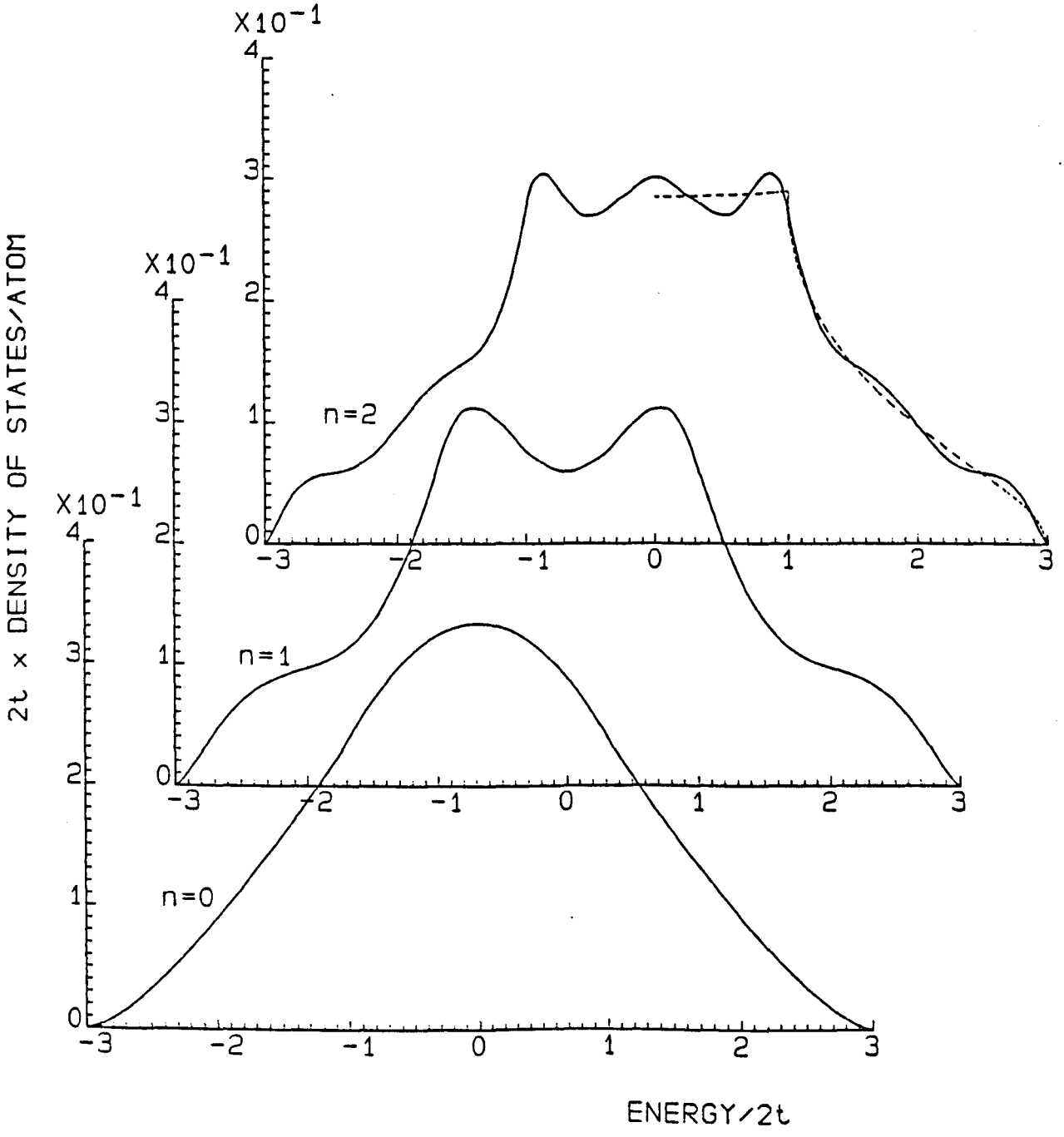

Fig.5. Local density of states for the surface(n=0) and th
First two interior planes in the presence of a (100) surfa
The surface perturbation U_o is zero .The dashed curve in th
upper figure is the infinite crystal density of states per
atom.

2.2 The transfer matrix method (TMM)

The aims of this section are :

(i) to explore the transfer matrix method (TMM) as a viable alternative to the KS method in the presence of degenerate bands

(ii) to introduce and clarify the concept of principal layer

The discussion of the TMM is necessary and very important for the future development of our overlayer method because KS method is not suitable for multi-orbital band structure. As we already stated, the method of adlayers can be generalized to realistic degenerate bands and it is hoped that this section on the TMM will give the reader some insight into the multi-orbital problem. Later on we shall illustrate the method for a two-orbital problem and determine for this model the bulk and surface DOS.

We now return to the TMM. There are three basic ingredients in the TMM (Lee and Joannopoulos 1981)

(i) reduction of any surface problem to a semi-infinite stack of principal layers

(ii) set of basis Bloch functions associated with each principal layer,

(iii) the transfer matrix which depends only on the Hamiltonian matrix elements between those basis Bloch functions.

Before the TMM is described, let us first discuss the general concept of a principal layer.

2.2.1 Principal layer concept

Consider a bulk crystal. We wish to think of it as

an infinite stack of principal layers. A principal layer is defined as the smallest stack of atomic layers such that there is nearest-neighbour interaction only between principal layers in the following sense: The interactions between atoms in the first principal and the second principal layer may be of nearst-neighbour or longer range but there is no interaction between any atom in the first principal layer and the third principal layer.

It should be noted that, in general, the interactions between different principal layers may be different. If periodicity in the direction paralell to the surface is preserved for all the atomic planes right up to the surface, then the wave vector $\underline{K}_{\parallel}$ is a good quantum number and, for each $\underline{K}_{\parallel}$, the surface problem further reduces to a one-dimensional chain in the direction (z) perpendicular to the surface.

We can now build Bloch orbitals for each atomic orbital ϕ_{α} along any atomic plane, for example, the λth atomic plane of the nth principal layer. Take m orbitals per atom and suppose each principal layer is composed of l atomic planes. We can then form column vector Bloch states for each principal layer:

$$\Psi_n(\underline{K}_{\parallel}) = \begin{pmatrix} \varphi_n^{11}(\underline{K}_{\parallel}) \\ \varphi_n^{12}(\underline{K}_{\parallel}) \\ \vdots \\ \varphi_n^{\lambda\alpha}(\underline{K}_{\parallel}) \\ \vdots \\ \varphi_n^{lm}(\underline{K}_{\parallel}) \end{pmatrix} \qquad (2.34)$$

where

$$\varphi_n^{\lambda\alpha}(\underline{K}_{\parallel}) = \frac{1}{\sqrt{N_{\parallel}}} \sum_{\underline{R}_{\parallel}} e^{i\underline{K}_{\parallel}\,\underline{R}_{\parallel}}\, \phi_n^{\lambda\alpha}(\underline{R}_{\parallel}) \qquad (2.35)$$

is the partial Bloch wavefunctions and $N_{\parallel}$, $\underline{R}_{\parallel}$ denote respectively the number of atoms and position vector of an atomic plane As an illustration of the principal layer concept, we shall give the following example

Example

A principal layer for (100) surface of a bcc lattice with d orbitals and with nearest-neighbour and second nearest-neighbour interaction is defined as follows

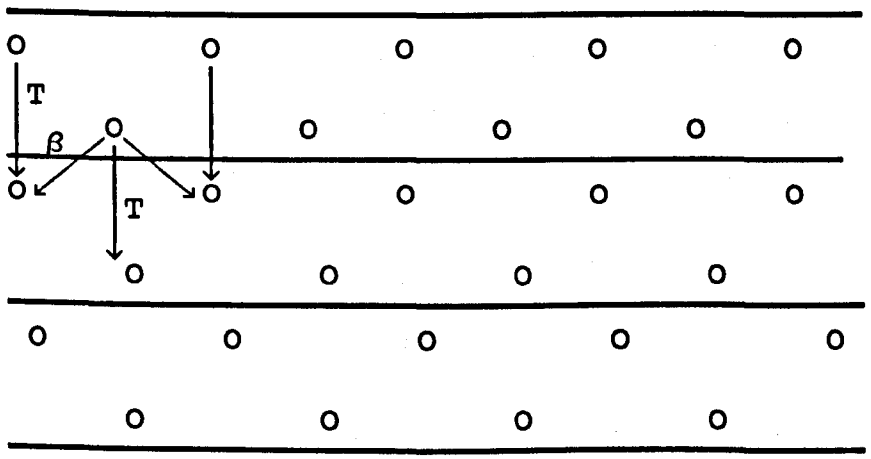

Fig.6 Stack of principal layers for a (100) surface of bbc lattice, where T is the nearest-neighbour and β the second nearest-neighbour interactions.

Since λ=1,2 for bcc (100) surface and α=1,2,...,5 for d-band only,we form column-vector $\Psi(K)$ following Eq(2.34) to obtain

$$\Psi_n(\underline{K}_\parallel) = - \begin{pmatrix} \varphi_n^{11}(\underline{K}_\parallel) \\ \varphi_n^{12}(\underline{K}_\parallel) \\ \vdots \\ \varphi_n^{15}(\underline{K}_\parallel) \\ \hline \varphi_n^{21}(\underline{K}_\parallel) \\ \varphi_n^{22}(\underline{K}_\parallel) \\ \vdots \\ \varphi_n^{25}(\underline{K}_\parallel) \end{pmatrix} -$$

—— These are for the first atomic layer orbitals 1 to 5.

—— and these are for the second atomic layer orbitals 1 to 5

(2.36)

2.2.2 Transfer matrix method of Lopez Sancho et al.

Consider the matrix equation for the Green's function G:

$$(\omega I - H)G = I \qquad (2.37)$$

where ω is the energy, H is the Hamiltonian written in a given basis $\{\Psi_n\}$ and I is the unit matrix. We write the matrix elements of the Green's function G in terms of Eq.(2.37) as follows

$$G_{nn'}(\omega, \underline{K}_\parallel) = \langle \Psi_n(\underline{K}_\parallel) | G(\omega) | \Psi_{n'}(\underline{K}_\parallel) \rangle$$

$$= G_{nn'}, \quad \text{for simplicity} \qquad (2.38)$$

Similarly, the matrix elements of Hamiltonian H may be defined as

$$H_{nn'}(\underline{K}_\parallel) = \langle \Psi_n(\underline{K}_\parallel) | H | \Psi_{n'}(\underline{K}_\parallel) \rangle$$

$$= H_{nn'} \qquad (2.39a)$$

and

$$H_{nn'} = H^*_{n'n} \qquad (2.39b)$$

represents different interactions between layers n' and n. We can now taking matrix elements of Eq.(2.37) between the Bloch states defined by Eq.(2.34) to obtain

$$\sum_{m} (\omega I - H)_{nm} G_{mn'} = \delta_{nn'} \qquad (2.40)$$

where

n denotes the nth principal layer

m denotes the nearest-neighbour principal layer.

We make a simplifying but not essential assumption of an ideal surface and set

$$\begin{aligned} H_{00} &= H_{11} = H_{22} = \ldots = H_{nn} = \ldots \\ H_{01} &= H_{12} = H_{23} = \ldots = H_{n-1,n} = \ldots \end{aligned} \qquad (2.41)$$

We let $n' = 0$ to obtain the usual chain of equations for the matrix elements of the Green function with fixed $\underline{K}_{\parallel}$

$$\begin{aligned} (\omega - H_{00}) G_{00} &= I + H_{01} G_{10} \\ (\omega - H_{00}) G_{10} &= H_{01}^{*} G_{00} + H_{01} G_{20} \\ (\omega - H_{00}) G_{20} &= H_{01}^{*} G_{10} + H_{01} G_{30} \\ &\vdots \\ (\omega - H_{00}) G_{n0} &= H_{01}^{*} G_{n-1,0} + H_{01} G_{n+1,0} \end{aligned} \qquad (2.42)$$

where $n = 0$ indicates the surface principal layer. We are now in a position to discuss the method of effective layers. From the general term in Eq.(2.42) we have

$$G_{n0}(\omega) = (\omega - H_{00})^{-1} (H_{01}^{*} G_{n-1,0} + H_{01} G_{n+1,0}) \qquad (2.43)$$

for all $n \geq 1$

Setting $n = 1$ into Eq.(2.43) and put the result into the first equation of the chain (2.42) to obtain

$$[\omega - H_{00} - H_{01} (\omega - H_{00})^{-1} H_{01}^{*}] G_{00} = I + H_{01} (\omega - H_{00})^{-1} H_{01} G_{20} \qquad (2.44)$$

which relates G_{00} to G_{20} .

Similarly can one obtained the general equation of the chain, Eq.(2.43), by replacing $G_{n-1,0}$ and $G_{n+1,0}$ after Eqs.(2.42)

$$
\begin{aligned}
(\omega-\varepsilon_{1s})G_{00} &= I + \alpha_1 G_{20} \\
(\omega-\varepsilon_{1})G_{n0} &= \beta_1 G_{n-2,0} + \alpha_1 G_{n+2,0} \qquad n \geq 2 \\
(\omega-\varepsilon_{1})G_{nn} &= I + \beta_1 G_{n-2,n} + \alpha_1 G_{n+2,n} \qquad (2.52)
\end{aligned}
$$

where

$$
\begin{aligned}
\alpha_1 &= H_{01}(\omega-H_{00})^{-1} H_{01} \\
\beta_1 &= H^{*}_{01}(\omega-H_{00})^{-1} H^{*}_{01} \qquad (2.46) \\
\varepsilon_{1s} &= H_{00} + H_{01}(\omega-H_{00})^{-1} H^{*}_{01} \\
\varepsilon_{1} &= \varepsilon_{1s} + H^{*}_{01}(\omega-H_{00})^{-1} H_{01}
\end{aligned}
$$

Eq.(2.46) defines an effective Hamiltonian describing a chainof effective layers of lattice constant 2a (twice the original one); each effective layer contains implicitly the effect of its nearest-neighbours in the original chain through the use of Eq.(2.43) Now taking only even values for n in Eq.(2.45), i.e., replacing n by 2n we obtain

$$
\begin{aligned}
(w-\varepsilon_{1s})G_{00} &= I + \alpha_1 G_{20} \\
(w-\varepsilon_{1})G_{2n,0} &= \beta_1 G_{2(n-1),0} + \alpha_1 G_{2(n+1),0} \qquad (2.47) \\
(w-\varepsilon_{1})G_{2n,2n} &= I + \beta_1 G_{2(n-1),2n} + \alpha_1 G_{2(n+1),2n}
\end{aligned}
$$

Eq.(2.47) defines a chain which couples the Green function matrix elements with even indices only $G_{2n,0}$ through effective nearest neighbour interactions given by the first two equations of Eq(2.46) and with effective zeroth order matrix elements already different for the surface (ε_{1s}) and the inner layer (ε_1). Except for the different zeroth order matrix elements, $\varepsilon_{1s} \neq \varepsilon_1$, Eq(2.47) are isormophic to

Eq.(2.42). It follows that the argument from Eq.(2.42) to Eq.(2.47) can be repeated if we start from Eq.(2.47). Now setting $\varepsilon_0 = H_{00}$, $\alpha_0 = H_{01}$ and $\beta_0 = H_{01}^*$ and repeating the argument i times we obtain the iterative sequence

$$\begin{aligned}
\alpha_i &= \alpha_{i-1}(w-\varepsilon_{i-1})^{-1}\,\alpha_{i-1} \\
\beta_i &= \beta_{i-1}(w-\varepsilon_{i-1})^{-1}\,\beta_{i-1} \\
\varepsilon_i &= \varepsilon_{i-1} + \alpha_{i-1}(w-\varepsilon_{i-1})^{-1}\,\beta_{i-1} + \beta_{i-1}(w-\varepsilon_{i-1})^{-1}\alpha_{i-1} \\
\varepsilon_i^s &= \varepsilon_{i-1}^s + \alpha_{i-1}(w-\varepsilon_{i-1})^{-1}\,\beta_{i-1}
\end{aligned} \tag{2.48}$$

The iteration is to be repeated until α_ν and β_ν are as small as we wish. Clearly, $\varepsilon_\nu \simeq \varepsilon_{\nu-1}$ and $\varepsilon_\nu^s \simeq \varepsilon_{\nu-1}^s$ and

$$\begin{aligned}
(\omega-\varepsilon_\nu^s)G_{00} &\simeq I \\
(\omega-\varepsilon_\nu)G_{2^\nu n,2^\nu n} &\simeq I \qquad \text{for all } n \geq 1
\end{aligned} \tag{2.49}$$

Thus we finally obtain the surface layer Green's function G_{00} to as good an approximation as we wish,

$$G_{00}(\omega) \approx (\omega-\varepsilon_\nu^s)^{-1} \tag{2.50}$$

and the bulk layer Green's function G_b by

$$\begin{aligned}
G_b &= \lim_{n\to\infty} G_{nn} \\
&= G_{2^\nu,2^\nu} \simeq (\omega-\varepsilon_\nu)^{-1}
\end{aligned} \tag{2.51}$$

As a demonstration of the TMM, we perform a numerical calculation for a simple cubic lattice with two bands and (100) surface. We shall obtain both the surface DOS and bulk DOS. In our model, one orbital generates an s-like wide band and the other a d-like narrow band.

The overlap and hybridization integrals are non-zero only

between orbitals centred at two nearest-neighbour sites and the numerical values are chosen to be (see Goncalves da Silva and B.Laks, 1977)

$$A_{2,2} = \begin{array}{c} \\ s \\ d \end{array} \begin{array}{c} \begin{array}{cc} s & d \end{array} \\ \begin{pmatrix} 1.0 & 0.2 \\ 0.2 & 0.1 \end{pmatrix} \end{array} \qquad (2.52a)$$

and

$$W_{2,2} = \begin{array}{c} \\ s \\ d \end{array} \begin{array}{c} \begin{array}{cc} s & d \end{array} \\ \begin{pmatrix} EC+4.GK & 4.GK+0.2 \\ 4.GK+0.2 & EC+2+4.GK+0.1 \end{pmatrix} \end{array} \qquad (2.52b)$$

where

$$GK = 0.5(\cos(K_x)+\cos(K_y)) \qquad (2.53)$$

In Fig.(7) we present the numerical results for the surface DOS and bulk DOS at the (100) surface.

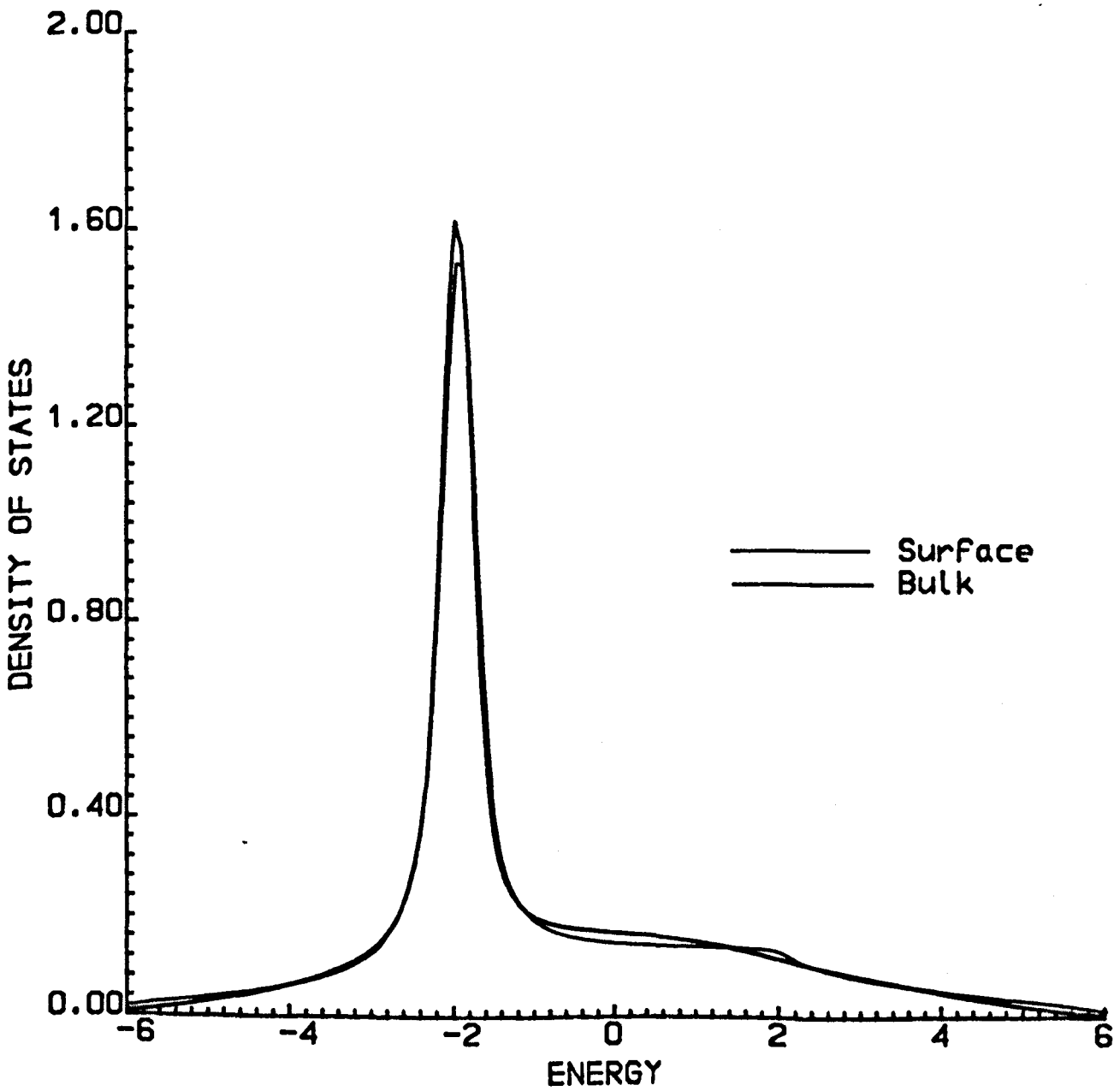

Fig.7 Surface and bulk density of states of a (100) surface of a square lattice, having two orbitals per site.

2.3 Method of Adlayer

In this section we describe a general recursion method for calculating the exact electron Green function in an arbitrary ferromagnetic overlayer.

The method we propose is very simple, computationally stable and so accurate that overlayers containing up to 10^3-10^4 atomic planes can be easily handled.

There are three basic ingredients in this method. The first is that we always start with a homogenous semi-infinite nonmagnetic substrate with a clean surface; in some cases, the substrate may also be ferromagnetic. The properties of the substrate are determined either the by KS formalism or by the transfer matrix method. We assume here that it is described by an s-band tight-binding Hamiltonian

The second ingredient is a ferromagnetic overlayer of N atomic layers labeled by n=1,2,...,N "deposite" on the substrate. These N atomic layers are characterized by different perturbations (diagonal matrix elements)V_i (i= 1,2,...,N) and also by different mean values of spin-up and spin-down electrons in each layer. For simplicity we model the overlayer by a simple s-band and assume that only nearest-neighbour (off-diagonal) elements T couple the subtrate to the overlayer; T is taken to be equal to the bulk value(see, e.g. Fig.6)

Finally, the third important feature on the method is that we use a set of basis wavefunctions which are taken in the mixed Bloch-Wannier representation. This is to take

advantage of the translational invariance of the system in the direction parallel to the surface.

As already stated, the aim of this chapter is to show that there is a general analytic method for calculating the LDOS in any atomic plane n=1,2,...N of the structure within the tight-binding approximation. The LDOS is obtained from

$$N_n(E) = -\frac{1}{\pi} \mathrm{Tr}\ \mathrm{Im} G^{+}_{nn}(E,q_{\parallel}) \quad , \tag{2.54}$$

where

$$G^{+}(E,q_{\parallel}) = \lim_{\delta \to o} G(E+i\delta,q_{\parallel}) \tag{2.55}$$

and the trace is over the wave vector $q_{\parallel}$ parallel to the structure surface. G^{+} is the local electron Green function written in the mixed representation.

To derive G_{nn} , we first assume that all the interaction matrix elements between the nonmagnetic substrate and the overlayer are switched-off so that the overlayer is physically removed from the subtrate.

Secondly, the matrix element of the exact electron Green function $G^{0}_{00}(E,q_{\parallel})$ in the now exposed surface plane of the substrate (n=0) is calculated, using generally, the Green functions of the bulk crystal. In fact, $G^{0}_{00}(E,q_{\parallel})$ is known already since it is given by Eqs(2.30) and (2.32).

As a next step, we reinstate the first atomic plane of the overlayer n=1 and give a prescription for calculating the matrix element G^{1}_{11} of the Green function in the new surface plane n=1 in terms of the old surface element G^{0}_{00} . The superscript '1' indicates that G^{1} refers to the substrate covered with one 'adlayer'.

Once G^1_{11} is known, the second layer n=2 is reinstated and G^2_{22} is expressed in terms of G^1_{11} which is a function of G^0_{00}. This procedure of depositing 'adlayers' is repeated until the whole overlayer is 'rebuilt'. After N recursion steps, we end up with the exact surface Green function $G^s \equiv G^N_{NN}$ in terms of the known substrate's Green function G^0_{00} The local Green function in any atomic plane is obtained from G^S.

Here we make the following important point: a generalization of the method to other geometries, to a longer range interaction and to a multi-orbital band structure is straightforward. In fact, it is sufficient to described the method for a simple cubic lattice and a nearest-neighbour exchange Hamiltonian since any layer structure can be reduced to this problem using the concept of principal layers (see section 2.2).

The layout of this section is as follows. First the details of single-adlayer formalism are outlined in subsection (2.3.1) where the surface Green function of one-layer system and its associated density of states are obtained. We next extend the method to an overlayer of N atomic layers and we examine theoretically the magnetic effect of a surface on bulk magnetism, in particular, we shall discuss, how LDOS, occupation numbers vary in each layer. An application of the overlayer formalism is presented in subsection 2.3.3, where we compute the LDOS, occupation number in each atomic layer of the structure.

2.3.1 Single-adlayer formalism for a non-magnetic system

Our aim in this subsection is to calculate the surface DOS of a single-adlayer system.We therefore require the diagonal matrix elements of the surface Green function

A.HAMILTONIAN

Assume that an atomic plane labeled by n = 1 'sits' on top of the (100) surface of a simple cubic non-magnetic substrate. This sub-strate occupies the half-space z<0.

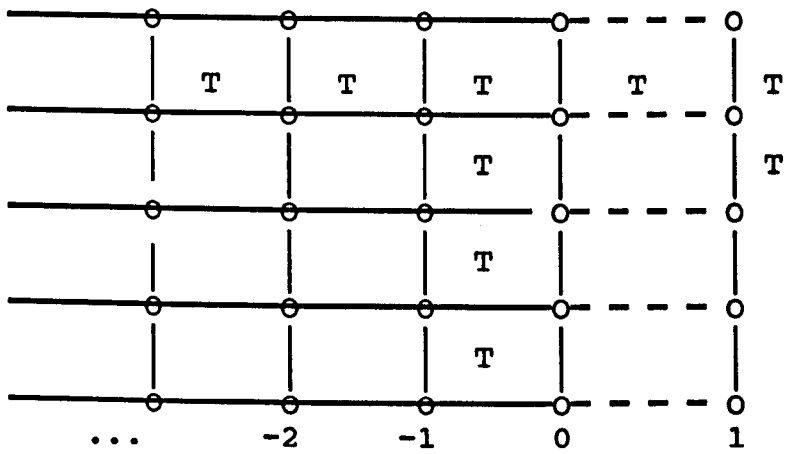

Fig.8 One atomic layer labeled by n = 1 is deposited on top of the substrate labeled by n = 0.

We shall first define the one-layer system Hamiltonian H^1 within the tight-binding approximation by

$$H^1 = H^0 + W$$

$$= \sum_{i,j} t_{ij}\, c_i^+ c_j + W \qquad (2.56)$$

where $c_i^+(c_j)$ are the creation (annihilation) operators of the s-type Wannier-type orbitals localized at sites i and j. We assume that the matrix elements t_{ij} are non-zero only when i and j are nearest neighbours.

The first term of Eq.(2.56) H^0 is the tight-binding Hamiltonian matrix corresponding to the semi-infinite nonmagnetic substrate without an overlayer.This Hamiltonian has a tridiagonal representation:

$$
H^0 = \begin{array}{c} \\ 0 \\ -1 \\ -2 \\ -3 \\ \vdots \\ \vdots \\ \vdots \end{array}
\begin{array}{c}
\begin{array}{cccccc} 0 & -1 & -2 & -3 & \cdots & \end{array} \\
\left(\begin{array}{cccccc}
H^0_{0,0} & H^0_{0,-1} & 0 & 0 & \cdots & \\
H^0_{-1,0} & H^0_{-1,-1} & H^0_{-1,-2} & 0 & \cdots & \\
0 & H^0_{-2,-1} & H^0_{-2,-2} & H^0_{-2,-3} & & \cdots \\
0 & 0 & H^0_{-3,-2} & H^0_{-3,-3} & & \cdots \\
\vdots & \vdots & \vdots & \vdots & & \cdots \\
\vdots & \vdots & \vdots & \vdots & & \cdots \\
\vdots & \vdots & \vdots & \vdots & & \cdots
\end{array}\right)
\end{array}
\qquad (2.57)
$$

Note that the indices n = 0,-1,-2,... denote the diagonal and the nearst-neighbour hopping elements between the nth and the (n-1)th or between the (n-1)th and the nth atomic planes. The second term W is the perturbation due to deposition of an adlayer to be discussed later.

The important point is that since we are depositing one atomic layer on top of the substrate, our recursion method requires the Hamiltonian H^0 to be written in a new basis of the single-adlayer system, i.e., in the space of dimension (N+1) layers. In this case H^0 extends to the following form

$$
H^0 = \begin{array}{c} \\ 1 \\ 0 \\ -1 \\ -2 \\ \vdots \end{array}
\begin{array}{c}
\begin{array}{ccccc} 1 & 0 & -1 & -2 & \cdots \end{array} \\
\begin{pmatrix}
0 & 0 & 0 & 0 & \cdots \\
0 & H^0_{0,0} & H^0_{0,-1} & 0 & \cdots \\
0 & H^0_{-1,0} & H^0_{-1,-1} & H^0_{-1,-2} & \cdots \\
0 & 0 & H^0_{-2,-1} & H^0_{-2,-2} & \cdots \\
\vdots & \vdots & \vdots & \vdots & \cdots \\
\end{pmatrix}
\end{array}
\qquad (2.58)
$$

Notice that the top column and row of zeros in Eq.(2.58) is just a mathematical device allowing us to extend H^0 to the new dimension.

B.GREEN FUNCTION

Let G^0 and G^1 be the Green functions for the substrate and single-adlayers system . Both G^0 and G^1 are written in the new space of dimension (N+1).

The single-adlayer Green function G^1 is defined by the following equation :

$$(EI-H^1+i\delta)G^1 = 1 \qquad (2.59)$$

where I is the (N+1)×(N+1) unit matrix, δ is a positive infinitesimal, and E is the energy.

The (100) surface Green function G^0 is related to the substrate Hamiltonian H^0 by the following equation :

$$(EI-H^0+i\delta)G^0 = 1 \qquad (2.60)$$

In the absence of an overlayer, the problem of finding G^0_{00}

in the basis of dimension N can be solved by the method of KS or by the transfer matrix method, ...(see e.g. section 2.1 and 2.2). The Green functions G^1 is related to G^0 via Dyson's equation

$$G^1 = G^0 + G^0WG^1 \qquad (2.61)$$

where the perturbation W is defined by

$$W = H^1 - H^0 \qquad (2.62)$$

As already discussed in section (2.1), the quantities G^1, G^0 and W in the mixed Bloch-Wannier representation are all diagonal in the wave vector $\underline{K}_{\parallel}$. Dropping $\delta(\underline{K}_{\parallel}-\underline{K}'_{\parallel})$, we shall denote by $G^1(m,n,\underline{K}_{\parallel})$, $G^0(m,n,\underline{K}_{\parallel})$ and $W(m,n,\underline{K}_{\parallel})$ the matrix elements of G^1, G^0 and W in the mixed representation. To simplify the notation even further we will generally drop the obvious $\underline{K}_{\parallel}$ dependence in these expressions.

Now from the discussion of the Hamiltonian given in part A. of subsection 2.3.1, it is obvious that there are two types of contribution which enter the perturbation W. First we have the offdiagonal matrix elements (also called the hopping integrals) which couple the (100) surface labeled n = 0 to the impurity plane of atoms labeled n = 1. Since the substrate Hamiltonian H^0 has no matrix elements connecting localized functions centrèd on planes 1 and 0 (see Eq.(2.58)), we obtain from Eq.(2.62) the following results

$$W(0,1) = \langle \underline{K}_{\parallel},0|W|\underline{K}_{\parallel},1\rangle$$

$$= \langle \underline{K}_{\parallel},0|H^1|\underline{K}_{\parallel},1\rangle = T \qquad (2.63a)$$

and

$$W(1,0) = \langle \underline{K}_{\parallel},1|W|\underline{K}_{\parallel},0\rangle$$

$$= \langle \underline{K}_{\parallel},1|H^{1}|\underline{K}_{\parallel},0\rangle = T \qquad (2.63b)$$

The other type of contribution is the diagonal matrix element of W. It arises due to deposition an atomic layer; we have

$$W(1,1) = \langle \underline{K}_{\parallel},1|W|\underline{K}_{\parallel},1\rangle$$

$$= \langle \underline{K}_{\parallel},1|H^{1}|\underline{K}_{\parallel},1\rangle = W_{1}$$

$$= V_{1} + 2T(\cos(K_{x}a + \cos K_{y}a)) = V_{1} + w(K_{\parallel}) \qquad (2.63c)$$

where V_1 is the on-site energy corresponding to atoms in plane 1 and $w(K_{\parallel})$ is the two-dimensional structure factor for planes parallel to the surface and it arises from the interaction of an atom with its four nearest-neighbours within a plane.

Here, we set W(0,0)=0 this is because we have taken it into account when we calculate the substrate. Note also that the nearest-neighbour hopping T and the on-site perturbation V_1, are either treated as adjustable parameters in a non-selfconsistent manner (as in KS) or V_1 can be treated in the HF approximation.

We now return to the calculation of the surface Green's function from the Dyson equation (2.61). In the mixed Bloch-Wannier representation, Eq.(2.61) reduces to a set of algebraic difference equation

$$G^{1}(i,j) = G^{0}(i,j) + \sum_{p,q} G^{0}(i,p)W(p,q)G^{1}(q,j) \qquad (2.64)$$

Using Eqs.(2.63a,b,c) we can transform Eq(2.64) to the form

$$G^1(i,j) = G^0(i,j) + W_1 G^0(i,1)G^1(1,j) + T\,[\,G^0(i,0)G^1(1,j) + G^0(i,1)G^1(0,j)\,] \qquad (2.65)$$

We are now in a position to evaluate the off-diagonal and diagonal matrix elements of the surface single-adlayer Green function G^1 in terms of the substrate Green function G^0_{00}. However, first we have to discuss the definition of $G^0(i,j)$ in the space of dimension (N+1). Now using Eq.(2.60) we obtain

$$G^0_{ij}(E,\underline{K}_{\parallel}) = (EI - H^0)^{-1}$$

$$= \begin{array}{c} \\ 1 \\ 0 \\ -1 \\ -2 \\ \\ \\ \end{array} \begin{array}{c} \begin{array}{cccc} 1 & 0 & -1 & -2 \end{array} \\ \begin{pmatrix} E & 0 & 0 & 0 \\ 0 & E-H^0_{0,0} & E-H^0_{0,-1} & 0 \\ 0 & E-H^0_{-1,0} & E-H^0_{-1,-1} & \cdot \\ 0 & 0 & E-H^0_{-2,-1} & \cdot \\ \cdot & \cdot & & \cdot \\ \cdot & \cdot & & \\ \cdot & \cdot & & \end{pmatrix} \end{array}^{-1} \qquad (2.66)$$

where I is the (N+1)×(N+1) unit matrix, H^0 is defined in Eq(2.58) It is obvious from Eq.(2.66) that the matrix elements of G^0 are given by :

$$G^0_{11}(E,\underline{K}_{\parallel}) = \frac{1}{E} \qquad (2.67a)$$

$$G^0_{10}(E,\underline{K}_{\parallel}) = G^0_{01}(E,\underline{K}_{\parallel}) = 0 \qquad (2.67b)$$

$$G^0_{00}(E,\underline{K}_{\parallel}) = (EI - H^0_{00})^{-1} \qquad (2.67c)$$

Eq.(2.67c) is just the definition of the known Green function for the (100) surface given by Eqs.(2.30) and (2.32) with m=0 and U_o=0

The Green's function (2.67c) is written explicitly as

For $\omega^2-4T^2 \leq 0$ we have $G^0_{00}(E,\underline{K}_{\parallel}) = 2\omega + i2\mu$ (2.68a)

For $\omega^2-4T^2>0$ we have $G^0_{00}(E,\underline{K}_{\parallel}) = 2/(\eta + \omega)$ (2.68b)

where $\mu = \sqrt{4T^2-\omega^2}$, $\eta = \text{sign}(\omega)\alpha$ and $\alpha = \sqrt{\omega^2 - 4T^2}$.

Setting i=j=1 into Eq.(2.65) and using Eqs.(2.67a,b,c) we get

$$G^1_{11}(E,\underline{K}_{\parallel}) = \frac{1}{E - W_1 - T^2 G^0_{00}(E,\underline{K}_{\parallel})}$$

$$= \frac{1}{\omega - V_1 - T^2 G^0_{00}(E,K_{\parallel})} \qquad (2.69)$$

where $\omega = E-w(K_{\parallel})$ and $w(K_{\parallel}) = 2T(\cos K_x a + \cos K_y a)$.

Eq.(2.69) is the diagonal matrix elements of the single-adlayer Green's function which is needed in the calculation of the local DOS given by

$$\rho^1(E) = -\frac{1}{\pi N_{\parallel}} \sum_{\underline{K}_{\parallel}} \text{Im} G^1_{11}(E,\underline{K}_{\parallel}) \qquad (2.70)$$

where $N_{\parallel}$ is the number of atoms in the surface plane and $\underline{K}_{\parallel}$ the summation over the first B.Z which must be done by numerically (see section 2.3.3).

In the next subsection, we shall extend the single-adlayer method to a general overlayer. We shall develop a systematic method of generating the whole matrix Green function of an overlayer. Once it is done, the associated DOSs in each layer are easily calculated.

2.3.2 Overlayer Formalism

We shall now describe how to generalise the method of subsection (2.3.1) to an overlayer of N atomic planes.

Once the Green's function for the one-layer system G^1_{11} is known, a second layer labeled n = 2 is reinstated, and the procedure of the single-adlayer formalism can now be repeated. The surface Green's function G^2_{22} is expressed in terms of G^1_{11}, and one finds that the diagonal matrix elements G^2_{22} is given by

$$G^2_{22}(E,\underline{K}_{\parallel}) = \frac{1}{E - W_2 - T^2 G^1_{11}} \qquad (2.71)$$

where $W_2 = V_2 + w(K_{\parallel})$. Again, G^2_{22} is now known, a third atomic layer labeled n=3 is reinstated and G^3_{33} is expressed in terms of G^2_{22}. Thus, in general, this procedure of depositing an atomic layer is repeated until the whole overlayer is 'rebuilt' (see Fig.9).

After N recursion steps, we arrive at

$$G^N_{NN}(E,K_{\parallel}) = \frac{1}{E - W_N - T^2 G^{N-1}_{N-1,N-1}}$$

$$= \frac{1}{\omega - V_N - T^2 G^{N-1}_{N-1,N-1}} \qquad (2.72)$$

for all N = 1,2,...

Where $W_N = V_N + w(K_{\parallel})$ and $\omega = E - w(K_{\parallel})$ have been used.

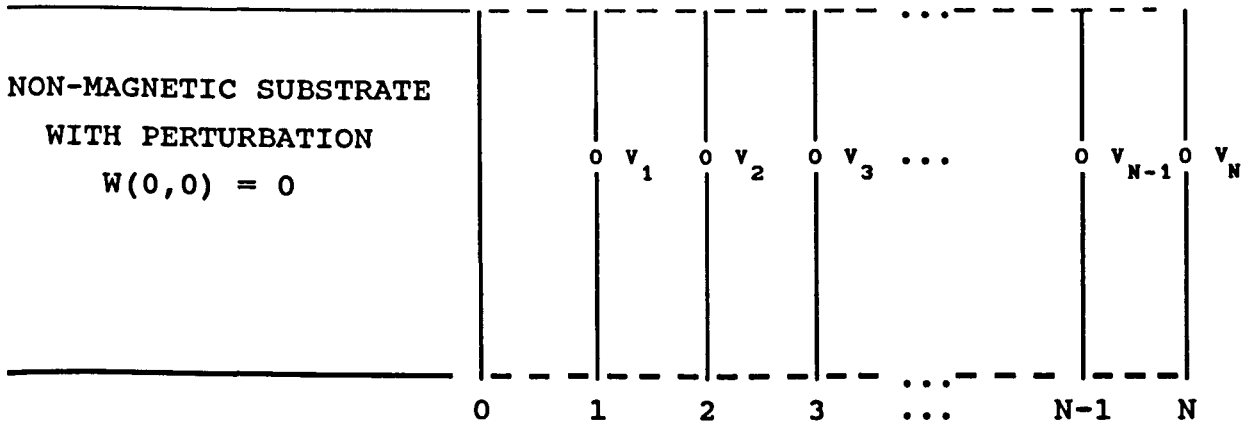

Fig.9 Numbering of atomic planes of an overlayer with the same nearest-neigbour hopping interactions but different perturbation V_i (for all i=1,2,...,N) in each layer.

Eq.(2.72) resembles the usual recursion step in conventional recursion methods. However, our recursion method is qualitatively different from all the traditional recursion methods since the Green function G^{N-1} and G^N in Eq.(2.72) describe two physically distinct systems. One is for an overlayer of N-1 atomic planes and the other for an overlayer on N atomic planes.This means,in particular, that all the intermediate G^{N-1},N=1,2,...N-2 are purely auxillary quantities and cease to have any physical significance when the whole overlayer is completed.

In constrast to the traditional recursion methods in which the proper termination is very important (see e.g. Haydock et al 1975) the present method does not involve any approximate termination of the recursion chain. Therefore, the Green's function in the overlayer surface plane G^N_{NN} is exact in terms of the exact substrate Green's function G^0_{00}.

Eq.(2.72) for the diagonal Green function $G^N_{NN}(E,\underline{K}_{\parallel})$ is the basis recursion formula for calculating the LDOS in the surface of a magnetic overlayer.

We now need to generalise the method to obtain all the matrix elements of G in the overlayer.The surface electron Green function G^N is related to the old G^{N-1} via Dyson equation

$$G^N = G^{N-1} + G^{N-1}WG^N \qquad (2.73)$$

where W is the perturbation matrix due to adding a layer N. Its diagonal and off-diagonal matrix elements are defined by

$$W_{NN} = W_N = V_N + 2T(\cos K_x a + \cos K_y a)$$
$$W_{N,N-1} = W_{N-1,N} = T \qquad (2.74)$$

In the matrix form, Eq.(2.73) becomes

$$G^N_{ij}(E,\underline{K}_{\parallel}) = G^{N-1}_{ij}(E,\underline{K}_{\parallel}) + \sum_{p,q} G^{N-1}_{ip} W_{pq} G^N_{qj} \qquad (2.75)$$

for all N = 1,2,...

Before the general matrix elements G^N_{ij} are calculated, G^{N-1} must again be extended to a space of dimension one higher than the space in which it is originally defined. [all the matrices in Eq.(2.73) must be of the same size]. This means that G^{N-1} acquires some additional matrix elements,

$$G^{N-1}_{ij}(E,\underline{K}_{\parallel}) = (EI-H^{N-1})^{-1}$$

$$= \begin{array}{c} \\ N \\ N-1 \\ N-2 \\ N-3 \\ \cdot \\ \cdot \\ \cdot \\ \cdot \end{array} \begin{array}{c} \begin{array}{cccccc} N & N-1 & N-2 & N-3 & \cdots & \end{array} \\ \left(\begin{array}{cccc} E & 0 & 0 & 0 & \\ 0 & E-H^{N-1}_{N-1,N-1} & E-H^{N-1}_{N-1,N-2} & 0 & \\ 0 & E-H^{N-1}_{N-2,N-1} & E-H^{N-1}_{N-2,N-2} & & \\ 0 & 0 & E-H^{N-1}_{N-3,N-2} & & \\ \cdot & \cdot & \cdot & \cdot & \\ \cdot & \cdot & \cdot & \cdot & \\ \cdot & \cdot & \cdot & \cdot & \\ \cdot & \cdot & \cdot & \cdot & \end{array}\right) \end{array}^{-1} \qquad (2.76)$$

Clearly, the diagonal additional matrix element is given by

$$G^{N-1}_{NN}(E,\underline{K}_{\parallel}) = 1/E \qquad (2.77)$$

where $H_{NN}(\underline{K}_{\parallel})$ is the Hamiltonian of a two-dimensional layer of electrons forming the Nth atomic plane of the overlayer and I is the unit matrix of dimension (N×N).

All other matrix elements connecting the adlayer N to the crystal below are zero, i.e.,

$$G^{N-1}_{iN} = G^{N-1}_{N,i} = 0 \qquad \text{for all } i = N-1,N-2,... \qquad (2.78)$$

Thus we are now in a position to solve Eq.(2.75) for G^{N}_{ij}. Using Eq.(2.74), we obtain

$$G^{N}_{ij} = G^{N-1}_{ij} + W_N G^{N-1}_{i,N} G^{N}_{N,j} + T\,[G^{N-1}_{i,N} G^{N}_{N-1,j} + G^{N-1}_{i,N-1} G^{N}_{N,j}] \qquad (2.79)$$

where N = 1,2,...

It is a straightforward matter to obtain the intermediate matrix elements $G^{N}_{N,j}$ and $G^{N}_{N-1,j}$. They are given by

$$G^{N}_{N,j} = \frac{EG^{N-1}_{N,j} + TG^{N-1}_{N-1,j}}{E - W_N - T^2 G^{N-1}_{N-1,N-1}} \qquad (2.80)$$

and

$$G^{N}_{N-1,j} = G^{N-1}_{N-1,j} + TG^{N-1}_{N-1,N-1} G^{N}_{Nj} \qquad (2.81)$$

for all N = 1,2,...
for all i,j = 0,1,2,...

Eqs.(2.79, 2.80 and 2.81) provided a very simple and efficient computational algorithm for calculating the exact surface Green function of an arbitrary overlayer.

After we have numerically generated all the matrix elements of the Green function G^{N}, we can calculate the DOS

in every atomic plane of an overlayer. From Eq.2.52) we write the LDOS as follows:

$$\rho_i(E) = -\frac{1}{\pi N_{\|}} \sum_{\underline{K}_{\|}} \mathrm{Im} G^{i}_{ii}(E,\underline{K}_{\|}) \qquad (2.82)$$

where $i = 1,2,\ldots,N$ and $N_{\|}$ is the number of atoms in the surface plane. Here, Im denotes the imaginary part of a complex analytic function and the surface BZ sum over $\underline{K}_{\|}$ is performed numerically using either Simpson's rule or the set of special Cunningham points (see e.g. Cunningham 1974). This will be described in the next subsection .

Once the LDOS of an overlayer has been calculated, other quantities such as the occupation number n_i or the energy of each layer E_i are easily determined. They are given by

$$n_i = \int_{-\infty}^{\infty} dE\ \rho_i(E) f(E) \qquad (2.83)$$

where f(E) is the Fermi-Dirac function and

$$E_i = \int_{-\infty}^{\infty} E\ f(E) \rho_i(E) dE \qquad (2.84)$$

Since we are interested in the ground-state (at $T=0^{0}K$), f(E) is a step function and Eq.(2.83) and (2.84) become

$$n_i = \int_{-\infty}^{E_F} \rho_i(E) dE \qquad (2.85)$$

and

$$E_i = \int_{-\infty}^{E_F} E\ \rho_i(E) dE \qquad (2.86)$$

where E_F is the Fermi-energy.

As it is shown in KS formalism (1971), there are two types of eigenfunctions associated with the surface.The first one extends through the entire crystal and the second wavefunction is associated with surface states, i.e.,states trapped (localized) at the surface and not present in the bulk. Since many surface properties are determined by surface states, it is desirable to discuss the properties of surface states.

In our method of adlayers with adjustable potentials, the presence of an adlayer may induced surface states. For a given $\underline{K}_{\parallel}$, the eigenvalues of possible surface states (if present) correspond to the poles of the Green function along the E-axis. These eigenvalues can be determined from the zero the denominator of Eq.(2.82).

The role of such surface states and how they can be included in our method will be discussed in sections (2.3.3.3). An application of the method of adlayers to a simple model will be given in the next subsection. The numerical results and discussion of the method are also presented there.

2.3.3 Numerical methods, results and discussions

In order to demonstrate the efficiency and accuracy of the method of adlayers and to interpret its results obtained in the previous subsections, we shall describe here our numerical calculation of the LDOS for an s-band in the tight-binding approximation.

In the present thesis, we have developed two distinct numerical methods for evaluating the two-dimensional Brillouin zone (BZ) sums appearing in the calculating of the LDOS of Eq.(2.82). The two numerical methods are called 'multiple integrals over a complex matrix (MIM) method and Cunningham points (CPs) method. Before we describe the methods, let us recall the Green function for an overlayer which appears in Eq.(2.72)

$$G^{i}_{ii}(E,\underline{K}_{\parallel}) = \frac{1}{\omega - V_i - T^2 G^{i-1}_{i-1,i-1}}$$

$$= G(E,K_x a,K_y a) \qquad (2.87)$$

where

$$W_i = V_i + w(K_{\parallel}) \ , \ \omega = E - w(K_{\parallel}) \qquad (2.88a)$$

and

$$w(K_{\parallel}) = 2T(\cos K_x a + \cos K_y a) \qquad (2.88b)$$

The bandwidth is determined by the hopping integral T and is equal to 12T (the centre of the band is at E=0). Throughout this thesis we put T=0.5 or one-twelfth of the bandwidth and we shall measure energy in units of 2T.

We can now describe the two numerical methods as follows.

2.3.3.1 Multiple integrals over a complex matrix (MIM) method

The aim of MIM method is twofold : first we want to find the limits and regions of integrations for LDOS. Secondly the two-dimensional BZ sums appearing in the LDOS for each energy region are computed by converting discrete sums to a double integral over a complex matrix (DIM).

A. Limits and regions of integrations for DOS

Eq.(2.82) gives the LDOS for an overlayer and it can be evaluated by passing to a continous representation for $\underline{K}_{\parallel}$, in which case we have to replace the two-dimensional BZ sum by an integral.

$$\frac{1}{N_{\parallel}} \sum_{\underline{K}} \longrightarrow \left(\frac{a}{2\pi}\right)^2 \int_{BZ} d\underline{K}_{\parallel} \qquad (2.89)$$

where the symbol BZ means that the integration must be restricted to the first BZ, $-\pi/a \leq K_x, K_y \leq \pi/a$ and K_x and K_y are components of $\underline{K}_{\parallel}$.

Thus Eq.(2.71) becomes

$$\rho_i(E) = -\frac{a^2}{4\pi^3} \int_{-\pi/a}^{\pi/a} \int_{-\pi/a}^{\pi/a} \mathrm{Im}\, G^i_{11}(E, K_x a, K_y a)\, dK_x dK_y \qquad (2.90)$$

Now since G^i_{11} is symmetic in K_x and K_y , the integration over $-\pi/a \leq K_x, K_y \leq \pi/a$ can be reduced to four times the integration over a quadrant $-\pi/a \leq K_x, K_y \leq 0$.

If we let $x = aK_x$ and $y = aK_y$ then Eq.(2.90) reduces to

If we let $x = aK_x$ and $y = aK_y$ then Eq.(2.90) reduces to

$$\rho_1(E) = -\frac{1}{\pi^3}\int_{-\pi}^{0}\int_{-\pi}^{0} \mathrm{Im}\, G^1_{11}(E,x,y)\,dxdy \qquad (2.91)$$

Upon substitution $X=\cos x$ and $Y=\cos y$ into Eq.(2.91) to get

$$\rho_1(E) = -\frac{1}{\pi^3}\iint_{\mathbb{R}} \mathrm{Im}\, G^1_{11}(E,X,Y)\,dXdY \qquad (2.92)$$

where the domain $\mathbb{R}$ is a section of the square of side 2. and is defined by the inequality

$$|\omega| \le 1 \qquad (2.93a)$$

or

$$|E - X - Y| \le 1 \qquad (2.93b)$$

Since $\rho_1(E)$ is an even function of K_x and K_y we restrict our calculations to the range of $-3 \le E \le 0$. There are three possibilities energy regions occur in this range :

(i) For $E < -3$ $\therefore$ it is empty so that $\rho_1(E) = 0$

(ii) For $-3 \le E \le -1$ $\therefore$ the region of integration is a triangle, $\mathbb{R}_1$ (see Fig.10) and Eq.(2.92) now becomes

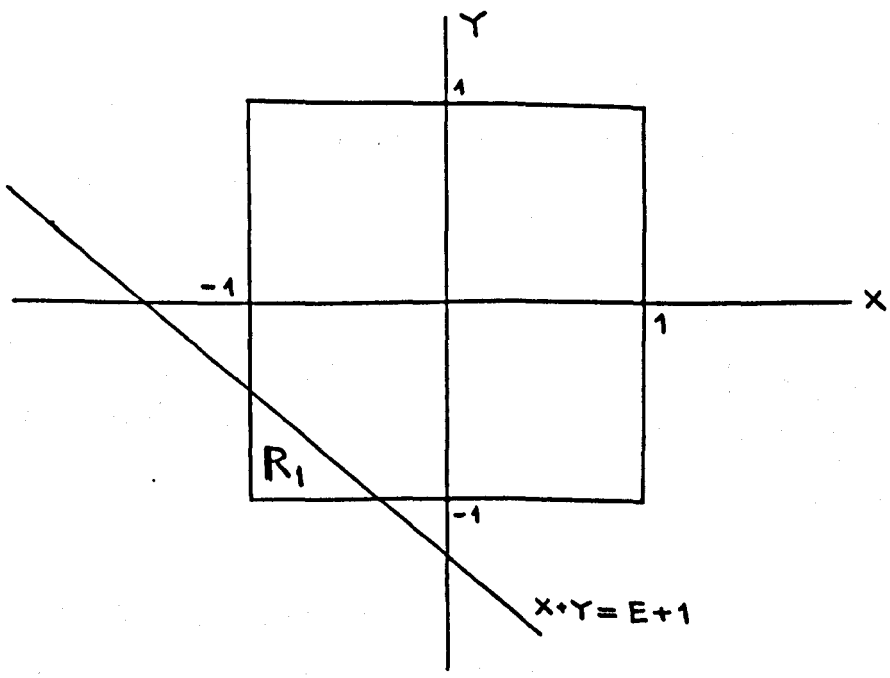

Fig.10 Domain of integration of Eq.(2.92) for $-3 \le E \le -1$

$$\rho_1(E) = -\frac{1}{\pi^3}\int_{X=-1}^{E+2}\int_{Y=-1}^{E+1-X} \mathrm{Im}\, G^1_{11}(E,X,Y)\,dXdY$$

$$= -\frac{1}{\pi^3}\int_{x=-\pi}^{-\cos^{-1}(E+2)}\int_{y=-\pi}^{-\cos^{-1}(E+1-\cos x)} \mathrm{Im}\, G^1_{11}(E,x,y)\,dxdy \qquad (2.94)$$

(iii) For $-1 < E \leq 0$ ∴ the region of integraion becomes ($\mathbb{R}_2+\mathbb{R}_3$) (see Fig.11)

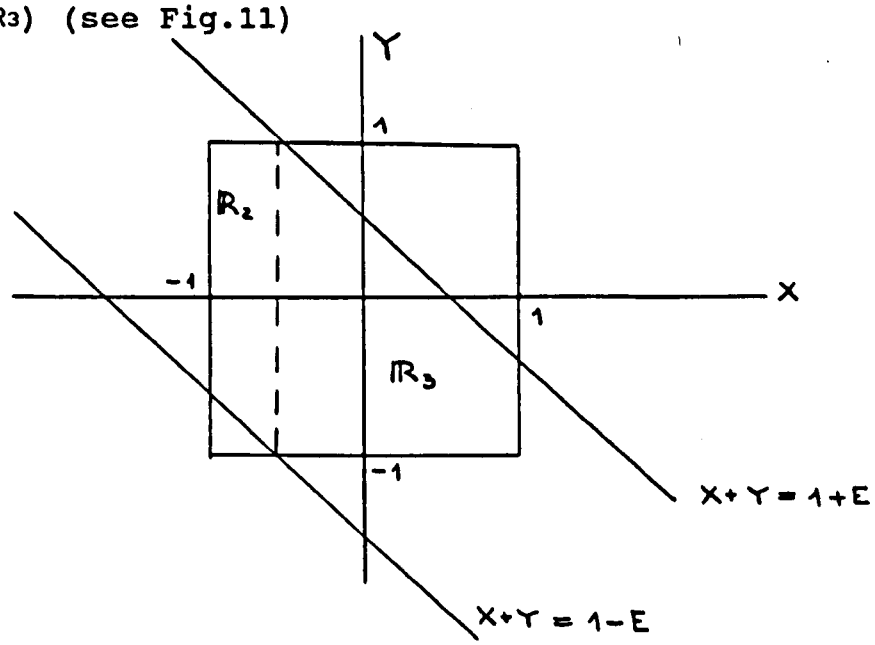

Fig.11 Domain of integration of Eq.(2.92) for $-1<E\leq 0$.

$$\rho_1(E) = -\frac{1}{\pi^3}\int_{X=-1}^{E}\int_{Y=E-1-X}^{1} \mathrm{Im}\, G^1_{11}(E,X,Y)\,dXdY + \int_{X=E}^{1}\int_{Y=-1}^{E+1-X} \mathrm{Im}\, G^1_{11}(E,X,Y)\,dXdY$$

$$= -\frac{1}{\pi^3}\int_{x=-\pi}^{-\cos^{-1}(E)}\int_{y=\cos^{-1}(E-1-\cos x)}^{0} \mathrm{Im}\, G^1_{11}(E,x,y)\,dxdy + \int_{x=-\cos^{-1}(E)}^{0}\int_{y=-\pi}^{-\cos^{-1}(E+1-\cos x)} \mathrm{Im}\, G^1_{11}(E,x,y)\,dxdy \qquad (2.95)$$

and the double integrals for each energy region are evaluated by using the DIM method which is described next.

B. Double integrals over a complex matrix (DIM)

The method is based on Simpson's algorithm and we shall refer to it as DIM. The only special feature in DIM is that the function to be double-integrated is a square complex matrix of dimension (N×N). It is, in fact, the Green's function G^1_{11} of Eq.(2.87) which is generated by the Subroutine EVA (see Appendix 1.)

The important point to note is that the energy E which appears in Eq.(2.88a) is a real quantity but the output of DIM is a square complex matrix (because G has real and imaginary parts). The DIM algorithm is given below

DIM's algorithm

Aim:to approximate the matrix integral $\rho_i(E)$ in Eqs.(2.94) and and (2.95)

Input : lower limit A, upper limit B, even positive integer N1 and N2, energy E, number of layers NMAX.

Output: Matrix S1=$\rho_i(E)$ where i=1,2,...,NMAX.

Step1 For M = 1,...,NMAX+1, set S1(M-1,M-1) = (0.0,0.0)

Step2 For J1 = 1,...,N1+1 do steps 3,4 and 11

Step3 For K=1,...,NMAX+1, set S2(K-1,K-1)=(0.0,0.0)

Step4 For J2=1,...,N2+1 do steps 5,6,7, and 8

Step5 Set H1=(B-A)/N1

Step6 Set X=A+H1*(J1-1)

If -3≤E≤-1 then

Set H2=(F22(X,E)-F11(X,E))/N2

Set Y+(J2-1)*H2+F11(X,E)

Else if -1≤E≤0 then

If A=-π then

```
          Set H2=(F44(X,E)-F33(X,E))/N2
          Set Y=(J2-1)*H2+F33(X,E)
   Else
          Set H2=(F22(X,E)-F11(X,E)/N2
          Set Y=(J2-1)*H2+F11(X,E)
   End if
Else
      Check 'E'
End if
```

Step7 Call subroutine EVA(NMAX,E,X,Y,RES)

Step8 For I1=1,...,NMAX+1 do steps 9 and 10

Step9 Set SS2=(H2/3)*DI(J2,N2)*RES(I1-1,I1-1)

Where

$$DI(J2,N2) = \begin{cases} 1 & \text{for } J2=1 \text{ or } N2+1 \\ 2 & \text{for odd } J2 \\ 4 & \text{for even } J2 \end{cases}$$

Step10 Set S2(I1-1,I1-1)=S2(I1-1,I1-1)+SS2

Step11 For I3=1,...,NMAX+1 do steps 12 and 13

Step12 Set SS1=(H1/3)*DI(J1,N1)*S2(I3-1,I3-1)

Step13 Set S1(I3-1,I3-1)=S1(I3-1,I3-1)+SS1/(π^3)

Step14 Output S1(I3-1,I3-1)

Step15 Stop.

2.3.3.2 Cunningham points (CP_s) method

In many theoretical calculations involving the electronic band-structure of solids, it is necessary to perform integrals over the first B.Z. The direct evaluation of such integrals as in the MIM method we described in (2.3.3.1) is not always possible. Other methods have, therefore, been developed for calculating BZ such as Gilat (1972), Noras (1980), Hardy et al.(1973) and Singhal (1972).

In constrast to MIM method, Baldereshi (1973), Chadi and Cohen (1973) proposed that such integrations can be accurately approximated by summing over a rather small selected number of special $\underline{K}$ points in the B.Z, with different weights asssociated with each point.Roughly speaking, a special $\underline{K}$ point is defined so that the value which any given periodic function of the wave vector assume at this point is an excellent approximation to the average value of the function over the B.Z.

Methods for finding such sets of special points have been further investigated by Monkhorst and Pack (1976), Cunningham (1974), Ren and Dow (1988) and Froyen (1988). In particular, Cunningham had applied the method of Chadi and Cohen to obtain the special point sets for the two-dimensional BZs. Our CPs method is based on the paper of Cunningham (1974) for a (100) surface simple cubic lattice.

The general theoretical method for generating all the special sets and their weights is described in Cunningham's paper. In the present thesis, we shall give an algorithm for the CP method for and arbitrary number of Cunningham points in one direction, say, K_x. We shall call this number NC and set $NC=2^n$, where n is an integer.

The CP method performs the same job as the MIM method except that the energy E which appears in Eq.(2.88a) is now complex $EC=E+i\varepsilon$ where ε is a small imaginary part. It is introduced to remove any singularity (if present) of the function to be integrated.

Usually a grid of 4NC(NC+1) points in the whole BZ is chosen for evaluating a two-dimensional B.Z integral. However, by taking symmetry considerations into account, the actual calculations are performed for only NC(NC+1)/2 points lying in the 1/8th of the BZ which is irreducible under symmetry operations.In order to obtain a greater degree of accuracy, the number of Cunningham point NC should be increased in the reduced symmetry until the results stabilize. This is the same requirement as in the calculations for the LDOS of an overlayer (see Fig.13). However, as we shall see later in chapter 3, a ten special point set corresponding to NC=4 gives a very satisfactory results for the calculation of the Goldstone mode and of spin-wave energies (see Fig.24 and Table 2.). To clarify the BZ summation using the CP method, we demonstrate a ten special point set in units of π/a for the simple square lattice as shown below :

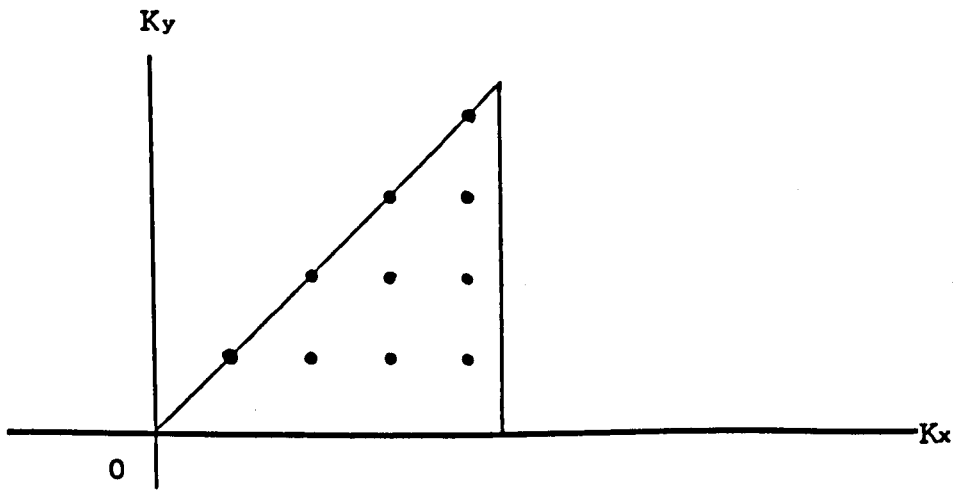

Fig.12 Ten points set for the square lattice.

It is clear from Fig.12 that the special points that fall on the diagonal of the square BZ have the weight 1/16 which is half of the weight of all the other points. This

is because the diagonal points are counted only once while the off-diagonal points are counted twice. The CP's algorithm for the (100) surface in the simple cubic lattice is described below:

CP's algorithm

Aim : to find the matrix DOS $\rho_1(E)$ of Eq.(2.82)

Input : number of Cunningham points NC, complex energy EC = E + iδ and NMAX is the number of layer

Output : matrix S prepared for the calculation of LDOS.

Step1 For I1 = 1,...,NMAX+1, set S(I1-1,I1-1) = (0.0,0.0)

Step2 For NK = 1,...,NC do steps 3,4 and 9

(generating special point sets for an arbitrary NC)

Step3 Set $K_x = [\pi(2NK-1)/2NC] - \pi$

Step4 For MK = 1,...,NK do steps 5,6,7 and 8

Step5 Set $KY = [\pi(2MK-1)/2NC] - \pi$

Step6 Call subroutine EVAL(NMAX,K_x,K_y,GS)

(see Appendix 2)

Step7 For I2 = 1,...,NMAX+1

set S1(I2-1,I2-1) = 2GS(I2-1,I2-1)/ NC^2

if NK = MK goto 990

990 For I7 = 1,...,NMAX+1

set S1(I7-1,I7-1) = 0.5*S1(I7-1,I7-1)

Step8 goto 991

991 continue

Step9 For I4 = 1,...,NMAX+1 set S(I4-1,I4-1) = S(I4-1,I4-1) + S1(I4-1,I4-1)

Step10 output S(I4-1,I4-1)

Step11 Stop.

This algorithm is used in the calculation of LDOS for an overlayer and is given in Appendix 2

2.3.3.3 Results and discussion

A. Non-magnetic overlayer

In Fig.13. we present the local DOS for an overlayer of seven atomic planes. The perturbation potential is set equal to zero across the overlayer and the LDOS for the surface (S), the first (S-1), second (S-2),..., and the sixth (S-6) layer below the surface are obtained. We also present the result for the bulk DOS (the dashed curve).

For $W_i=0$, $i=1,2,\ldots,$ N in the overlayer, the LDOS is symmetric above the middle of the band,i.e., we only need to calculate the LDOS for ($-3.0 \leq E \leq 0.0$). Comparing the LDOS for an overlayer with the bulk LDOS, we note the following results:

(i) A narrowing of the surface DOS is obtained. The difference between the surface and bulk DOS is an oscillating, algebraically decreasing function of distance into the bulk. It is interesting to see that the LDOS has healed to the bulk value no more than two or three atomic layers from the surface. This is because the atoms in those layers are now in a bulk-like enviroment.

The rapid recovery to the bulk properties as we proceed into the crystal is a very well-known and general result and was already described by KS [see Figs.2. and 3. of KS (1971) where small and large surface perturbations had been incluced]. This result has also been verified by the

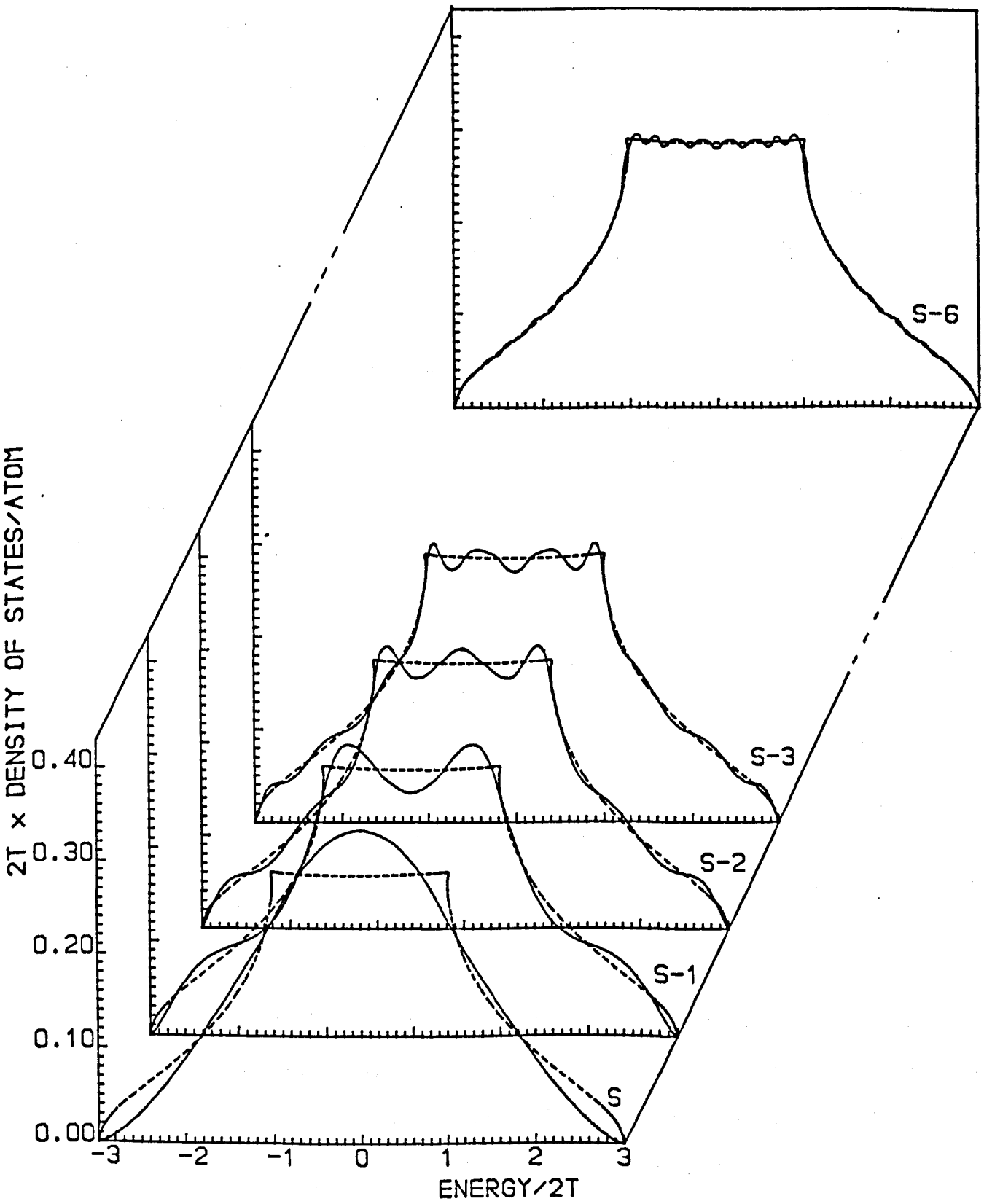

Fig.13 Local density of states of a non-magnetic overlayer of seven atomic planes. The surface layer (S), the first (S-1), second (S-2), third (S-3),...and the sixth (S-6) layer below the surface. The broken curves are the bulk density of states

recursion method of Haydock et al (1973), the method of moments of Cyrot-Lackmann et al (1973) and now by our method of adlayer (see Fig.13.)

(ii) At E = ± 1 (or 2T), the bulk DOS exhibits an infinite discontinuity in its slope (Van Hove singularities) while the curve for the surface layer has no singularities.

(iii) At the band egdes, the surface DOS rises more gradually than the bulk DOS. The surface DOS behaves like $E^{3/2}$ at the band edges while $E^{1/2}$ applied for the bulk DOS (see Fig.14.)

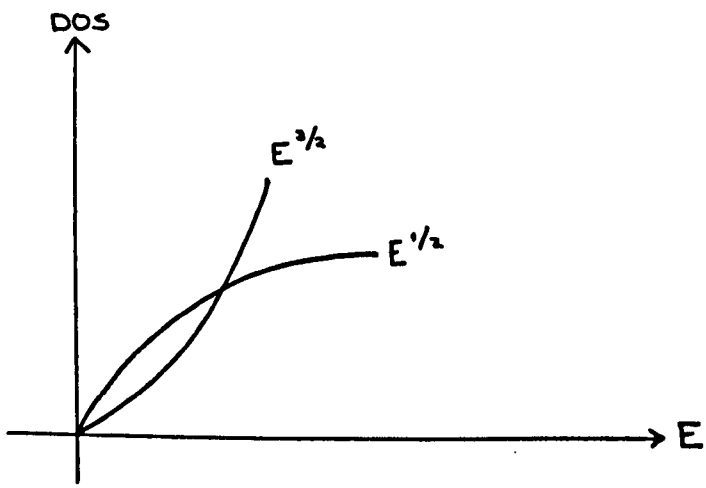

Fig.14

The LDOSs shown in Fig.13. were obtained numerically by the MIM and CPs methods. They are in complete agreement to several decimal points. The only difference is in the computing time. For example, to compute the LDOS for an overlayer of seven atomic planes by CPs method takes approximately 1/4 of that required for the MIM method Note that the results in Fig.13. were obtained by CPs method and correspond to sampling over 2080 points (corresponding to

nc=64) in 1/8th of the Brillouin zone and the calculations were done using double-precision arithmetic on a CRAY X-MP.

To check the results in Fig.13. we also evaluate the sum rule

$$\int_{-\infty}^{\infty} \rho_i(E)dE = 1 \qquad (2.96)$$

for an overlayer. It is clear from Table.1. that the sum rule is satisfied.

The sum rule in each layer	
Layer number	$\int_{-3}^{+3} \rho_i(E)dE$
1	0.993
2	0.994
3	0.996
4	0.998
5	0.999
6	0.999
7	0.9997

Table.1.

B. Magnetic overlayer

The HF potentials for an overlayer are defined by

$$V_{i\sigma} = V_i + U^{eff} n_{i,-\sigma} \qquad (2.97)$$

where V_i is the spin-independent potential and $U^{eff} n_{i,-\sigma}$ is the HF exchange potential. More explicitly, we can write

$$V_{i_\uparrow} = V_i + U^{eff} n_{i_\downarrow} \qquad (2.98a)$$

$$V_{i_\downarrow} = V_i + U^{eff} n_{i_\uparrow} \qquad (2.98b)$$

For simplicity, we set $V_{i_\uparrow} = 0$, i.e.,the centre of the spin-up band is no longer at zero but is now different for each atomic layer. We note that by setting $V_{i_\uparrow}=0$, we end up with $V_i=-U^{eff}n_{i\downarrow}$ after $n_{i\downarrow}$ is calculated self-consistently. In other words, each adlayer plane will represent a material characterized by a V_i which exactly cancelled $U^{eff}n_{i\downarrow}$, making $V_{i_\uparrow} \equiv 0$, hence

$$V_{i_\downarrow} = U^{eff}(n_{i_\uparrow} - n_{i_\downarrow}) \qquad (2.99)$$

where the number of spin-down, $n_{i\downarrow}$, particles has to be determined self-consistently for each layer.In fact, they are obtained by solving the HF equations

$$n_{i\sigma} = \int_{-\infty}^{E_F} dE\ \rho_i^\sigma(E) \qquad (2.100)$$

where E_F is the Fermi energy of the system and $\rho_i^\sigma(E)$ is the DOS for electrons in the i-th layer with spin-σ and is defined by

$$\rho_i^\sigma(E) = -\frac{1}{\pi N_\parallel} \sum_{K_\parallel} \mathrm{Im}\ G_{ii}^{i\sigma}(E) \qquad (2.101)$$

Here, G^σ denotes the Green's function with spin σ which is defined as in Eq.(2.79) but the diagonal perturbation V_N is now defined by

$$V_N = \begin{cases} 0 & \text{for } G^\uparrow \\ V_{i_\downarrow} & \text{for } G^\downarrow \end{cases} \qquad (2.102)$$

Our aim is to find self-consistently the HF potentials $V_{i_\downarrow}$ and hence the LDOS of spin-down particles for an overlayer. We proceed as follow:

First the perturbation in an overlayer is switched off, i.e, we set $V_N=0$ for all N = 1,2,... .The HF occupation numbers of spin-up particles can be found as in part A, i.e,

$$n_{i_\uparrow} = \int_{-\infty}^{E_F} dE\ \rho_i^{\uparrow}(E) \qquad (2.103)$$

where $\rho_i^{\uparrow}(E)$ can be determined with the help of Eqs(2.101 and 2.102).To determine $n_{i\downarrow}$ we need the following parameters $n_{i_\uparrow}$,U^{eff} and $V_{i\downarrow}$. We treat U^{eff} as a parameter and $n_{i_\uparrow}$ were already calculated in part A.Since $V_{i_\downarrow}$ is a function of $n_{i_\downarrow}$ (see Eq.(2.99), we have develop the following algorithm to to determine $n_{i_\downarrow}$ and $V_{i_\downarrow}$ self-consistently:

Algorithm for $n_{i_\downarrow}$ and $V_{i_\downarrow}$

Aim : To calculate $n_{i_\downarrow}$ and $V_{i_\downarrow}$ self-consistently

Input : $n_{i_\uparrow}$, U^{eff}, number of layer NMAX and tolerance δ

Output : $n_{i_\downarrow}$ and $V_{i_\downarrow}$

Step1 : For i=1,...,NMAX, set $n_{i_\downarrow}^{old} = 0.0$

Step2 : For i=1,...,NMAX, set $V_{i_\downarrow} = U^{eff}(n_{i_\uparrow} - n_{i_\downarrow}^{old})$

Step3 : Calculate $n_{i_\downarrow}^{new}$ from Eq.(2.103) with the parameters $n_{i_\downarrow}^{old}$ and $V_{i_\downarrow}$

Step4: For i=1,...,NMAX, set the difference $C_i=|n_{i_\downarrow}^{old}- n_{i_\downarrow}^{new}|$

Step5 : If $C_i < \delta=0.00001$ then output $n_{i_\downarrow}$ and $V_{i_\downarrow}$ Stop.

Step6 : If $C_i > \delta=0.00001$ then do steps 7,8

  Step7 : For i=1,...,NMAX+1 set $n_{i_\downarrow}^{old} = n_{i_\downarrow}^{new}$

  Step8 : Goto Step2

Step9 : Stop.

Once $V_{1\downarrow}$ is known, the calculation of the LDOS of spin-down band for the magnetic overlayer is straightforward. To illustrate the method, we first deposit one atomic layer on top of the (100) surface of a a non-magnetic substrate.

The surface perturbation $V_{1\downarrow}$ is treated in the HF approximation as described and the LDOS of spin-down particles are determined for several values of the Coulomb interaction U^{eff} (see Fig.15.). Here we wish to make the following important point: in the process of computing the HF LDOS by the CPs method with a complex energy EC=E+iε, the imaginary part ε has a strong influence on the shape of the DOS curve. For example, if ε is too small say 0.001, the DOS curve contains many peaks. This is because the DOS is a collection of delta function like peaks and the value of ε determines the width of these peaks. On the other hand, if ε is too big, say 0.3, then the peaks in the DOS curve are averaged out to a single peak but its width is too large. A convenient value of ε for each set of CPs must be determined so that a reasonable DOS curve is obtained in the two parameters space ε and nc. For the ten point set of CPs, ε=0.1 leads to a stable DOS.

In Fig.(16), the self-consistent results for the number of spin-down particles $n_{1\downarrow}$ are shown as a function of U^{eff} (E_F=-1.5). It is obvious that the stronger the Coulomb repulsion energy U^{eff}, the smaller is the number of spin-down electrons per atom.

As already discussed in section (2.3.2), the presence of an impurity layer of atoms may induce surface states. Our

tight-binding model of a semi-infinite crystal leads to surface states if a strong enough perturbation occurs at the surface. When such surface states are present, they remove some spectral weights from the perturbed bulk states (see Fig.15e.).

In some simple case, the Green's function method allows us to separate the surface states from bulk states by searching for isolated poles of the Green function. This will be now demonstrate for the single adlayer overlayer. The poles of the Green function which determine the energy values of surface states can be found by setting the denominator of Eq.(2.69) equal to zero. i.e,

$$\omega - V_{i_\downarrow} - T^2 G^0_{00}(E,K_\parallel) = 0 \qquad (2.104)$$

provided the conditions $\omega^2-4T^2 > 0$ and $|V_{i_\downarrow}| > T$ are satisfied simultaneously (KS 1971).

For a given $K_\parallel$, an isolated pole can be located either below or above or inside the band states ($-3.0 \leq E \leq 3.0$) but since the Coulomb interaction U^{eff} is always positive, there is an isolated pole only for $\omega > 1$. Let us first investigate when the surface states lie completely outside the band states, i.e., above $E_{min} = +3.0$. For $\omega>1$, we have

$$\omega = E_{min} - w(K_\parallel) \qquad \text{hence}$$

$$\omega_{max} = 3 - (-2) \qquad \text{see (Eq.2.23b)}$$

and

$$G^0_{00}(E,K_\parallel) = \frac{2}{\omega + \sqrt{\omega^2 - 1}} \qquad \text{(see Eq.2.68b)}$$

It is clear from Eq(2.104) that $V_{1\downarrow} \propto 4.9495$. Since the position of each surface state depend on the parameter $V_{1\downarrow}$, the centre of gravity of the band of surface states shifts with changing $V_{1\downarrow}$. It can be seen from Fig(15) that there are three different situations

(i) If $V_{1\downarrow} < 0.5$ then there are no surface states and the only contribution to the LDOS comes from bulk states. The number of particle sum rule is satisfied by the band state alone (see Fig.15a).

(ii) If $0.5 < V_{1\downarrow} < 4.9495$ then the surface states lie inside the band of bulk state, i.e., we have a situation where surface and bulk states coexist (see Fig.15.b,c and d). Both states contribute to the sum rule.

(iii) If $V_{1\downarrow} > 4.9495$ then surface states are fully separated from the bulk states (see Fig.15e). Again the sum rule is satisfied by both states.

One of the advantages of our method of adlayers using a complex energy is that it allows us to treat both bulk and surface states in one computation. This is now illustrated for a magnetic overlayer of seven atomic planes.

We deposit seven atomic layers on top of a (100) surface and determine again the HF potential $V_{1\downarrow}$ for all i=1,2,...,7 self-consistently. Fig.17 shows the LDOS for

the spin-down band with U^{eff}= 30.5. It is clear that the number of spin-down electrons per atom at the Fermi energy E_F =-1.5 must be very small compared with that of spin-up electrons. This is illustrated in Fig.(18) We have, therefore, an "almost strong" ferromagnetic overlayer in this particular example.

We can summarise the main results of chapter 2. as follow: the method of adlayers allows us to compute within the tight-binding formalism very accurately and efficiently all the matrix elements of the one-electron Green function for an arbitrary ferromagnetic overlayer. We have implemented such a calculation for a single-orbital model but we can have also indicated that the method can be readily extended to a multiorbital band. We shall now use the results of chapter 2. to investigate spin waves in a magnetic overlayer.

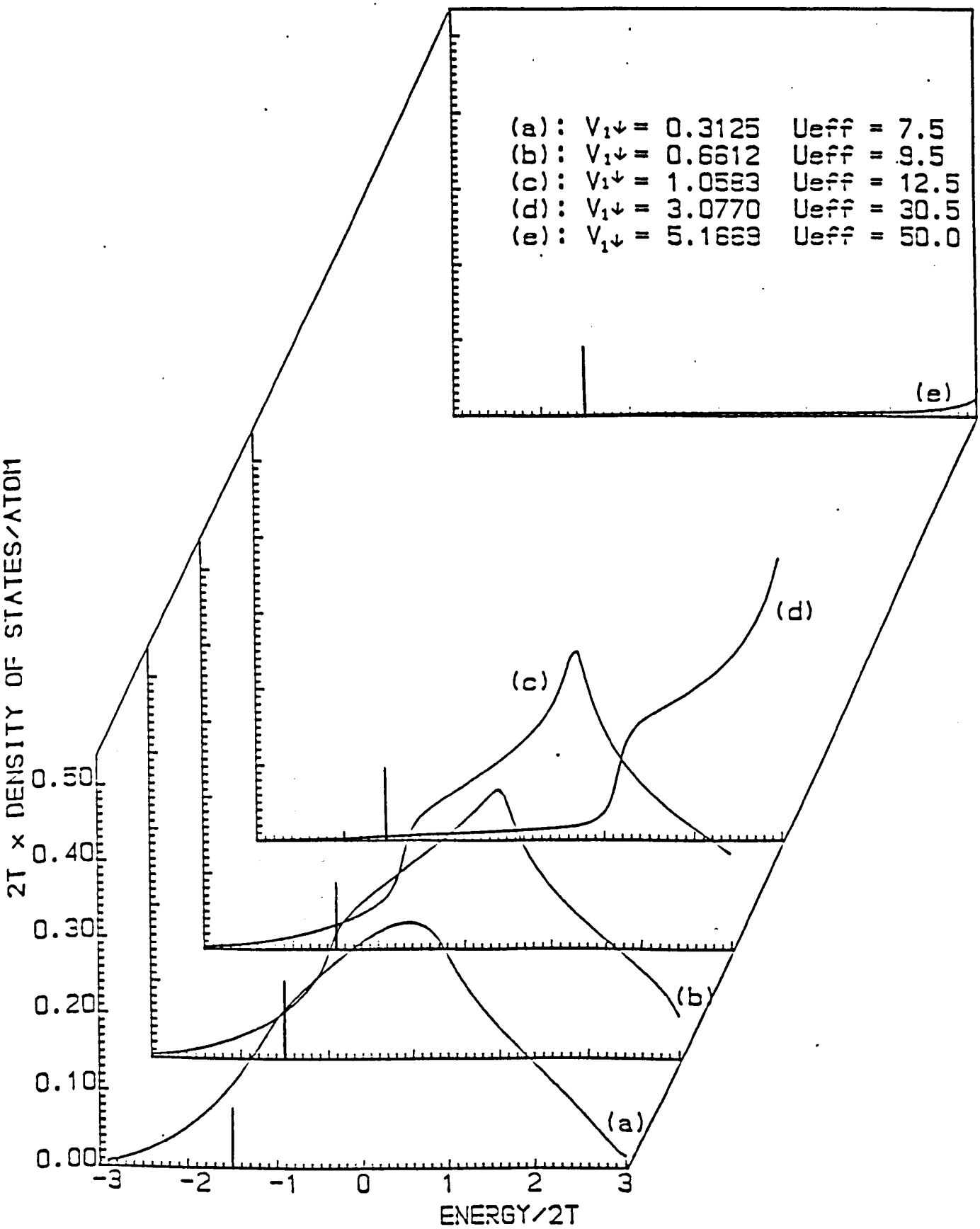

Fig.15 Local density of states of spin-down band of a single adlayer system for different values of surface perturbations These perturbations are treated in the HF approximation. The vertical line indicates the Fermi energy EF=-1.5 .

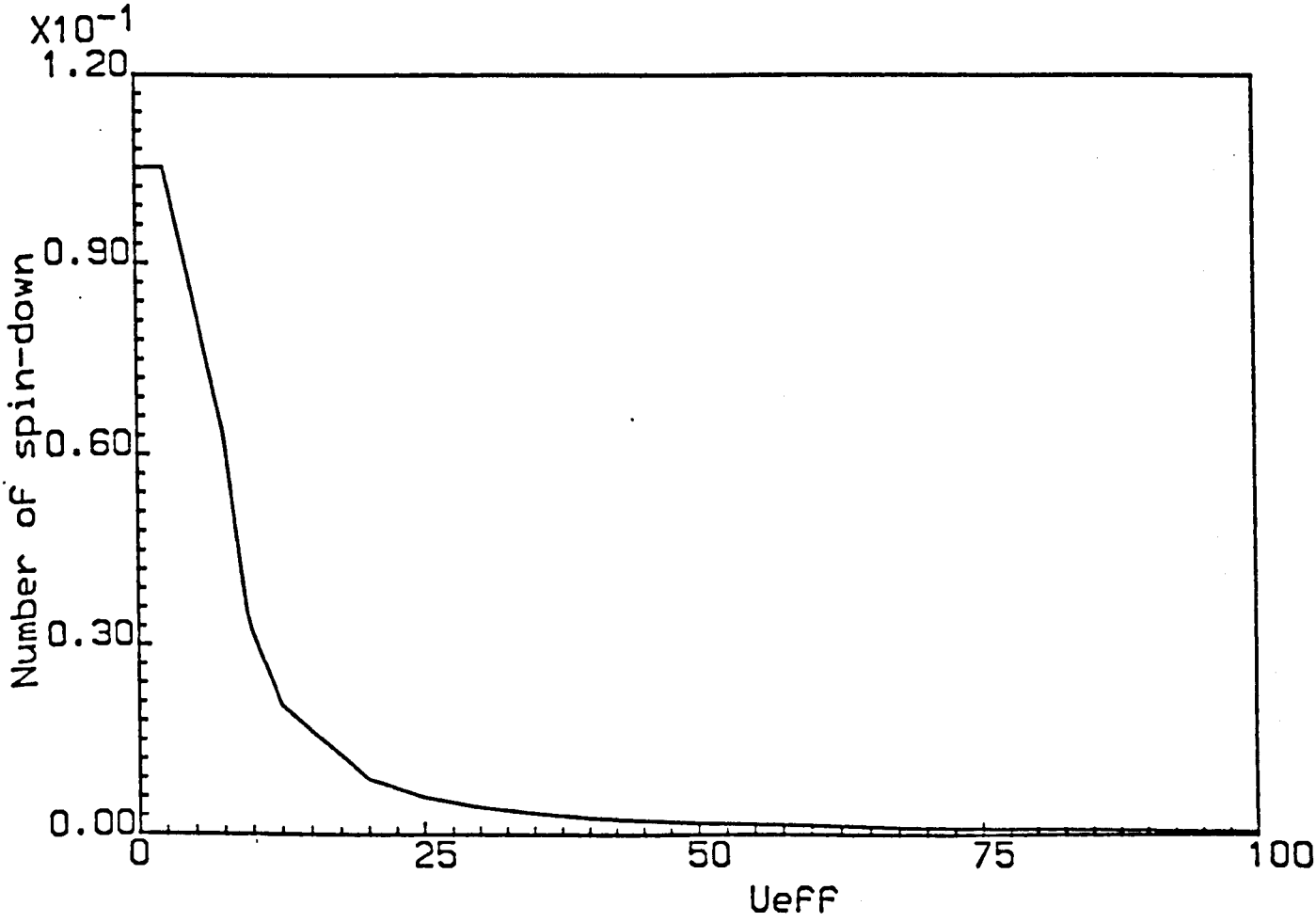

Fig.16 Dependence of spin-down particles per atom on Coulomb repulsion energy UeFF for a single adlayer system at Fermi energy Ef=-1.5 .

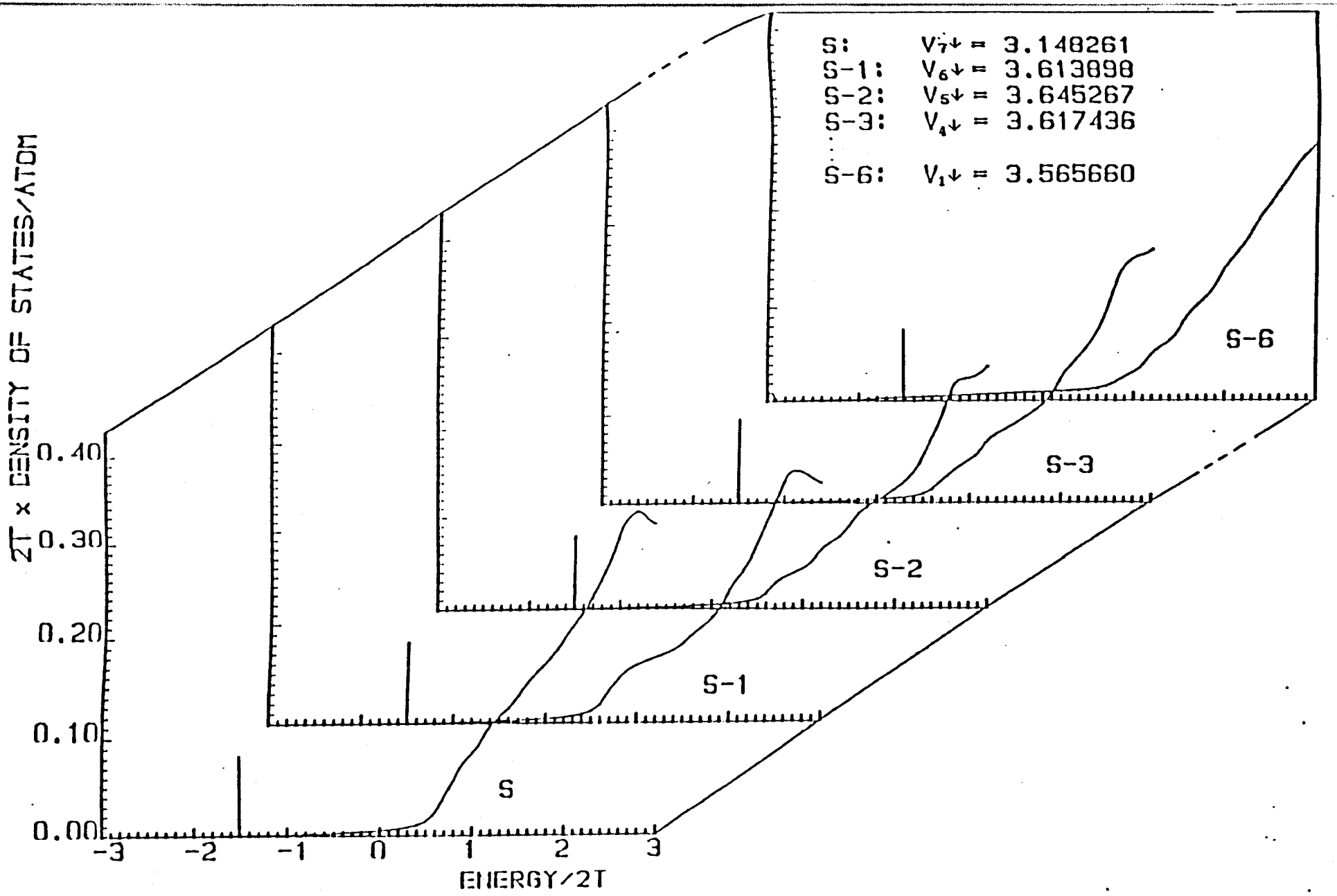

Fig.17 Local density of states of spin-down band for a magnetic overlayer of seven atomic planes. The surface layer (S), the first (S-1), second (S-2), third (S-3),..., the sixth (S-6) layer below the surface. The vertical line indicates the Fermi level EF=-1.5, UeFF=30.5 and NC=61.

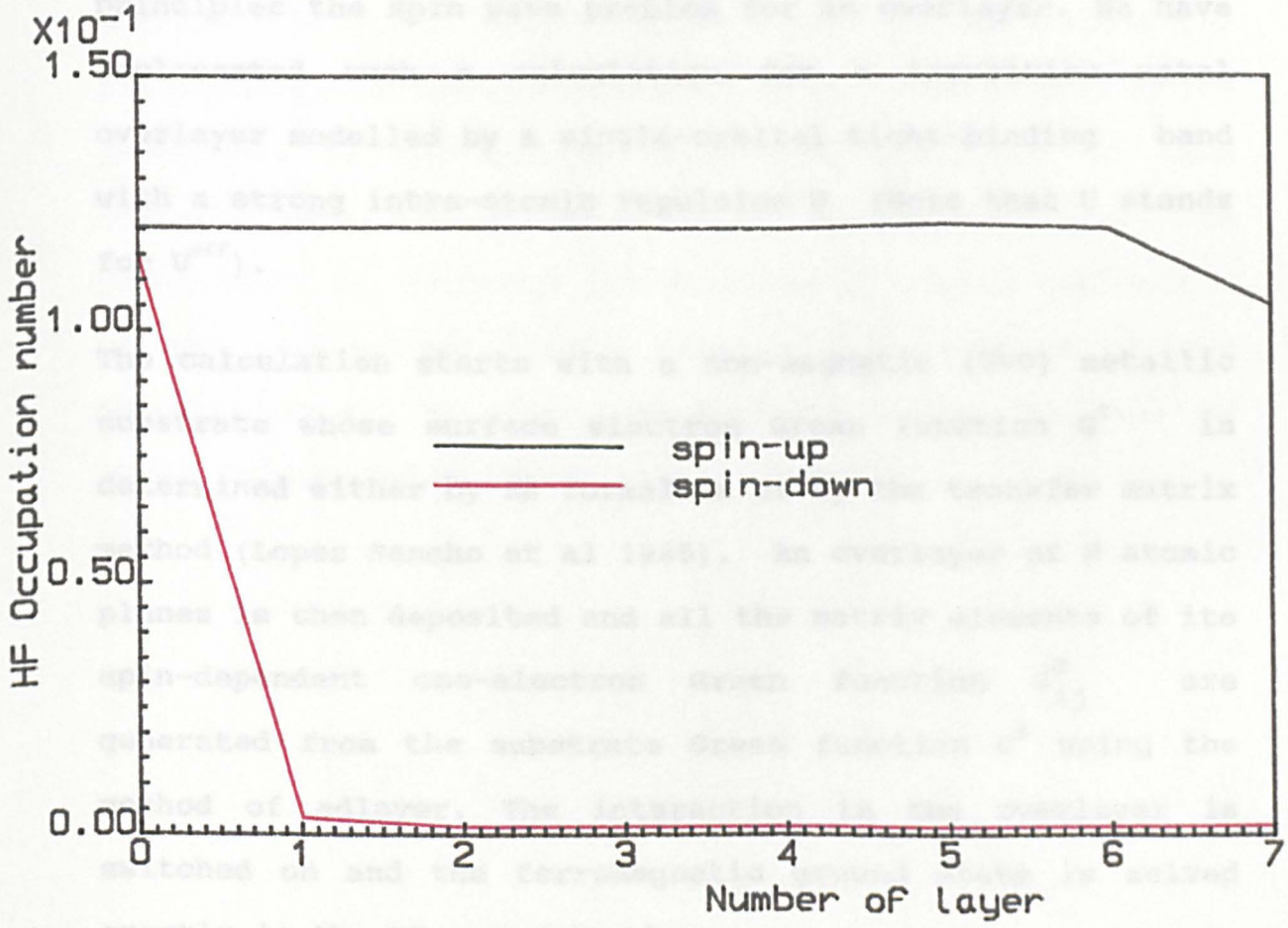

Fig.18 Distribution of spin-up and spin-down particles per atom at Fermi energy EF=-1.5, UeFF=30.5 and NC=64.

First principle calculation of spin waves in an overlayer

3.1 Introduction

The goal of this chapter is to solve from the first principles the spin wave problem for an overlayer. We have implemented such a calculation for a transition metal overlayer modelled by a single-orbital tight-binding band with a strong intra-atomic repulsion U (Note that U stands for U^{eff}).

The calculation starts with a non-magnetic (U=0) metallic substrate whose surface electron Green function G^0 is determined either by KS formalism or by the transfer matrix method (Lopez Sancho et al 1985). An overlayer of N atomic planes is then deposited and all the matrix elements of its spin-dependent one-electron Green function G^{σ}_{ij} are generated from the substrate Green function G^0 using the method of adlayer. The interaction in the overlayer is switched on and the ferromagnetic ground state is solved exactly in the HF approximation.

All the matrix elements of the HF dynamic unenhanced susceptibility $\chi^{HF}_{ij}(\omega,q_{\parallel})$ in the overlayer are then computed from the HF one-electron Green's function G^{σ} (see sections 1.5 and 2.3.3.3). The ground is now prepared to attack the spin wave problem. We recall that spin waves are poles of the full dynamic transverse spin susceptibility $\chi^{-+}(\omega,q_{\parallel})$ which is given in the RPA by $\chi^{-+} = (I-U\chi^{HF})^{-1}\chi^{HF}$. The eigenfrequencies ω of all spin wave modes in the

overlayer can thus be determined from the secular equation:

$$\text{Det} \mid I - U\chi^{HF}(\omega, q_{\parallel}) \mid_{NxN} = 0$$

where I is the NxN unit matrix.

The plan of chapter 3 is as follow: first the theoretical formulation for the full dynamic susceptibility χ^{RPA} of an overlayer is given. Next we compute the spin wave modes for a single-adlayer system for a range of Hubbard interaction parameters U. The adlayer spin wave spectrums is then compared with the spectrum in an unsupported layer. In particular, we determine the exchange stiffness constant D of the unsupported layer. Finally, the results of our calculation of the spin wave energies of an overlayer of seven ferromagnetic layers are presented.

3.2 Theoretical formulation of χ^{RPA} for an overlayer.

Our aim is to calculate the dynamic susceptibility χ^{RPA} for an overlayer and there are at least three reasons why we have chosen an overlayer rather than an unsupported thin film:

(i) In the past theoretical studies of the dynamic susceptibility and of spin waves in thin films have been carried out mostly for magnetic insulators described by the Heisenberg model. As far as we know, there is no theoretical work on metallic films on a substrate based on the itinerant model of ferromagnetism.

(ii) It is computationally more convenient to study an overlayer because one-electron Green functions are less singular for a semi-infinite system than for a free-standing metallic thin film. It is also preferable to consider an overlayer rather than surface because the overlayer problem can be solved exactly.

(iii) Films studied experimentally are always on a substrate.

To determine spin waves in the surface and in any other layer of the overlayer system, we must be able to solve for the dynamic susceptibility matrix $\chi^{-+}_{ij}(\omega,q_{\parallel})$ in all atomic planes $M \leq i,j \leq N$, where N is the thickness of the overlayer and M is the thickness of the substrate (see Fig.19).

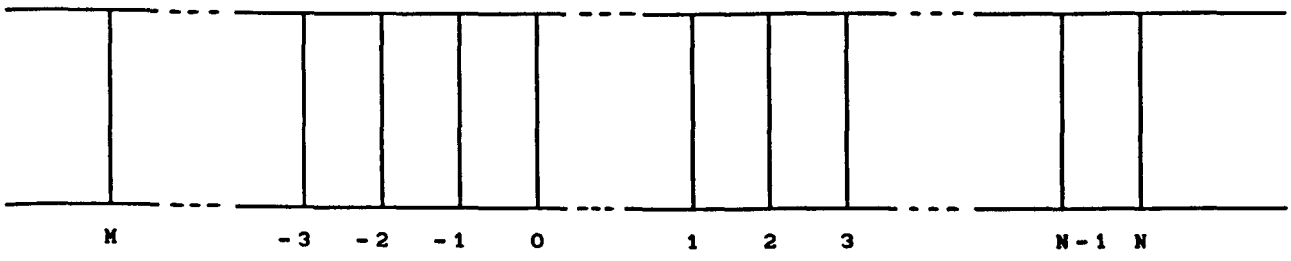

Fig.19

The RPA susceptibility $\chi^{-+}_{ij}(\omega,q_\parallel)$ can be found from the general matrix equation (1.100) derived in Section 1.4 $\chi^{-+}= \chi^{HF}+ \chi^{HF}U\chi^{-+}$ This matrix equation is equivalent to the following system of linear equations:

$$\chi^{-+}_{N,N}(\omega,q_\parallel) = \chi^{HF}_{N,N}(\omega,q_\parallel) + \sum_{j=1}^{N} \chi^{HF}_{N,j}\, U_j\, \chi^{-+}_{j,N}(\omega,q_\parallel)$$

$$\chi^{-+}_{N-1,N}(\omega,q_\parallel) = \chi^{HF}_{N-1,N}(\omega,q_\parallel) + \sum_{j=1}^{N} \chi^{HF}_{N-1,j}\, U_j\, \chi^{-+}_{j,N}(\omega,q_\parallel)$$

$$\vdots$$

$$\chi^{-+}_{1,N}(\omega,q_\parallel) = \chi^{HF}_{1,N}(\omega,q_\parallel) + \sum_{j=1}^{N} \chi^{HF}_{1,j}\, U_j\, \chi^{-+}_{j,N}(\omega,q_\parallel) \qquad (3.1a)$$

- - - - - - - - - - - - - - - - - -

$$\chi^{-+}_{0,N}(\omega,q_\parallel) = \chi^{HF}_{0,N}(\omega,q_\parallel) + \sum_{j=1}^{N} \chi^{HF}_{0,j}\, U_j\, \chi^{HF}_{j,N}(\omega,q_\parallel)$$

$$\chi^{-+}_{-1,N}(\omega,q_\parallel) = \chi^{HF}_{-1,N}(\omega,q_\parallel) + \sum_{j=1}^{N} \chi^{HF}_{-1,j}\, U_j\, \chi^{-+}_{j,N}(\omega,q_\parallel)$$

$$\vdots$$

$$\chi^{-+}_{M,N}(\omega,q_\parallel) = \chi^{HF}_{M,N}(\omega,q_\parallel) + \sum_{j=1}^{N} \chi^{HF}_{M,j}\, U_j\, \chi^{-+}_{j,N}(\omega,q_\parallel) \qquad (3.1b)$$

where

$$U_j = \begin{cases} U & \text{if } 1 \le j \le N \\ 0 & ; \text{ otherwise} \end{cases} \qquad (3.1c)$$

The system of N equations (3.1a) is for an overlayer containing N unknowns $\chi^{-+}_{N,N}$, $\chi^{-+}_{N-1,N}$, ... , $\chi^{-+}_{1,N}$. The system (3.1b) is for the susceptibility matrix elements in the non-magnetic substrate.

Therefore, in general, we have N+|M|+1 equations for N+|M|+1 unknowns $\chi^{-+}_{N,N}$,$\chi^{-+}_{N-1,N}$, ... , $\chi^{-+}_{M,N}$. However, we first solve the NxN system for $\chi^{-+}_{N,N}$, $\chi^{-+}_{N-1,N}$, ... , $\chi^{-+}_{1,N}$ and then show that $\chi^{-+}_{0,N}$, $\chi^{-+}_{-1,N}$, ... , $\chi^{-+}_{M,N}$ can be expressed in terms of $\chi^{HF}_{ij}(\omega,q_{\parallel})$ and in terms of the first N elements $\chi^{-+}_{j,N}$ for all j = 1,2, ... ,N.It follows that it is sufficient to solve a system of linear equations whole size is equal to the number of atomic planes in the overlayer

The solution of the first N equations for the overlayer is given by

$$(\chi^{-+})_{NxN} = [I-U(\chi^{HF})]^{-1}_{NxN} (\chi^{HF})_{NxN} \qquad (3.2)$$

where I is the unit matrix of dimension (NxN),

$$(\chi^{-+})_{NxN} = \begin{pmatrix} \chi^{-+}_{N,N} \\ \chi^{-+}_{N-1,N} \\ \cdot \\ \cdot \\ \cdot \\ \chi^{-+}_{1,N} \end{pmatrix} \qquad (3.2a)$$

and

$$(\chi^{HF})_{N\times N} = \begin{pmatrix} \chi^{HF}_{N,N} \\ \chi^{HF}_{N-1,N} \\ \cdot \\ \cdot \\ \cdot \\ \chi^{HF}_{1,N} \end{pmatrix} \qquad (3.2b)$$

It is now clear from the form of the system (3.1b) that all other elements $\chi^{-+}_{0,N}$, ... , $\chi^{-+}_{M,N}$ in the substrate can be expressed in terms of the same inverse matrix that appears in Eq.(3.2).

Clearly, the spin wave modes in each layer of the overlayer are determined from the condition that the inverse matrix becomes singular, i.e. , from zeros of the determinant in Eq.(3.2),

$$\text{Det} \mid I - U(\chi^{HF}) \mid_{N\times N} = 0 \qquad (3.3)$$

Since the Goldstone condition $q_{\parallel} \to 0$ as $\omega \to 0$ must be satisfied for an overlayer, $\text{Det}[I-U(\chi^{HF})]_{N\times N}$ is a continous function for small ω and, therfore, by plotting the determinant against the frequency we may obtain all spin wave modes. This is illustrated qualitatively in Fig.(20).

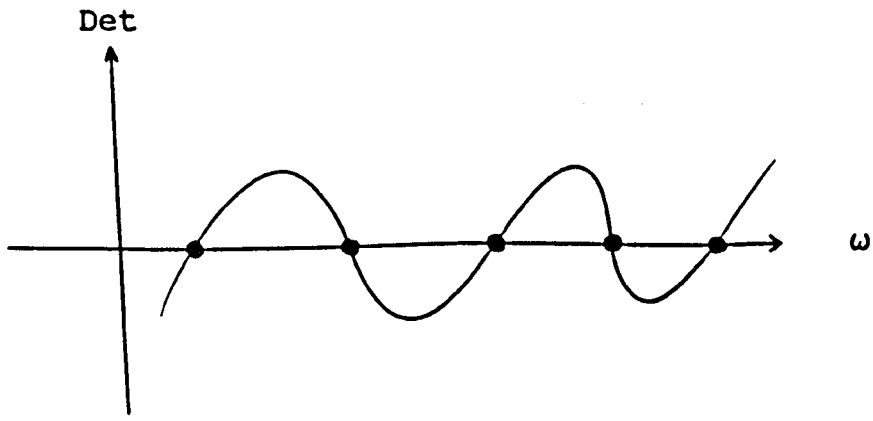

Fig.20 • spin wave modes

3.3 Calculation of χ^{RPA} for a single-adlayer

Our aim in this section is to apply the general theoretical formulation for χ^{RPA} in an overlayer (see section 3.2) to an overlayer consisting of a single adlayer.

Spin wave energies for a single-adlayer system (see Fig.9) can be obtained from the general Eq.(3.3)

$$\text{Det } |I-U\chi^{HF}_{ij}(\omega,q_{\parallel})|_{1x1} = 0 \qquad (3.6)$$

where U is the effective Coulomb interaction and the kernel $\chi^{HF}_{ij}(\omega,q_{\parallel})$ is the usual transverse susceptibility of non-interaction electrons moving in a spin dependent HF potential $V_{i\sigma} = V_i+U<n_{i\sigma}>$.

Here, $\chi^{HF}_{ij}(\omega,q_{\parallel})$ can be expressed in terms of the one-electron HF Green's function $G^{\sigma}_{ij}(E)$ as shown in section 1.5

Since $Im\chi^{HF}_{ij}(\omega,q_{\parallel})$ is zero outside the Stoner continuum, the spin wave energies for a single-adlayer are determined from the following equation :

$$1 - U\,Re\,\chi^{HF}_{11}(\omega,q_{\parallel}) = 0 \qquad (3.7)$$

To calculate the spin wave spectrum we must first determine numerically the kernel $Re\,\chi^{HF}_{11}(\omega,q_{\parallel})$ (see Eq.1.119 with i=j=1). We recall here that

$$Re\chi^{HF}_{11}(\omega,q_{\parallel}) = -\frac{1}{\pi N_{\parallel}} \sum_{K_{\parallel}} \int_{-\infty}^{E_F} dE \; [\; Im G^{\uparrow}_{11}(E,K_{\parallel})\; Re G^{\downarrow}_{11}(\omega+E,K_{\parallel}+q_{\parallel}+G)$$

$$+ \; Im G^{\downarrow}_{11}(E,K_{\parallel})\; Re G^{\uparrow}_{11}(E-\omega,K_{\parallel}+q_{\parallel}+G)\;] \qquad (3.8)$$

where $q_{\parallel}$ is the wave vector from the first B.Z and the reciprocal lattice vector G keeps the points $K_{\parallel}+q_{\parallel}$ within the first B.Z (i.e. take care of Umklapp-process). Since our Green function is inversely proportional to cosine functions, we can drop G in Eq.(3.8).

We wish to point out that since our HF one-electron Green funtion $G^{\sigma}_{11}(E,K_{\parallel})$ in the adlayer is determined exactly, our calculation of $Re\chi^{HF}_{11}$ is also exact.

3.3.1 Numerical calculations and discussion

We present in this section our numerical results for the spin wave spectrum of a single-adlayer, of an unsupported layer and also for the exchange stiffness constant D_{2d} of a two dimensional layer.

Let us first compute the energies of spin wave modes in an overlayer consisting of a single atomic plane on a (100) s.c non-magnetic metallic substrate. To calculate the spin wave spectrum we solve Eq(3.7) for $0 \leq q_{\parallel} \leq \pi/a$, where $q_{\parallel}=(q_x,q_y)$ is from the first B.Z.

For an arbitrary wave vector $q_{\parallel}$,there is no symmetry and we have to perform numerically the summation in $\mathrm{Re}\chi^{HF}_{11}(\omega,q_{\parallel})$ in Eq.(3.8) over the whole two-dimensional B.Z. Alternatively we can perform the summation over the irreducible B.Z (here 1/8th of the B.Z in our CP$_\alpha$ method) by applying full point group symmetry operations to the function in Re $\chi^{HF}_{11}(\omega,q_{\parallel})$.

In either case, the summation is computationally much more demanding than the calculation of the density of states. For simplicity, we consider the wave vector $q_{\parallel}$ in the x-direction only, i.e., we set $q_y = 0$. This choice of the wave vector q_x reduces the summation over the two-dimensional B.Z to one half of the B.Z.

This is due to the reflection symmetry along the x-axis (see Fig.21). Again any point $K_{\parallel}+ q_x$ which lies outside the upper-half B.Z will be brought back into the zone by a reciprocal vector G.

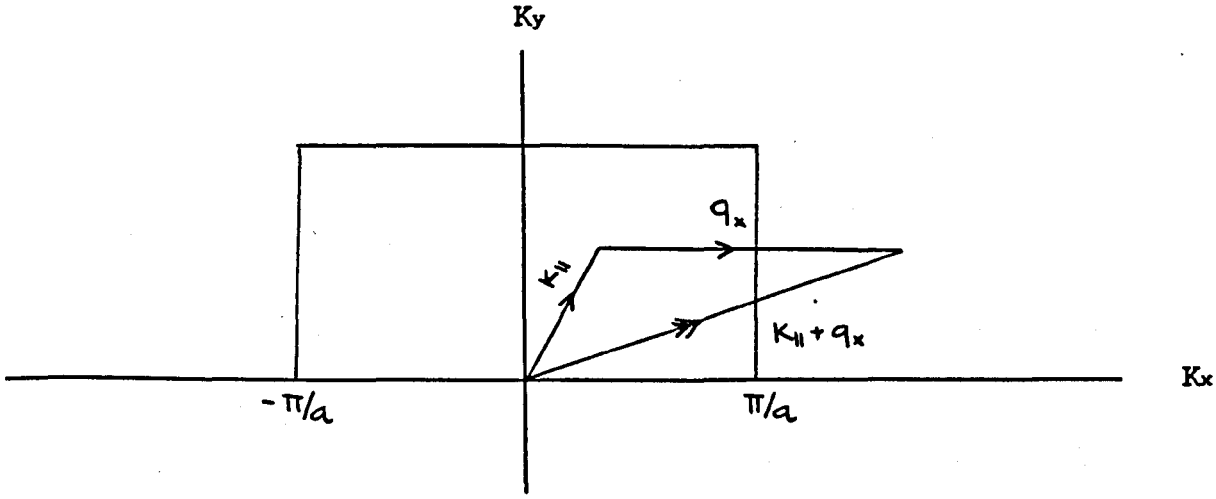

Fig.21 Summation of the Re $\chi^{HF}_{ij}(\omega,q_x)$ over the upper-half of a two-dimensional B.Z for an arbitrary wave vector q_x.

Before computing the spin wave modes we have developed a test to find a pole of the spin wave spectrum from a graphical solution. For any given q_x from the first B.Z we can plot Re $\chi^{HF}_{11}(\omega,q_x)$ as a function of ω and the pole of χ^{-+} is obtained from the intersection of the curve Re $\chi^{HF}_{11}(\omega,q_x)$ with the straight line 1/U. This is shown qualitatively in Fig.(22).

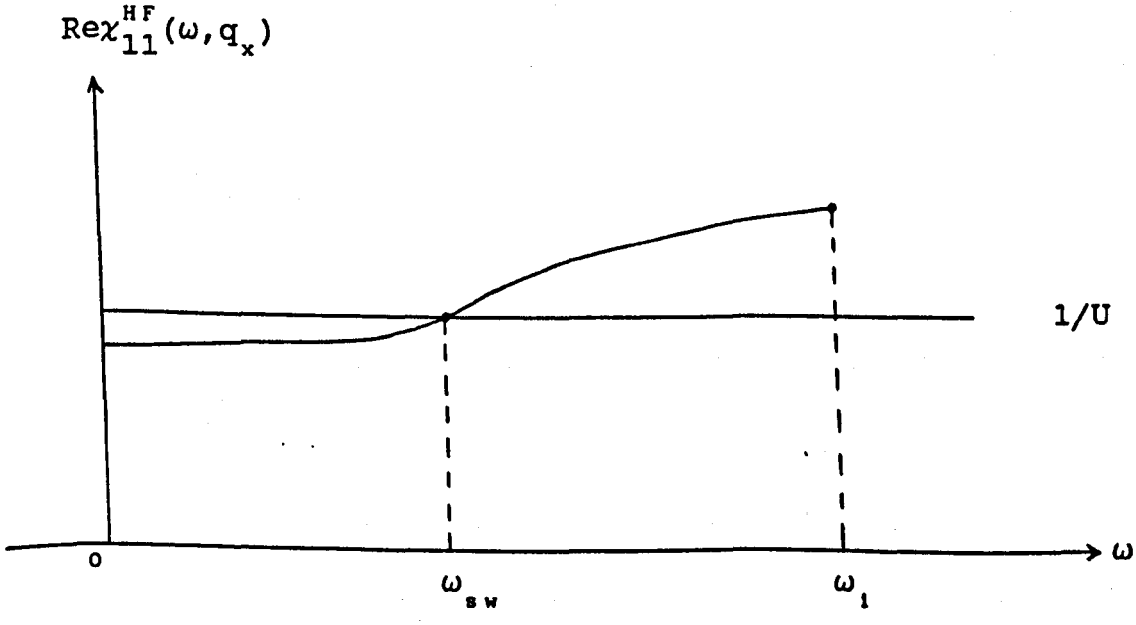

Fig.22 Graphical solution of the transcendental equation (3.7).

The Goldstone mode is then determined by solving $\mathrm{Det}|I-U\mathrm{Re}\chi_{11}^{HF}|=0$ at zero wave vector $q_{\parallel}$ for zero frequency ω

Table 2. below illustrates that our spin wave spectrum at $q_{\parallel} = 0$, $\omega = 0$ is very accurate for any single-adlayer itinerant ferromagnet including a very weak one. It is espencially interesting to note that excellent Goldstone mode is obtained even for a small number of NC say NC = 4. To explain this remarkable and unexpected result we propose the following physical argument. The set of Cunningham points (see Fig.12) forms a regular grid in the reciprocal space. It follows that there is a set of corresponding fictitious lattice points in the direct space (in the x,y-plane). Since we have replaced the B.Z. integral by the sum over the Cunningham points we are effectively evaluating the B.Z. sums exactly for a fictitious small set of atoms sitting on a regular lattice in the x,y-plane. Because of the spin-rotational invariance of the Hubbard Hamiltonian, the Goldstone theorem must be satisfied exactly for any collection of atoms no matter how small the sample may be. We believe that our results reflect precisely this fact.

It is also important to note that the Goldstone mode in our overlayer depends very much on the accuracy of calculation of the kernel $\chi_{11}^{HF}(\omega,q_{\parallel})$.

The Goldstone theorem is broken if the kernel is not treated exactly in the HF approximation.This will be discussed in detail later.

After this preliminary discussion, we can now describe our

Goldstone mode

$$U\mathrm{Re}\chi_{11}^{HF}(\omega=0,q_{\parallel}=0) = 1$$

NC	U	$n_{1\uparrow}$	$n_{1\downarrow}$	$V_{1\downarrow}$(or Δ)	$U\mathrm{Re}\chi_{11}^{HF}$
4	100.0	0.09732	0.000251	9.706808	0.99999
	39.97	0.09732	0.001497	3.830190	0.99999
	30.50	0.09732	0.002525	2.891331	0.99994
	20.50	0.09732	0.005451	1.883260	0.99995
	15.50	0.09732	0.009457	1.361940	0.99993
	10.50	0.09732	0.021152	0.799776	0.99995
	9.50	0.09732	0.026449	0.673331	0.99991
	6.90	0.09732	0.062485	0.240399	0.9998
	6.50	0.09732	0.077867	0.126488	0.99995
32	100.0	0.09882	0.000246	9.857267	0.99999
	39.97	0.09882	0.001472	3.891143	0.99999
	30.50	0.09882	0.002483	2.938373	0.99995
	20.50	0.09882	0.005358	1.916017	0.99995
	15.50	0.09882	0.009272	1.388057	0.99994
	10.50	0.09882	0.020620	0.821175	0.99990
	9.50	0.09882	0.025709	0.694591	0.99992
	6.90	0.09882	0.058703	0.276857	0.9998
	6.50	0.09882	0.071464	0.177864	0.9997

Table 2. Testing Goldstone mode for a single-adlayer with E_F =-1.5 and ε = 0.001.

spin wave energies calculated (we use energy units W=6). The Fermi energy is chosen at E_F=-1.5. It is situated in the majority up-spin hole band while the minority spin-down band is assumed to be almost occupied as there is only a long tail extending downward to the bottom of the band as shown in Fig.23. below :

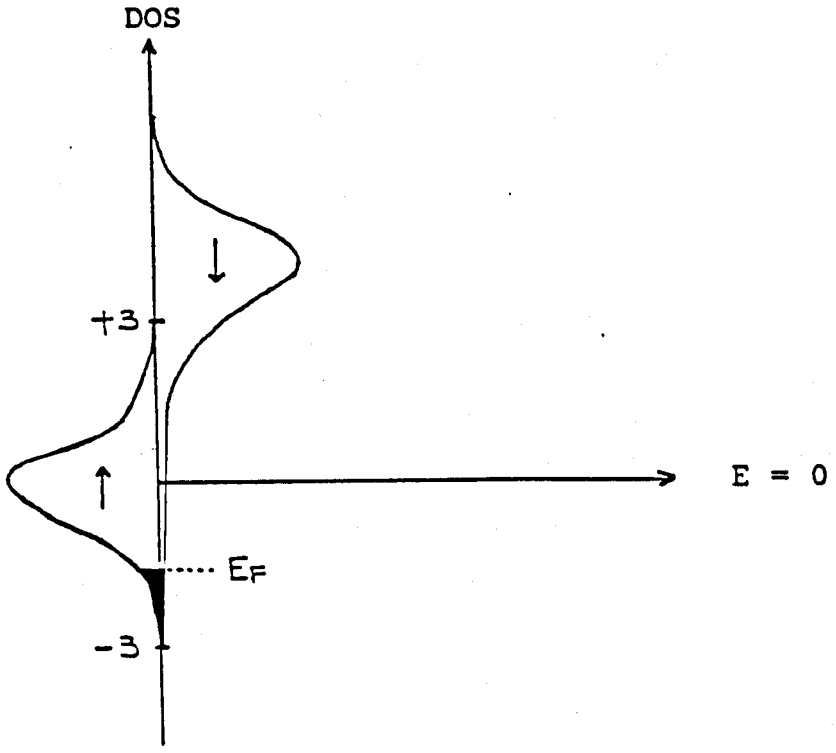

Fig.23.

This long tail may be explained in terms of quantum tunnelling. This phenomenon of tunnelling is clearly to be seen as a result of overlapping wavefunctions between the non-magnetic substrate and a single ferromagnetic layer. In other words, some of the down spin holes in the substrate still penetrate into the overlayer of a single atomic plane. Their density depends very much on how high or wide the potential energy barrier is. For example, from Table.2 we can see that if the barrier is high (i.e. $\Delta \rightarrow \infty$) then the tunnelling becomes very difficult and a smaller number

of spin-down particles penetrates the surface layer. Fig.(18) shows that how deep the holes can penetrate depends also on the thickness of the overlayer. As we can see from Fig.18 the number of spin-down holes can only penetrate the first or, to a lesser extent,the second layer

Given the values of E_F and U, we can determine $n_{1\uparrow}$, $n_{1\downarrow}$ and $V_{1\downarrow}$ (or Δ) self-consistently. Once this is done, the spin wave energies are then computed for $0 \leq q_{\parallel} \leq \pi/a$ from Eq.(3.7) using a bisection method.

We would like to emphasize that our method of adlayers is applicable to strong, weak and even very weak ferromagnetic overlayers provided the Fermi level and U are chosen so that the HF ground state remains ferromagnetic, i.e, the Stoner criterion $UN(E_F) > 1$ is satisfied.

In Fig.24 we show two spin wave dispersion curves for two different values of NC. One curve is computed for NC=4, and the other for NC=32. It is remarkable that the complete two curves are in argreement up to 70% of the first B.Z. We wish to remark that the degree of accuracy obtained with the CPs method in computing the spectrum of spin wave is very high and the spin wave spectrum is almost independent of the choice of the number of NCs.

It is important to note that the same number of CPs NCs must be used consistently throughout the calculations of the HF ground state and of spin wave energies. Altering NC in either stage of the calculation will seriously affect the Goldstone mode and the spin wave spectrum.

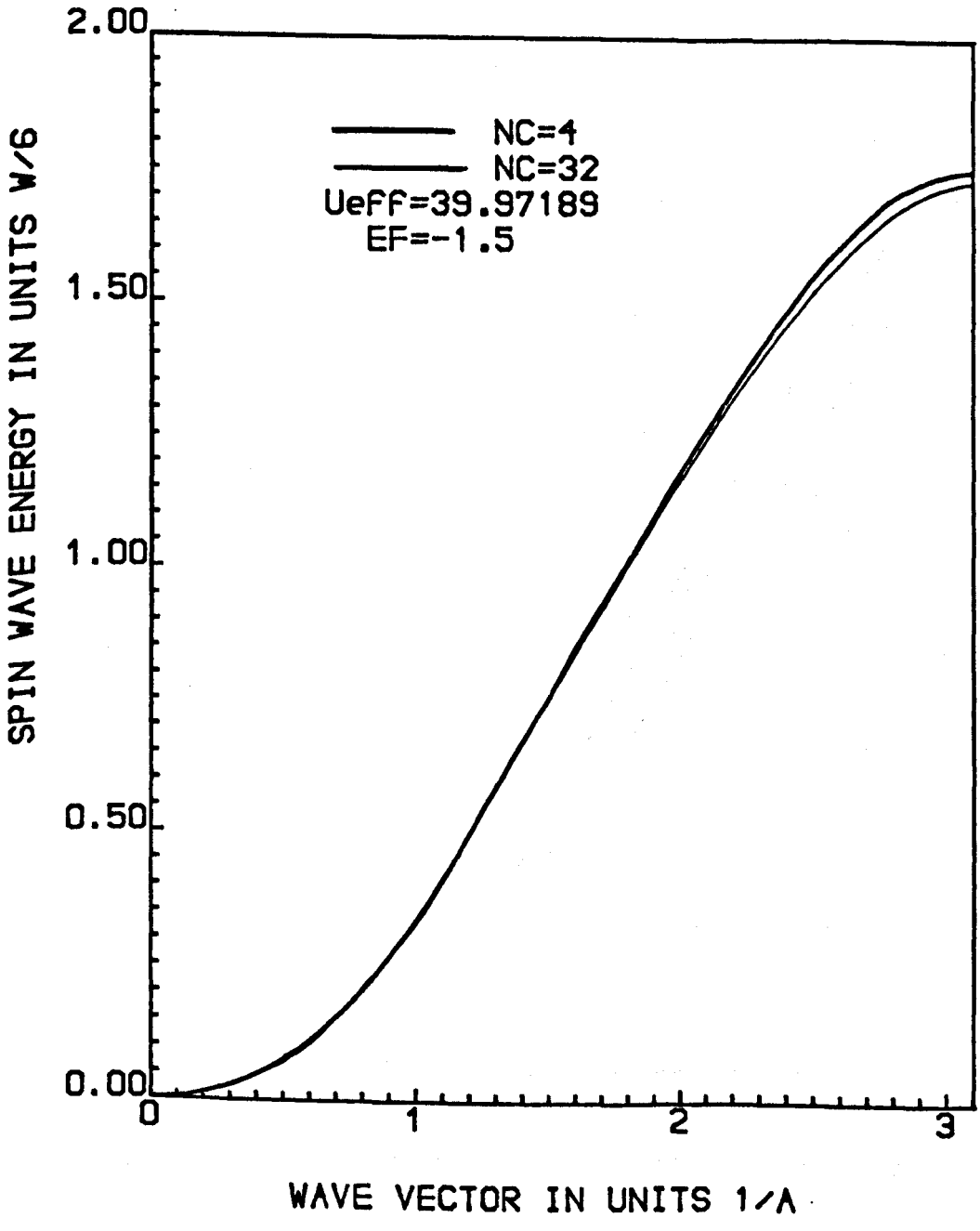

Fig.24. Spin wave dispersion curves for a single-adlayer on top of a (100) non-magnetic substrate. The two curves are plotted together with different values of NC for the purpose of comparison.

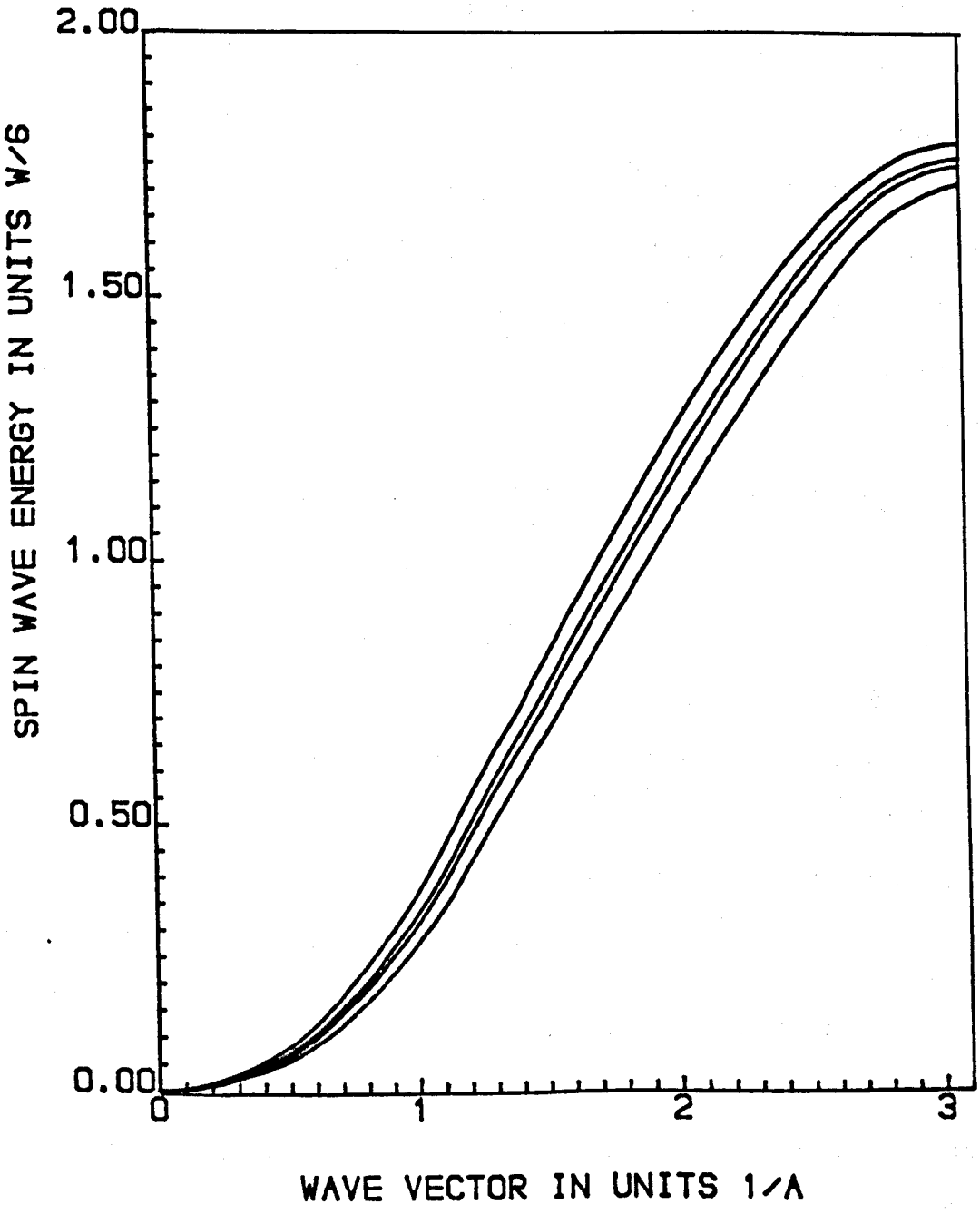

Fig.25. Spin wave spectrums for a single-adlayer on top of a (100) non-magnetic metallic substrate with different coulomb interactions U = 100.0, 39.97, 30.5 and 20.5 starts from top to bottom curve respectively. Here Ef=-1.5 and NC=4 in all four spectrums of spin wave.

We next calculated the spin wave energies for a range of U. We have investigated two different limits.

In the first case, we calculated the spectrum of spin waves for large values of U: 100, 39.97189033, 30.5 and 20.5. We found that the spectrums did not change much and this is illustrated in Fig.25 It is interesting to interprete these results in terms of an effective exchange stiffness constant D for a single-adlayer system We define D as a coefficient in the dispersion law $\omega = Dq_{\|}^2$ of a spin wave with a small $q_{\|}$. For a single-adlayer we can estimate D by fitting a $\omega=Dq_{\|}^2$ curve for small $q_{\|}$. The interpretation of the the results shown in Fig.(25) in terms of D is that the values of D reach a saturation value, say D_o, in the limit $\Delta \rightarrow \infty$.

In the second case, we computed the spectrum of spin wave for several small values of U: 15.5, 9.5 and 6.9.The spin wave spectrum satisfies the Goldstone theorem and ω increases with the wave vector q_x. The calculated spin waves are undamped until they enter the Stoner continuum at some critical wave vector q_x^c.

We estimate that with U= 15.5 and 9.5 the spin waves intersect the continuum at $q_x^c \approx 2.$ and 1.2 and become strongly damped for $q_x > q_x^c$. For U=6.9, we found that the spin wave spectrum is undamped until it decays into the continuum at a $q_x^c \approx 0.7$. For $q_x > q_x^c$ the spectrum becomes oscillating and it completely disappeared at $q_x = 0.89$ (see Fig.26).

We recall that when the spectrum of spin wave is inside the

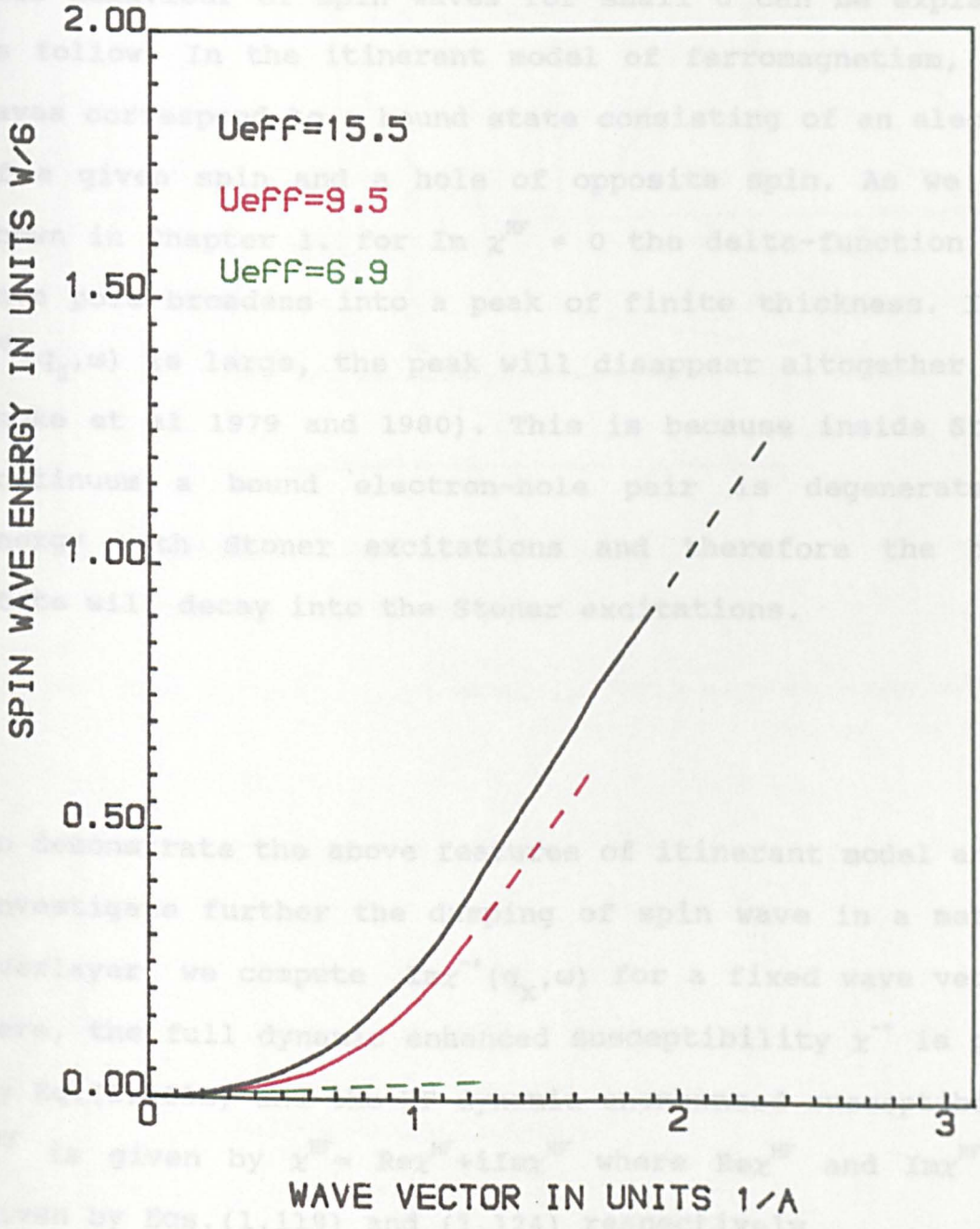

Fig.26. Spin wave spectrums for a single-adlayer on top of a (100) non-magnetic metallic substrate. Here, EF=-1.5 and NC=4 in all three spectrums of spin waves. The dashed lines indicate the spin waves enter the Stoner continuum.

Stoner continuum Im $\chi^{HF}_{ij}(q_{\parallel},\omega)$ no longer vanishes. Thus for a fixed value of q_x we may possibly find several Stoner poles in the continuum and this we have observed for $q > q^c$.

This behaviour of spin waves for small U can be explained as follow: In the itinerant model of ferromagnetism, spin waves correspond to a bound state consisting of an electron of a given spin and a hole of opposite spin. As we have shown in Chapter 1. for Im $\chi^{HF} \neq 0$ the delta-function spin wave pole broadens into a peak of finite thickness. If Im $\chi^{HF}(q_{\parallel},\omega)$ is large, the peak will disappear altogether (see Cooke et al 1979 and 1980). This is because inside Stoner continuum a bound electron-hole pair is degenerate in energy with Stoner excitations and therefore the bound state will decay into the Stoner excitations.

To demonstrate the above features of itinerant model and to investigate further the damping of spin wave in a metalic overlayer, we compute $Im\chi^{-+}(q_x,\omega)$ for a fixed wave vector. Here, the full dynamic enhanced susceptibility χ^{-+} is given by Eq.(1.103b) and the HF dynamic unenhanced susceptibility χ^{HF} is given by $\chi^{HF} = Re\chi^{HF} + iIm\chi^{HF}$ where $Re\chi^{HF}$ and $Im\chi^{HF}$ are given by Eqs.(1.119) and (1.124) respectively.

In Fig.26a. we plot $Im\chi^{-+}_{11}(q_x,\omega)$ versus the spin wave energy ω for a single-adlayer for U^{eff}=15.5, ε=0.05, NC=32 and q_x = 0.5, 1.5 and 3.0. There are several features in Fig.26a

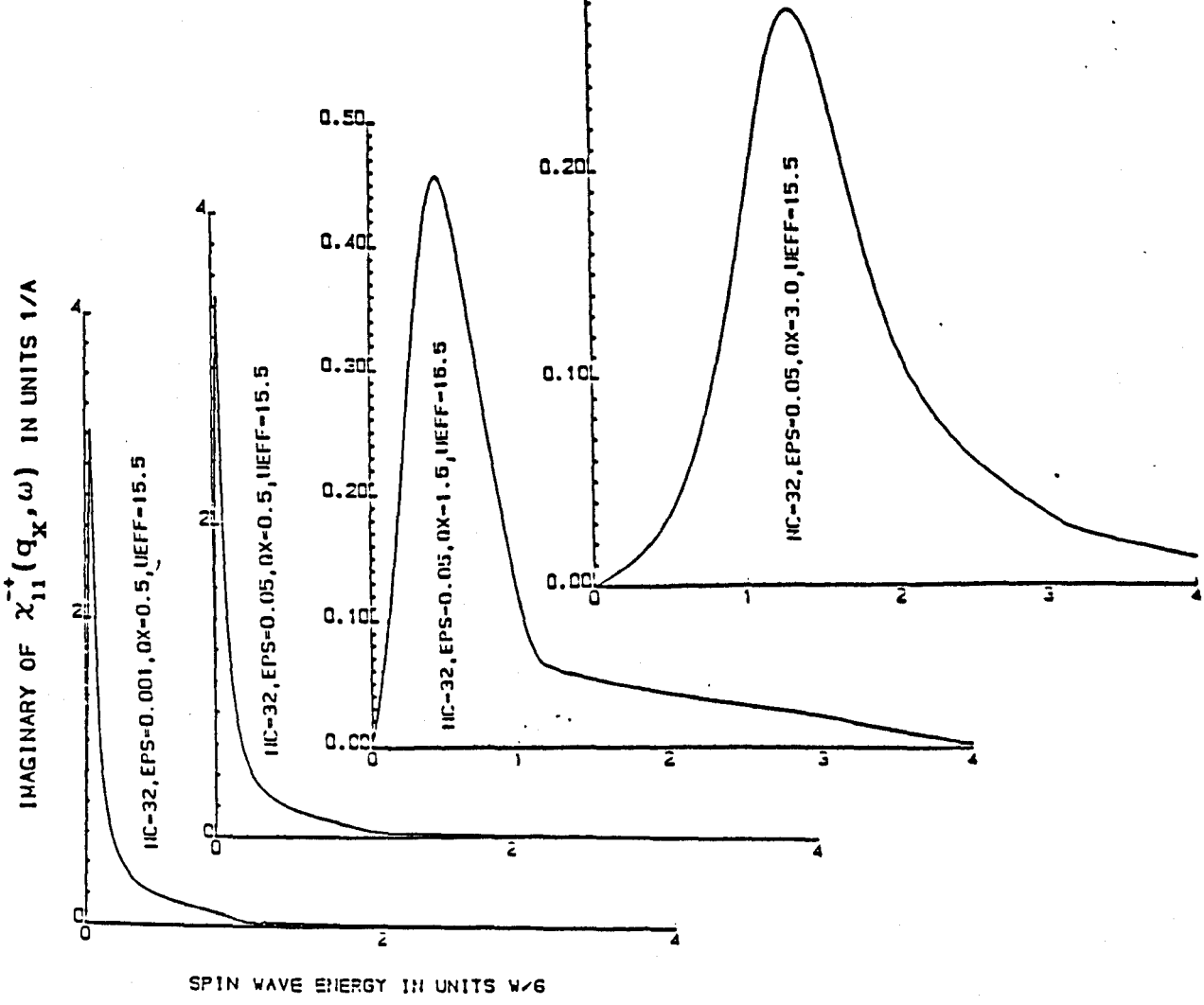

Fig.26a. Plot of Im $\chi^{-+}_{11}(q_x,\omega)$ versus ω for a single-adlayer system

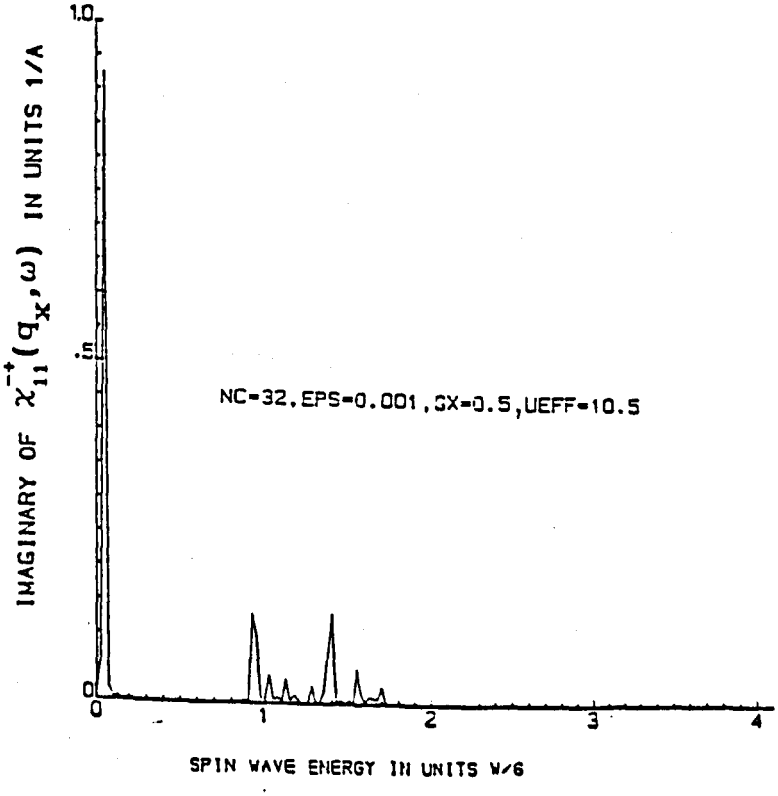

Fig.26b. Plot of Im $\chi^{-+}_{11}(q_x,\omega)$ versus ω for an unsupported layer

we wish to discuss. The spin waves show up as peaks and the positions of the peaks determine the spin wave energies. The widths of the peaks in $Im\chi^{HF}_{11}(q_x,\omega)$ is inversely related to the spin wave lifetime. The spin wave peak is very sharp for wave vector below 1.0, but always has a finite lifetime. The peak width broadens and the peak height drops as we increases the wave vector from the B.Z. centre. The broadening of the spin wave peak almost does not change as we decrease the values of ε from ε=0.05 to ε=0.001, meaning that such a broadening is not an artifact of our finite ε but genuine effect.

It is clearly noticeable that the spin wave peak and the Stoner continuum of the single-adlayer are superimposed on one another. This result indicates that down-spin electrons from the substrate can tunnel into the overlayer at energy below the exchange splitting and hence there is a long tail in the majority up-spin hole band (see Fig.23). As a result, the spin wave spectrums of a metallic overlayer is always damped. In fact, this is a striking feature of the magnetic metallic overlayer on top of a metallic substrate.

To demonstrate the above statement more explicitly, we plot in Fig.26b., $Im\chi^{-+}(q_x,\omega)$ versus ω for an unsupported two-dimensional layer (see section 3.3.1.1, Fig.30). In constrast to the single-adlayer, the spin wave peak which

has an infinite lifetime and the Stoner continuum in a free-standing layer are completely separated from each other and this is because the system has no tail.

In summary, our result indicates that for a magnetic metallic overlayer deposite on top of a metallic substrate, the Stoner continuum exists everywhere even in a small region around the Brillouin zone centre. This result shoud not be found for a metallic overlayer deposited on top of an insulator substrate. This is because the electrons are localized at the substrate and hence there is no tail.

Finally we would like to investigate the dependence of the Goldstone mode on the accuracy of $\chi_{ij}^{HF}(q_{\parallel},\omega)$ for a single-adlayer system.

For illustration, we choose U=100.0 and E_F=-1.5. The numbers of spin-up and spin-down particles computed self-consistently are shown in Table 2. The number of spin-down particles is about 0.26% of spin-up particles. One might, therefore, be tempted to neglect the second contribution in Eq.(3.8). However, this leads to a serious error and the Goldstone mode at $q_{\parallel}$=0, ω=0 is violated, i.e. we obtain a finite frequency pole at zero wave vector. This large unphysical gap in the spectrum of spin waves is clearly seen in Fig.(27).

This example illustrates how important it is to calculate the kernel χ_{ij}^{HF} exactly in the HF approximation. Griffin and Gumbs (GG) (1976,1980) applied the Hubbard model to a semi-infinite ferromagnet and tried to find the surface spin waves. As a first step, they approximated χ^{HF} in the so called 'classical infinite barrier model' (CIBM) which assumes that the static electron density near the surface is the same as in the bulk. GG were then able to solve Eq.(1.100) and obtained a surface spin wave above the bulk spin wave band as $q_{\parallel} \to 0$. However, it is clear that the kernel χ^{HF} in the CIBM approximation is not the correct HF kernel. Since our example shows that even a very small error in the calculation of χ^{HF} leads to a large unphysical gap in the spin-wave spectrum, the results of Griffin and Gumbs are clearly incorrect. This was already discussed by Mathon (1981a,b) in the case of a strong ferromagnet but our calculation is the first quantitative illustration how serious the error of Griffin and Gumbs really is.

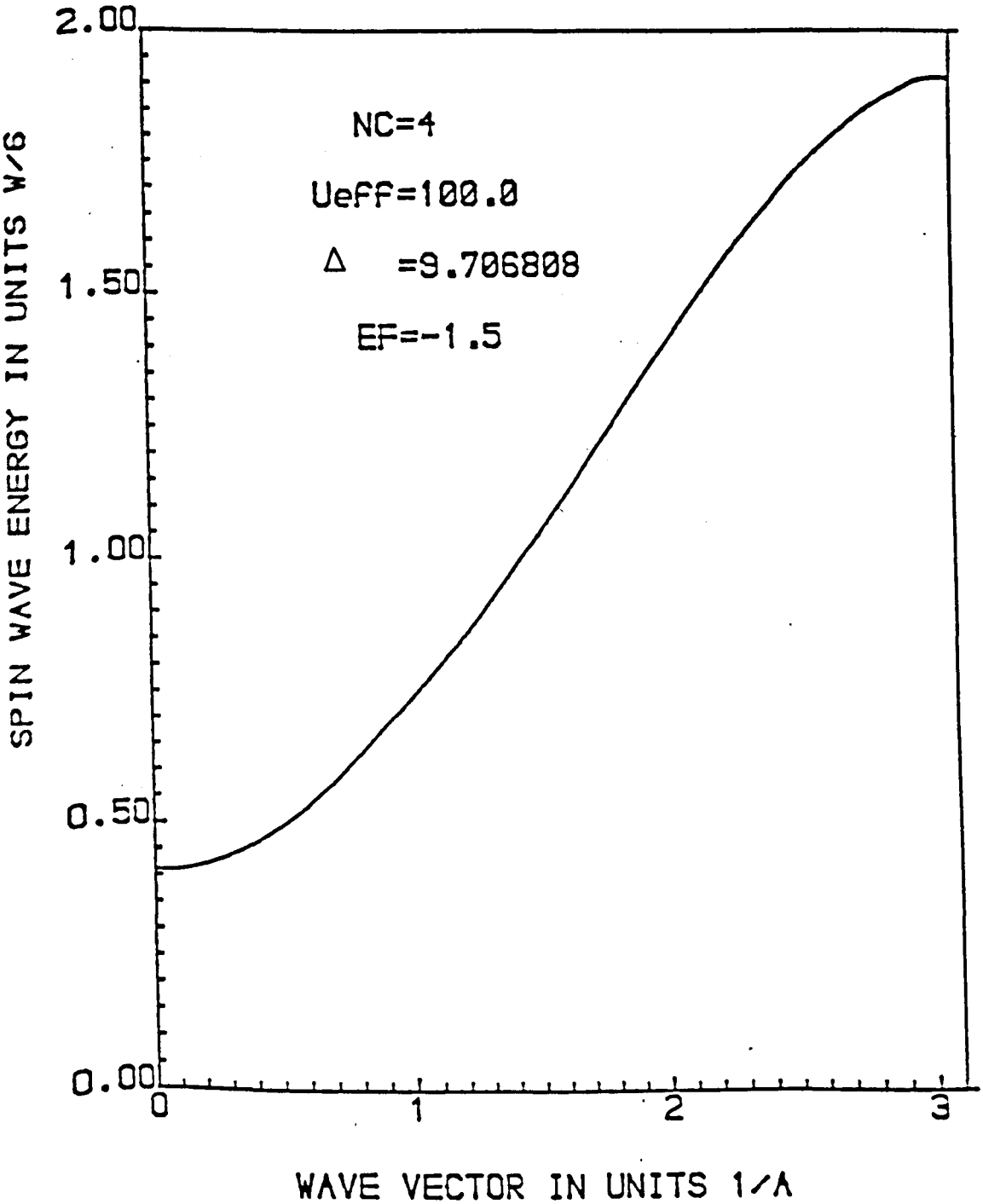

Fig.27. Spin wave energies for a single-adlayer system calculated from Eq.(3.8) without $ImG_{11\downarrow}$. This is an example of not treating the $\chi^{HF}(w,q_{\parallel})$ exactly in the HF approximation which gives rise to an unphysical gap and breaks the Goldstone theorem

3.3.1.1 Comparison between spin waves in an unsupported layer and a single-adlayer

A. Introduction

The aim of this subsection is to compute the spin wave spectrum of a single-adlayer for a range of U and for a fixed total number of particles $n = n_{\uparrow} + n_{\downarrow}$. The results are then compared with the spin wave spectrum of an unsupported layer having the same values of U and n. We shall also compare these two spectra with the spin wave dispersion law calculated from the exchange stiffness constant D_{2d} of an unsupported layer.

We begin with the derivation of the RPA formula for the exchange stiffness D_{2d} of a two-dimensional ferromagnet using the Edwards formula (Edwards, 1967) for a D in a simple cubic crystal.

B. Exchange stiffness constant of a two-dimensional unsupported layer

We shall briefly describe the calculation of the exchange stiffness constant D_{2d} of an infinite two-dimension ferromagnet. The exchange stiffness constant D is defined by $\hbar\omega = D_{2d} q_{\parallel}^2$. For a two-dimensional layer, D_{2d} is given by

$$D = \frac{U}{2N} \sum_{k} \left(\frac{f_{k\uparrow} + f_{k\downarrow}}{2\Delta} \nabla^2 E_k - \frac{f_{k\uparrow} - f_{k\downarrow}}{\Delta^2} |\nabla E_k|^2 \right) \qquad (3.9)$$

which can be derived from Eq.(1.104).

Following Edwards (1967), Eq.(3.9) may be further simplified by employing the Green theorem to obtain

$$\frac{D}{a^2} = \frac{U}{2\Delta^2} \int_{\mu_\downarrow}^{\mu_\uparrow} E(\mu - E) N(E) dE \qquad (3.10)$$

where $\mu_{\uparrow\downarrow}$ are the spin up and down spin energies, N(E) is the density of states per atom and a is the lattice constant. At $T=0^0K$ μ is defined by

$$\begin{aligned} \mu_{\uparrow\downarrow} &= \mu \pm \Delta/2 \\ \Delta &= nU\xi \end{aligned} \qquad (3.11)$$

Let us first calculate the number of spin-up particles $n_\uparrow$. By definition, we have

$$n_\uparrow = \int_{-2.}^{E_F} N(E) dE \qquad (3.13)$$

where

$$N(E) = \frac{1}{N} \sum_{K_\parallel} \delta[E - E(K_\parallel)] \qquad (3.14)$$

with $E(K_\parallel) = 2T(\cos aK_x + \cos aK_y)$

Thus Eq.(3.13) becomes

$$n_{\uparrow} = \frac{a^2}{(2\pi)^2} \iint_{E(K)\leq EF} dK_x dK_y$$

$$= \frac{1}{4\pi^2} \cdot 4 \cdot \iint_{\Delta} dK_x dK_y \qquad (3.15)$$

where Δ is the region of integration defined as follows

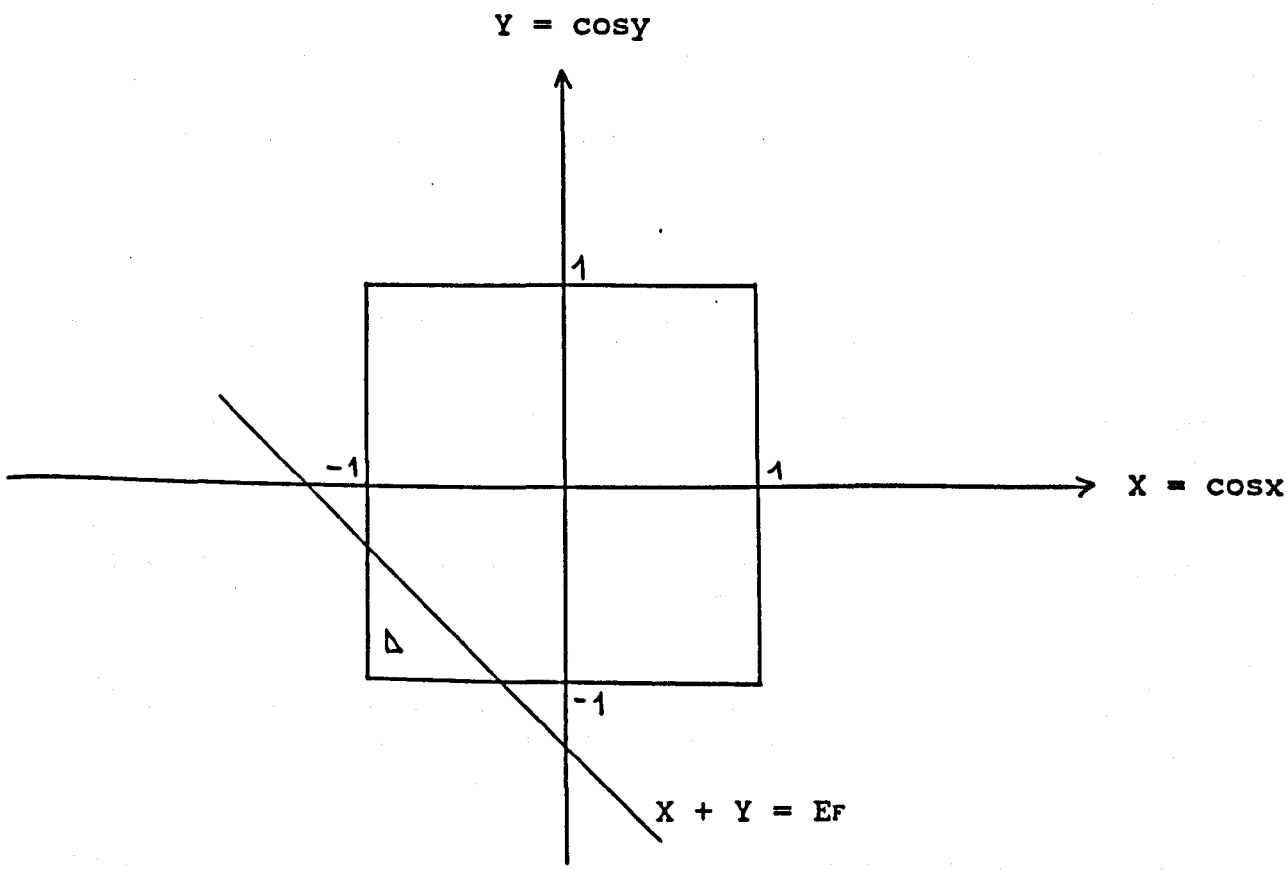

Fig.28 Region of integration of Eq.(3.15)

Finally Eq.(3.15) reduces to

$$n_{\uparrow} = \frac{1}{\pi^2} \int_{x=-\pi}^{-\cos^{-1}(EF+1)} dx \, [\pi - \cos^{-1}(E_F - \cos x)] \qquad (3.16)$$

We now return to Eq.(3.10) which yields

$$\frac{D_{2d}}{a^2} = \frac{U}{2\pi^2 \Delta^2} \iint_{\Delta} E(K_{\parallel})[\mu - E(K_{\parallel})] \, dK_x \, dK_y \qquad (3.16')$$

where Δ is defined in Fig.(28).

We finally obtain the following an expression for the exchange stiffness constant D_{2d}:

$$\frac{D_{2d}}{a^2} = \frac{U}{2\Delta^2\pi^2}\int_{x=-\pi}^{-\cos^{-1}(EF+1)} dx \{ (\mu\cos x-\cos^2 x)(\pi-C)+(2\cos x-\mu)\sin C + 0.25\sin(2C)+ 0.5C-\pi/2) \quad (3.17a)$$

where

$$C = \cos^{-1}(E_F - \cos x)$$

$$\mu = E_F - \Delta/2 \quad (3.17b)$$

with $\Delta = Un_{\uparrow}$ and $n_{\uparrow}$ is given in Eq.(3.16).

C. Spin-wave spectrum for an unsupported layer

The Green's functions for an unsupported layer are defined as follow:

$$G^{\uparrow}(E,K_{\parallel}) = \frac{1}{E - 2T(\cos K_x a+\cos K_y a) + i\varepsilon} \quad (3.18a)$$

and

$$G^{\downarrow}(E,K_{\parallel}) = \frac{1}{E -2T(\cos K_x a+\cos K_y a) - \Delta + i\varepsilon} \quad (3.18b)$$

Before we can calculate the spin wave spectrum, we need the density of states which is given by

$$N^{unsup.}(E) = -\frac{1}{\pi}\sum_{K_{\parallel}} \mathrm{Im}\, G^{\uparrow}(E,K_{\parallel}) \quad (3.19)$$

Because Eq.(3.19) is the sum of delta functions, we need a large number of CPs in the summation in the K space. We found that NC = 256 and ε = 0.0056 lead to a smooth density of states with a bandwith W = 4. Again the usual sum rule is well satisfied with ε=0.0056 (see Fig.29).

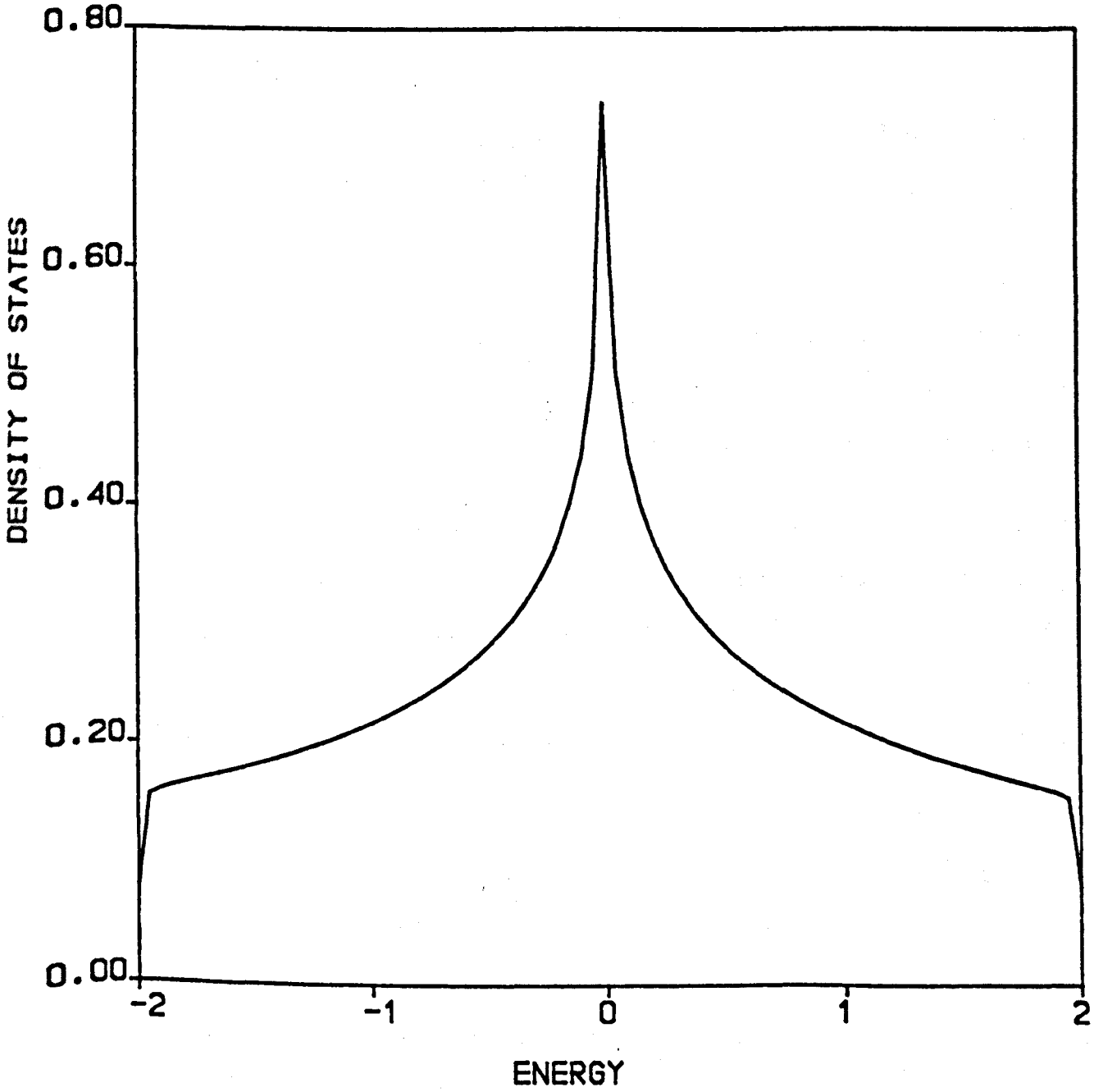

Fig.29. Density of states of an unsupported layer in two-dimensional with EF=-1.5, NC=256 and ε =0.0056.

The spin wave energies for an unsupported layer are easily obtained from

$$1 - U^{eff}\ \mathrm{Re}\ \chi^{HF}_{11}(\omega, q_{\parallel}) = 0 \qquad (3.20)$$

where the unenhanced susceptibility of a strong ferromagnetic system is given by

$$\mathrm{Re}\ \chi^{HF}_{11}(\omega, q_{\parallel}) = -\frac{1}{\pi N_{\parallel}} \sum_{K_{\parallel}} \int_{-2}^{E_F} dE\ \mathrm{Im}\ G^{\uparrow}_{11}(E, K_{\parallel})\, \mathrm{Re}\ G^{\downarrow}_{11}(E+\omega, K_{\parallel}+ q_{\parallel}) \qquad (3.21)$$

We remark that the DOS for a two-dimensional layer has a rectangular shape, which indicates that the system is always a strong ferromagnet. Therefore $\mathrm{Im}\ G^{\downarrow}_{11} = 0$ and there is no contribution of the second term in Eq.(3.21).

Eq.(3.21) was evaluated using the CPs method to perform the B.Z. summation and the Simpson rule to perform the energy integration. Spin modes were again obtained by a bisection method from Eq.(3.20). We can now compare the spin wave spectra for a single-adlayer and for an unsupported layer.

First we choose the parameters assuming that it is a strong ferromagnet such as nickel for a single-adlayer. We thus determine the Fermi energy from the condition that the total number of particles per atom in the surface layer is ≈ 0.12. We find with $n = n_{1\uparrow} + n_{1\downarrow} \approx 0.118472$ that E_F=-1.5, U=10.5, the magnetization $m = n_{1\uparrow} - n_{1\downarrow} = 0.0782$ and $\Delta = 0.821175$ (see Table.2). The spin wave spectrum is then computed in the usual manner.

Once the spin wave dispersion curve is obtained, we remove

the non-magnetic substrate which means that the single-adlayer system is now reduced to an unsupported ferromagnetic layer. We keep the two parameters n=0.12 and U=10.5 unchanged. With these parameters we have determined the Fermi level of the unsupported layer, from its density of states (see Fig.29). As already discussed, we have also determined the exchange stiffness constant D_{2d} from Eq.(3.17a) for E_F=-1.3125 and Δ=1.2455484.

All these results are compared in Fig.(30). We first note that there is an excellent agreement between D_{2d} and the spin wave spectrum for an unsupported layer obtained from Eq.(3.20). This is important because it demonstrates that our method of calculating the spin wave spectrum from one-electron propagators in the mixed representation is very accurate.

It is also interesting that there is very little difference between spin wave energies in the adlayer and in the unsupported layer at the bottom of the spin wave band.

Finally, we wish to point out that spin waves in the single-adlayer become damped for $q_x \geq 1.5$. This is because the single-adlayer is a weak ferromagnet.

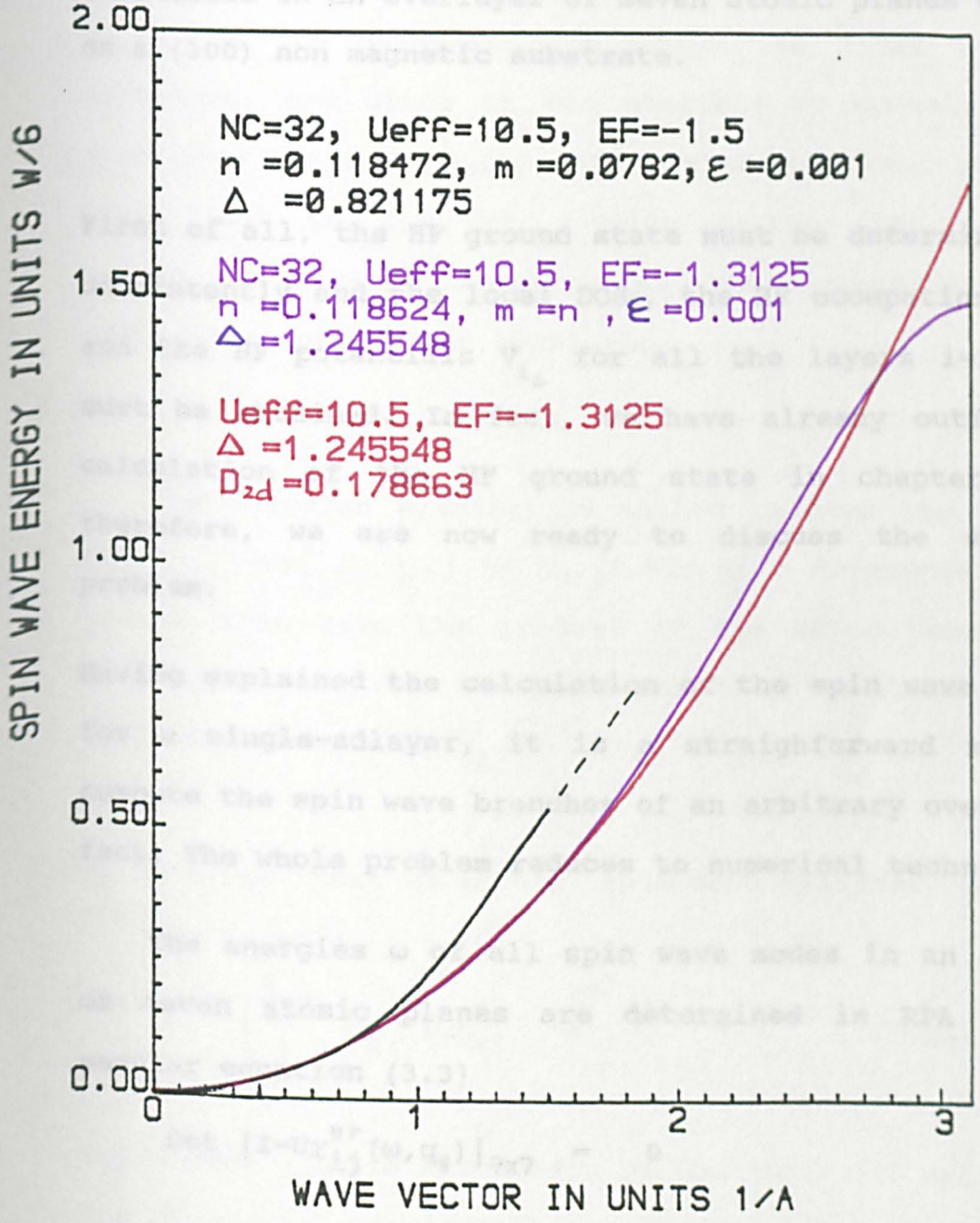

Fig.30. A comparison between spin wave energies of a single-adlayer (black colour) and an unsupported layer (purple colour) are presented. The red curve represents the Dq_x^2 relation with D in two-dimensional of an infinit ferromagnetic system. The dashed line indicates the spin wave enters the Stoner continuum.

3.4 Spin waves in an overlayer

Our aim in this section is to compute all the spin wave modes in an overlayer of seven atomic planes deposited on a (100) non magnetic substrate.

First of all, the HF ground state must be determined self-consistently and the local DOSs, the HF occupation numbers and the HF potentials $V_{i\downarrow}$ for all the layers i=1,2,...,7 must be obtained. In fact, we have already outlined the calculation of the HF ground state in chapter 2 and, therefore, we are now ready to discuss the spin wave problem.

Having explained the calculation of the spin wave energies for a single-adlayer, it is a straighforward matter to compute the spin wave branches of an arbitrary overlayer.In fact, The whole problem reduces to numerical techniques.

The energies ω of all spin wave modes in an overlayer of seven atomic planes are determined in RPA from the secular equation (3.3)

$$\text{Det } |I-U\chi^{HF}_{ij}(\omega,q_{\parallel})|_{7x7} = 0 \qquad (3.22)$$

where I is the 7x7 unit matrix and i,j denote planes parallel to the surface, $1 \leq i,j \leq 7$.

The determinant in Eq.(3.22) can be evaluated by several numerical techniques. In particular, it is possible to

reformulate Eq.(3.22) as an eigenvalue problem and then use one of the standard techniques to solve the eigenvalue problem.

Another more direct method for evaluating the determinant (3.22) is the Gaussian elimination. We first tried this technique, and since it was possible to compute all the spin wave branches using this method and also because of time limit we did not develop further the eigenvalue method. It is clear, however, that the eigenvalue method is preferable for thicker overlayer.

The Gaussian elimination method reduces the whole 7x7 matrix $[I-U\chi^{HF}_{ij}(\omega,q_{\parallel})]$ in Eq.(3.22) to a triangular matrix, and we then take the product of the seven terms on the diagonal to evaluate the determinant. We shall denote these diagonal elements by $\tilde{\chi}_i$.

It is clear that to obtain spin wave energies we have to solve

$$\prod_{i=1}^{7} \tilde{\chi}_{ii}(\omega,q_{\parallel}) = 0 \qquad (3.23)$$

where each $\tilde{\chi}_{ii}$ is a function of the whole 7x7 matrix $Re\chi^{HF}_{ij}$ The branches of spin wave spectrum for an overlayer correspond to zeroes of Eq.(3.23). As already discussed in section (3.1) there are seven spin wave branches. We shall assume that the Coulomb interaction U takes the following form:

(i) $U = U$ throughout the overlayer,

(ii) $U = U + \Delta U$ for $i = 7$

$= U$ for $i \neq 7$

The second alternative takes into account that the HF potential in the surface layer may differ from the "bulk" potential in all the other layers. We intended to vary ΔU and search for surface spin waves in the overlayer. Unfortunately, the computation of all the branches of the spin wave spectrum proved to be time consuming and we were able to complete the computation of spin wave energies only in the case (i). The results are described next.

We first solved the HF ground state problem as described in chapter 2. The values of the HF potentials in all the layers and the corresponding $n_{i\uparrow}$, $n_{i\downarrow}$ are given in Table 3. for E_F=-1.5 and U=30.5.

U	NC	E_F		$n_{i\uparrow}$	$n_{i\downarrow}$	$V_{i\downarrow}$
30.5	4	-1.5	i=0	0.095404	0.108591	0.000000
			i=1	0.097844	0.002621	2.904507
			i=2	0.1070170	0.000072	3.261820
			i=3	0.1011204	0.000022	3.083504
			i=4	0.1142068	0.000017	3.482772
			i=5	0.1095104	0.000018	3.339500
			i=6	0.1103062	0.000018	3.363777
			i=7	0.0973175	0.000021	2.967540

Table 3.

Next we solved Eq.(3.23) for $q_{\parallel}$=0 and ω=0 to test the Goldstone mode. We found that the Goldstone theorem for an overlayer of seven atomic planes is very well satisfied.

$$\prod_{i=1}^{7} \tilde{\chi}_{ii}(0,0) = 0.9999999999953 \qquad (3.24)$$

Finally, all the spin wave modes of the seven layer thin film were computed using the bisection method. Normally the method for determining zeroes of a function $\prod_{i=1}^{7} \tilde{\chi}_{ii}(\omega, q_{\parallel})$ involve the evaluation of its derivatives.

Since it would be very difficult or even impossible to obtain the derivative of the above function, we look for methods that do not make use of derivatives. The bisection method has emerged as the most convenient technique for solving our spin wave problem. Our method of solving Eq.(3.23) can be described as follows: we first solved Eq.(3.23) at $q_{\parallel}$ = 0 to obtain seven 'principal' spin wave modes, say, ω_{ip} for i = 1,2, ... ,7. Each of the values ω_{ip} acts as a head-mode of the spin wave dispersion curve and only one spin wave branch is computed at a time. Usually, we compute the top branch of spin wave first where the largest $\omega_{ip}(\omega_{ip}^{max})$ is its head-mode. This top spin wave branch gives a general guide in determining other branches of spin wave.

We now describe briefly how the top branch of spin wave is computed. We start with an interval $[\omega_{ip}^{max}, \Delta]$ containing a

spin wave containing a spin wave mode at a fixed wave vector say q_x^1. Then a mid-point ω_{sw} is found from $\omega_{sw} = (\omega_{ip}^{max} + \Delta)/2$

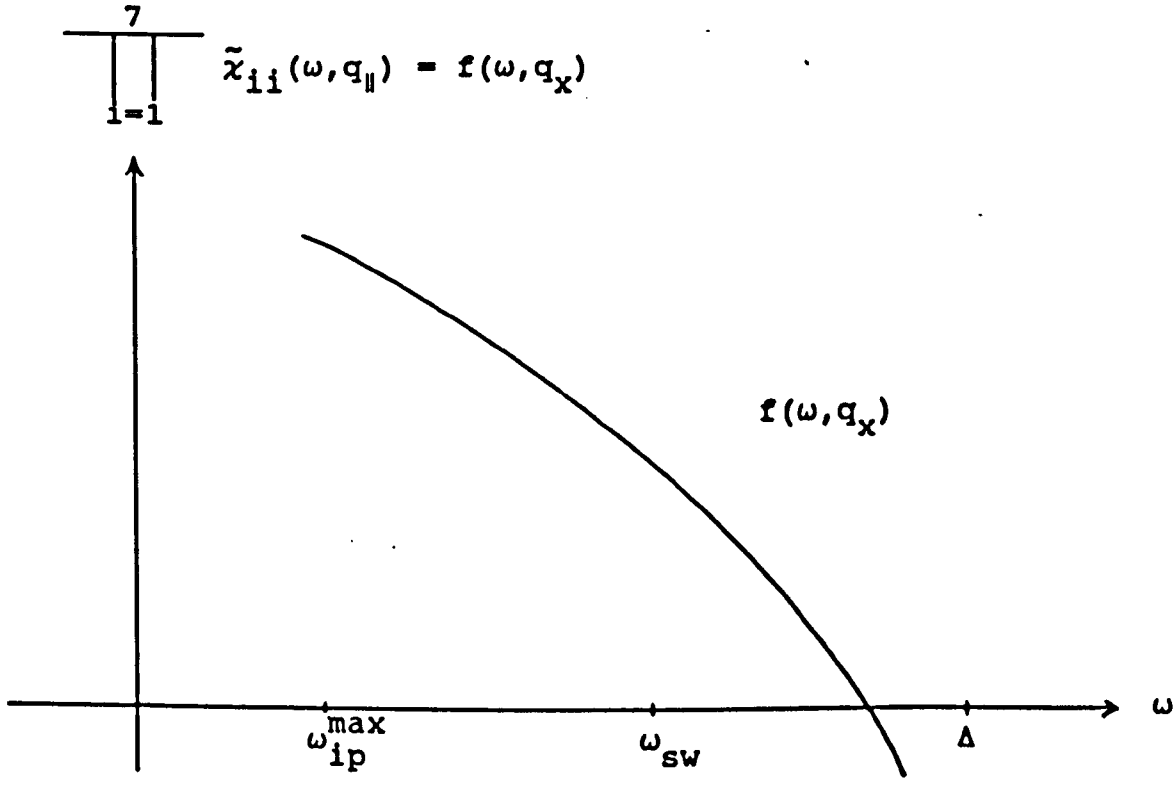

Fig.31 Algorithm for bisection method in searching for a spin wave mode.

Next $f(\omega_{sw}, q_x^1)$ and $f(\omega_{ip}^{max}, q_x^1)$ are calculated (see Fig.31). If the product of the above two functions is less than zero then the spin wave mode must lie in the interval $[\omega_{ip}^{max}, \omega_{sw}]$. However, if the product is ≥ 0 then the spin wave mode must lie in the interval $[\omega_{sw}, \Delta]$. In either case, the size of the interval containing a spin wave mode has been halved. The bisection method continues with a new smaller interval and the procedure is repeated as required. After n steps the interval will have a size $(\Delta - \omega_{ip}^{max})/2^n$

If this interval reaches a given specified tolerance δ then a spin wave mode ω^1_{sw} is found. The next spin wave mode ω^2_{sw} at a given wave vector say $q^2_x > q^1_{sw}$ can be found in a similar manner but this time the bisection starts with an interval $[\omega^1_{sw}, \Delta]$.

Once the top branch of spin waves have been computed, the second branch from top with the second largest ω_{ip} being its head-mode is calculated in an exactly the same manner. This procedure is repeated until the last spin wave branch with the smallest $\omega_{ip} = 0$ is computed.

As an illustration, we present in Fig.32 the results of our calculation of all spin wave modes in an overlayer of seven atomic planes on top of a (100) non-magnetic substrate. There are 0.12 holes in its spin majority band and the average exchange splitting is $\Delta \approx 0.5W$.

There are several features in Fig.32 we wish to discuss. Firstly, the lowest spin wave branch approaches continously $\omega=0$ in the limit $q_{\parallel} \to 0$ and an effective D at the bottom of the band can clearly be defined. This is, of course, a consequence of the spin-rotational invariance of the Hubbard Hamiltonian but it is gratifying to see that our numerical method can reproduce this result accurately.

Here we would like to make an important remark that all the seven branches of spin wave are computed by solving Det $|I-U^{eff}Re\chi^{HF}_{ij}(q_{\parallel},\omega)|_{7x7} = 0$. We therefore have not

investigate the lifetime of the spin wave spectra. Although , a large effective intra-atomic Coulomb integral U have been used, some branches of spin wave at large wave vector may have some considerable damping as we have already discussed in subsection 3.3.1.

Finally, it is clearly noticeable that the two lowest branches approach one another in the limit $\omega \to 0$. This could be an indication that a surface spin wave branch is about to develop (it is known from previous work of Mathon, 1981 that the surface and bulk spin waves should be degenerate at $\omega=0$). We, therefore, aim to investigate this problem in future by varying ΔU in the surface layer.

To conclude, we wish to point out that the whole computational scheme based on the method of adlayers can be immediately generalized to a multi-orbital band structure using the method of principal layers. We intend to carry out such calculations for nickel and iron overlayers in future.

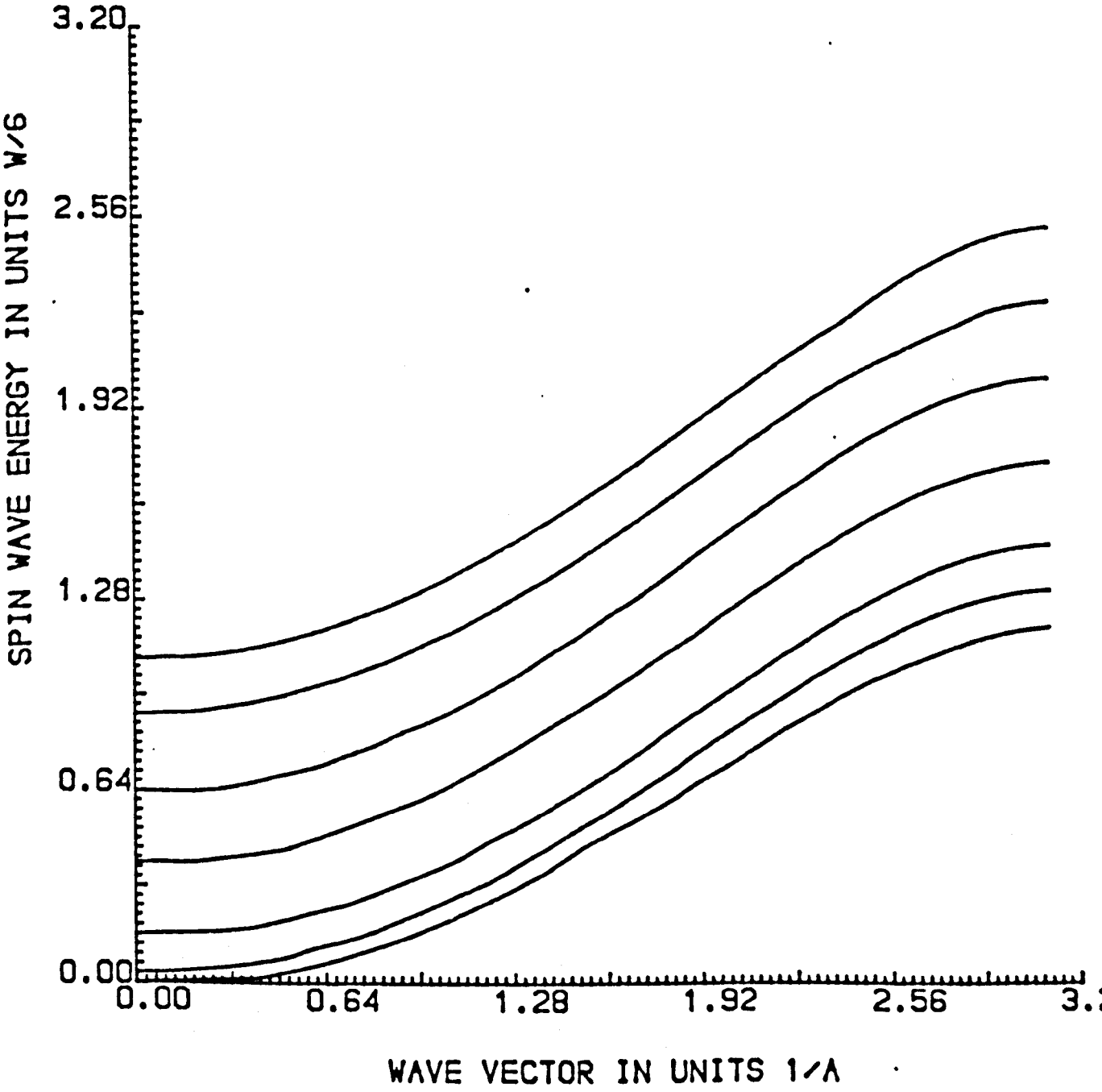

Fig.33. Spin wave modes in an overlayer of seven atomic planes above a (100) non-magnetic metallic substrate wit EF=-1.5, UHUB=30.5 and NC=4. The dashed lines indicate spin waves decay into the Stoner continum.

```
SUBROUTINE DIM(A,B,N1,N2,E,NMAX,S1)
COMPLEX S1(0:NMAX,0:NMAX),S2(0:NMAX,0:NMAX),RES(0:NMAX,0:NMAX),
       SS1,SS2
REAL A,B,H1,H2,X,Y,E,PI,PIE,F11,F22,F33,F44
INTEGER I1,I3,DI,NMAX,J1,J2,M
PI=4.0*ATAN(1.0)
PIE=PI**3
   DO 10 M=1,NMAX+1
      S1(M-1,M-1)=(0.0,0.0)
10 CONTINUE
   DO 11 J1=1,N1+1
       DO 12 K=1,NMAX+1
          S2(K-1,K-1)=(0.0,0.0)
12     CONTINUE
       DO 13 J2=1,N2+1
          H1=(B-A)/N1
           X=A+H1*(J1-1)
           IF (E.GE.-3.0.AND.E.LE.-1.0) THEN
              H2=(F22(X,E)-F11(X,E))/N2
               Y=F11(X,E)+H2*(J2-1)
           ELSE IF (E.GT.-1.0.AND.E.LE.0.0) THEN
              IF (A.EQ.-PI) THEN
                 H2=(F44(X,E)-F33(X,E)/N2
                  Y=F33(X,E)+H2*(J2-1)
              ELSE
                 H2=(F22(X,E)-F11(X,E))/N2
                  Y=F11(X,E)+H2*(J2-1)
              END IF
           ELSE
                PRINT*,'CHECK VALUE OF E'
                STOP
           END IF
  CALL EVA(NMAX,E,X,Y,RES)

(* note that subroutine EVA generate a complete matrix Green
function of an arbitrary overlayer, see Chapter 2 Eqs.2.79, 2.80
and 2.81 *)

    DO 14 I=1,NMAX+1
       SS2=(1.0/3.0)*DI(J2,N2)*H2*RES(I-1,I-1)
       S2(I-1,I-1)=S2(I-1,I-1)+SS1
14  CONTINUE
    DO 15 I=1,NMAX+1
       SS1=(1.0/3.0)*DI(J1,N1)*H1*S2(I-1,I-1)
       S1(I-1,I-1)=S1(I-1,I-1)*SS1/PIE
15  CONTINUE
11  CONTINUE
    RETURN
    END
```

```
INTEGER FUNCTION DI(I,N)
DI=3-(-1)**(I-1)
IF (I.EQ.1.OR.I.EQ.N+1) DI=1
RETURN
END


REAL FUNCTION F11(X,E)
F11=-4.0*ATAN(1.0)
RETURN
END


REAL FUNCTION F22(X,E)
REAL E,X,Y
Y=E+1.-COS(X)
IF (Y.GE.1.0) Y=1.0
IF (Y.LE.-1.0) Y=-1.0
F22=-ACOS(Y)
RETURN
END


REAL FUNCTION F33(X,E)
REAL E,X,Y
Y=E-1.-COS(X)
IF (Y.GE.1.0) Y=1.0
IF (Y.LE.-1.0) Y=-1.0
F33=-ACOS(Y)
RETURN
END


REAL FUNCTION F44(X,E)
F44=0.0
RETURN
END
```

APPENDIX II: CUNNINGHAM POINTs METHOD

(* This subroutine performs the two-dimensional B.Z integration using Cunningham points for (100) surface in s.c lattice, see S.L Cunningham, Phys.Rev. B10, 4988 (1974). It is used to integrate a function of K_x, K_y and complex energy EC=E+ic. This function is supplied as subroutine EVAL(NC,EC,K_x, K_y,GS) where EVAL generates a complete matrix Green function of an arbitrary overlayer, see Chapter 2. Eqs. 2.79, 2.80 and 2.81. Here, the matrix S is the integrated result depending on EC and other parameters. NC is the number of Cunningham points in one direction (e.g K_x) NC=2**N where N is an integer and the total number of points in 1/8 of B.Z is NC*(NC+1)/2 *)

```
SUBROUTINE CINT2(NC,EC,NMAX,S)
COMPLEX S(0:NMAX,0:NMAX),S1(0:NMAX,0:NMAX),GS(0:NMAX,0:NMAX),EC
REAL KX,KY,PI
PI=ACOS(-1.0)
   DO 1 I=1,NMAX+1
      S(I-1,I-1)=(0.0,0.0)
1  CONTINUE
   DO 1000 NK=1,NC
      KX=PI*(2*NK-1)/(2*NC)-PI
   DO 1000 MK=1,NK
      KY=PI*(2*MK-1)/(2*NC)-PI
      CALL EVAL(NC,EC,KX,KY,GS)
      DO 2 I=1,NMAX+1
        S1(I-1,I-1)=2.*GS(I-1,I-1)/(NC**2)
2     CONTINUE
      IF (NK.EQ.MK) GO TO 990
      GO TO 991
990   DO 7 I=1,NMAX+1
        S1(I-1,I-1)=0.5*S1(I-1,I-1)
7     CONTINUE
991   CONTINUE
         DO 8 I=1,NMAX+1
           S(I-1,I-1)=S(I-1,I-1)+S1(I-1.I-1)
8        CONTINUE
1000  CONTINUE
      RETURN
      END
```

Ahmad S B, J Mathon and Phan M S 1988 J.de.Physique C8 1639

Arrot A S, Heinrich B, Purcell S T and Cochran J F 1987 J.Appl.Phys. 61 3721

Al-Asadi M 1980 PhD Thesis The City University (unpublished)

Bader S D and Moog E R 1987 J.Appl.Phys. 61 3729

Baldereshi A 1973 Phys.Rev. B7 5212

Bloch 1929 Z.Phys. 57 545

Carcia P F, Meinhaldt A D and Suna A 1985 Appl.Phys.Lett. 47 178

Chadi D J and Cohen M L 1973 Phys.Rev. B8 5747

Cooke J F 1979 J.Appl.Phys. 50 7439-7444

Cooke J F, Lynn J W and David H L 1980 Phys.Rev. B21 4118

Cunningham S L 1974 Phys.Rev. B10 4988

Cyrot-Lackmann F 1973 Surf.Sci. 40 423

Desjonqueres M C and Cyrot-Lackmann F 1975 J.Phys. F5 1368

Edwards D M 1977 Physica 91B 3-13

Edwards D M 1967 Phys.Lett. 24A 350

Einstein T L and Schrieffer J R 1973 Phys.Rev. B11 3629

Falicov L M and Moran-Lopez J L (ed) 1986 Magnetic Properties of Low-Dimensional Systems (Berlin:Springer)

Falicov L M and Yndurain F 1975 J.Phys. C8 (Solid state phys.) 147

Freemann A J, Fu C L, Onishi C and Weinert M 1985 Polarised Electron In Surface Physics ed.R.Feder (Singapore:World Scientific) p3

Freemann A J, Fu C L 1987 J.Appl.Phys. 61 3356-61

Fulde P, Luther A and Watson R E 1973 Phys.Rev. B8 440

Gilat G 1972 J.Com.Phys. 10 432

Goncalves da Silva and B Laks 1977 J.Phys. C10 851

Gradmann U 1985 Thin Solid Films 126 107

Griffin A and Gumbs G 1976 Phys. Revs. Lett. 30 371

Gumbs G and Griffin A 1980 Surf. Sci. 91 669-93

Hardy R, Morrison I W and Bijanki S 1973 J.Com.Phys. 13 591

Haydock R, Heine V and Kelly M J 1972 J.Phys. C5 2845

Haydock R and Kelly M J 1973 Surf.Sci. 38 138

Herring C and Kittel C 1951 Phys.Rev. 81 869

Herring C Magnetism IV ed.G T Rado and H Suhl (Academic Press, Newyork 1966)

Hohenberg P and Kohn W 1964 Phys.Rev. 136 B864

Hubbard J 1963 Proc.R.Soc. A276 238-57

Hubbard J 1964 Proc.R.Soc. A281 401-19

Iwasaki Shun-ichi 1984 IEEE Trans.Mag. MAG-20 657

Izuyama T, Kim D J and Kubo R 1963 J.Phys.Soc. Japan 18 1025-42

Jelitto R J 1969 J.Phys.Chem.Solids 30 609

Kalkstein D and Soven P 1971 Surf.Sci. 26 85

Kanamori J 1963 Prog.Theor.Phys. 30 275

Kanamori J 1981 Electron Correlation And Magnetism In Narrow-Band System ed.T Moriya (Springer Series 29 p.102)

Katsuki A and Wohlfarth E P 1966 Proc.R.Soc. A295 182

Kittel C 1971 Introduction to Solid State Physics (NewYorK:Wiley)

Kohn W and Sham L J 1965 Phys.Rev. 140 A1133

Lee D H and Joannopoulos J D J.Vac.Sci.Technol. 1981 19(3) 355

Liebsch A 1979 Phys.Rev.Letts. 43 1431

Liebermann L N, Fredkin D R and Shore H B 1969 Phys.Rev.Lett. 22 539-41

Lopez Sancho M P,Lopez Sancho J M and Rubio J 1975 J.Phys. F15 851

Lowde R D and Windsor C G 1970 Adv. Phys. 19 813

Mathon J 1981a Phys.Rev. B24 6588

Mathon J 1981b Inst.Phys.Conf.Ser.No.55: Chapter 4 p311

Mathon J 1988a Rep.Prog.Phys. 51 1

Mathon J 1988b Physica 1988 B149 31

Mathon J and Ahmad S B 1988 Phys.Rev. B37 660

Mathon J 1989 J.Phys.: Condensed Matter 1 2585

Mathon J and Phan M S 1989 J.Phys.:Condensed Matter 1 7983

Mattis DC 1964 Phys.Rev. 132 2521

Mauri D, Scholl D and Siegmann H C 1988 Phys.Rev.Lett. 61 31

Mills D L, Beal-Monod M T and Weiner R A 1972 Phys.Rev. 135 4637

Mills D L and Lederer P 1967 Phys.Rev. 160 590

Monkhorst HJ and Pack JD 1976 Phys.Rev. B13 5188

Mott N F 1964 Adv.Phys. 13 325

Mott N F 1935 Proc.R.Soc. 47 571

Penn D 1979 Phys.Rev.Letts 42 921

Raimes S 1972 Many-Electron Theory Amsterdam-London North-Holland

Rajagopal A K 1980 Advances in Chemiscal Physics Vol.41,ed I Prigogine and S A Rice (New York:Wiley) p 59

Ren S Y and Dow J D 1988 Phys.Rev. B38 1999

Schrieffer J R and Soven P 1975 Physics Today 24-30

Siegmann H C, Mauri D, Scholl D and Kay E
1989 Plenary talk at ICM88 , Proc.ICM88, Paris (in Press)

Singhal S P 1972 J.Com.Phys. 10 316

Shimizu M 1981 Rep.Prog.Phys. 44 329

Slater J C 1953 Rev.Mod.Phys. 25 139

Stoner E C 1938 Proc.R.Soc. A165 372

Stoner E C 1936 Proc.R.Soc. A154 654

Takayama H, Baker K and Fulde P 1974 Phys.Rev. B10 2022

Thompson E D 1963 Ann. Phys. N.Y. 22 309

Thompson E D,Wohlfarth E P and Bryan A C 1964 Proc.Phys.Soc. 83 59

Van Vlech J H 1953 Rev.Mod.Phys. 25 220

Victoria R H 1986 Magnetic Properties Of Low-Dimensional Structures ed. L M Falicov and J L Moran-Lopez (Berlin:Springer Verlag) p.25

Welling F 1980 J.Phys. F10 1975-93

Wohlfarth 1980 Ferromagnetic Materials Vol.1 ed.E P Wohlfarth (Amsterdam : North Holland) pp3-70

Wohlfarth E P 1953 Rev.Mod.Phys. 25 211

Wolfram T 1969 Phys.Rev. 182 573

Ziman J M 1972 Principles of The Theory Of Solids Cambridge University Press

Zubarev D N 1960 Usp Fiz Nauk 71 71 Translation ; Soviet Phys. Usp 3 320-330